AN ANALYSIS OF HYDROGEN
CONTROL MEASURES AT
MCGUIRE NUCLEAR STATION

Revision 2
January 22, 1982

Remove and insert pages according to the following tabulations:

Remove these pages: Insert these pages:

Volume 1

                                             Chapter 2 Table of Contents
                                               (Page 2)
2.2-1   2.2-1
2.6-2   2.6-2
2.7-2   2.7-2
2.8-2   2.8-2
2.9-1   2.9-1
2.9-2   2.9-2

Volume 2

                                             Insert Tabs 2H, 2I, 2J, 2K
                                             Appendix 2H, 2I, 2J, 2K

Volume 3

6.2-3   6.2-3
6.2-4   6.2-4

TABLE OF CONTENTS (cont.)

2.2 HALON INTERING

2.2.1 Purpose

Quickly inerting a containment with Halon after a serious accident to prevent
hydrogen combustion is not a new concept. The Maritime Administration of
the Department of Commerce funded a three year program in the mid-1970's to
study the use of Halon 1301 in the reactor containment of a nuclear powered
ship. The concept was found to be completely suitable and would have been the
system of choice had such reactors been built. However, due to the differences
in size and design of the containments, it was not known whether a Halon system
would be feasible for an ice condenser containment. To answer this question,
Atlantic Research Corporation conducted a feasibility study on the use of
Halon 1301 in an ice condenser containment.

2.2.2 Summary

Three major considerations were to be addressed in the study: 1) preliminary
design of a Halon inerting system, 2) evaluation of the potential for inerted
mixture combustion to be initiated by a postulated local detonation, and
3) evaluation of the effects of a change in water chemistry due to Halon decom-
position and solubility. This project was conducted based on experimental
data available in the literature and that obtained from the studies associated
with the Maritime Administration project. It became evident early in the
project that very little information was available on the corrosion effects of
Halon 1301 and of low concentrations of hydrogen bromide and bromide ions. To
assist in addressing the third consideration, corrosion studies were conducted
at the Singleton Engineering Materials Laboratory. Chemical conditions were

chromatograph was used to determine the vessel atmosphere constituents at the conclusion of each test. Test results are presented in Appendix 2H.

Static and transient tests were conducted in Phase 2. The igniter assembly was located near the bottom of vessel for all tests. Static tests were conducted without water fog and with water fog at two different droplet sizes and concentrations. Transient tests were conducted with hydrogen injection and with hydrogen/steam injection. Comparisons were made with similar tests in Phase 1, both with and without sprays. Vessel atmosphere constituents were determined with a gas chromatograph after each test. Results of the Acurex tests are presented in Appendix 2H.

Test results demonstrated that both the ignitor location and the presence of water fogs affect the characteristics of hydrogen deflagrations. These tests demonstrated that:

1) For an enclosed vertical compartment with hydrogen injected near the bottom, higher ignitor locations appear to result in a higher pressure rise.

2) The addition of steam, water sprays, or water fogs reduce the pressure rise resulting from hydrogen combustion.

Although the presence of a water fog results in a pressure reduction, containment analyses discussed in Chapter 4 show that adequate safety margin is present without a pressure suppressant system. Therefore, further research on the effect of water fog is not being pursued. Additionally, results of the ignitor location tests appear to be consistent with existing knowledge on hydrogen combustion. Therefore, additional research on ignitor location effects is not anticipated.

Anticipated tests are very similar to those conducted in Phase 1.

Data has been obtained on glug plug performance in various hydrogen-steam-air mixtures. The glow plug has been operated at 12 and 14 volts in quiescent and turbulent conditions. These test results are consistent with the Fenwal tests discussed in section 2.1 and agree reasonably well with the Shapiro-Moffette flammability curve. Tests are currently underway with an AC ignitor developed by Tayco Engineering, Inc. These tests should be completed by February 1, 1982. An interim report is included in Appendix 2I.

with fans and grating. Tests are to be conducted with both items individually and jointly. Fan flow is varied from zero to a combined maximum of approximately 3000 cfm. The grating consists of a 1/4 inch plate perforated with 1 inch diameter holes, resulting in a blockage of 50%. Plates are located one third and two thirds the vessel height. Hydrogen concentrations are varied from 6 to 20 v/o. In Phase 4, a pipe approximately one foot in diameter and 20 feet long is attached to the sphere. Tests are to be conducted with uniform and non-uniform hydrogen concentrations varying from 6 to 20%. Ignition will be in the pipe and in the sphere. These tests provide data on the effects of flame propagation from one geometry into another, as well as the effects of propagation from one concentration to another.

Test results obtained to date appear to confirm that steam and turbulence have competing effects on hydrogen combustion. Steam tends to reduce the rate and degree of combustion, while turbulence promotes rapid and more complete combustion. Additional turbulence testing is underway, with the pipe-sphere tests to follow. Completion of all testing is anticipated around mid-February, 1982. An interim report is included in Appendix 2J.

2

2.9 HYDROGEN MIXING AND DISTRIBUTION

2.9.1 Purpose

Concerns have been expressed regarding the potential for localized accumulation of hydrogen at detonable concentrations. Previous analyses have shown that as a result of the mixing induced by the air return fans and the steam-hydrogen jet itself, the formation of detonable concentrations is precluded. Additionally, the design of the hydrogen mitigation system assures that the released hydrogen starts burning once a flammable concentration is reached. However, to provide additional assurances that localized hydrogen accumulation will not occur, tests are being conducted by the Hanford Engineering Development Laboratory (HEDL) to verify the mixing characteristics of the air return fans and the steam-hydrogen jet.

2.9.2 Summary

Tests are being conducted at HEDL's Containment Systems Test Facility (CSTF). This facility has a height of 67 feet and a diameter of 25 feet. Volume of the facility is approximately 3×10^4 cubic feet. The CSTF has been modified to resemble a simplified ice condenser containment. A schematic of the modified CSTF is shown in Figures 2.9-1 and 2.9-2. Atmospheric temperature and hydrogen concentration are being measured as a function of time at various locations. Additional measurements include flow velocity and water vapor concentration.

The test program includes tests with and without the air return fans. In addition, the injection rate of the jet will be varied. Although a majority of the tests are being conducted with helium, tests will be conducted with hydrogen to assure applicability of the helium tests. | 2

All testing has been completed. Results appear to indicate that the lower compartment is well mixed; thus precluding the formation of pockets containing significantly higher concentrations of hydrogen. More specifically, the data appears to show that:

1) The air return fans minimize the peak concentration and the maximum concentration difference within the test compartment.

2) Test compartment mixing is not strongly dependent on the orientation of the source jet.

Final data reduction and analysis is anticipated to be complete by February 1, 1982. A preliminary project report is included in Appendix 2K.

Revision 2
Entire Page Revised

APPENDIX 2H

COMBUSTION CONTROL STUDIES

PROJECT REPORT

EFFECT OF IGNITOR LOCATION AND WATER
FOGS ON HYDROGEN COMBUSTION WITHIN AN ENCLOSED COMPARTMENT

PROJECT REPORT

December, 1981

Prepared by:

F. G. Hudson, Duke Power Company
K. K. Shiu, American Electric Power
R. C. Torok, Acurex Corporation
J. J. Wilder, Tennessee Valley Authority

Project Conducted by:

Acurex Corporation
485 Clyde Avenue
Mountain View, California

Project Sponsors:

TABLE OF CONTENTS

Section 1

Introduction

Approximately ten hours into the accident at Three Mile Island, a hydrogen burn occurred inside the containment. Although this burn posed no real threat to the TMI containment, it did create interest in hydrogen combustion and its effects on containment structures. The operating license applications for McGuire and Sequoyah Nuclear Stations contributed to the growth of this interest into a major safety concern, especially for ice condenser containments. The individual and joint activities of the three utilities owning ice condenser stations (American Electric Power, Duke Power Company, and the Tennessee Valley Authority) are well documented in various licensing submittals or licensing proceedings and will not be repeated here. However, when the three utilities decided to install a distributed ignition system as a hydrogen mitigation system, the question of ignitor location within a compartment arose. Additionally, concurrent with the design of a distributed ignition system, several independent organizations suggested coupling a water fog system with the distributed ignition system to act as a pressure suppressant during combustion. To investigate the effect of ignitor location on hydrogen combustion within a compartment, the three utilities, in conjunction with the Electric Power Research Institute, contracted with Acurex Corporation to conduct a series of tests. These tests were conducted at the SRI International Explosives Test Site near Livermore, California. Although analyses had shown a pressure suppressant was not necessary for ice condenser containments, the utilities believed that investigating the effect of water fogs on hydrogen combustion could be of some potential interest to the

industry. Therefore, an investigation of water fog effects on hydrogen combustion was added to the Acurex project. This report presents the results of that project.

Section 2

Test Facility

2.1 TEST VESSEL AND MECHANICAL SYSTEMS

The test vessel selected for this project has a volume of approximately 630 ft^3. Vessel dimensions are: internal diameter - 7 ft., overall height - 21 ft., and "barrel" height - 17 ft. Auxiliary mechanical systems provide the ability to: 1) inject hydrogen or a hydrogen/steam mixture into the lower portion of the test vessel, 2) supply a water spray or microfog from the upper portion of the test vessel, 3) obtain pre-test and post-test vessel atmosphere samples, and 4) provide a means of premixing the vessel atmosphere for quiescent tests. Additionally, the capability to ignite the vessel atmosphere from the top, middle or bottom of the vessel was provided. A schematic of the test vessel and its auxiliary mechanical systems is presented in Figure 2-1.

A propane-fueled boiler supplied steam for the facility. This steam served as a parameter for several tests, as well as to preheat the test vessel to the desired temperature. The steam flowrate was monitored with an annular flow sensor and a differential pressure gauge. When steam was not required as a test parameter, the boiler was isolated from the test vessel after preheating was completed. Bottled hydrogen served as the hydrogen source for the test vessel. The hydrogen flowrate was monitored with a rotameter and controlled with a control valve.

A three horsepower electric motor and gear pump supplied water to the test vessel spray nozzles. A bypass loop was included to control the flowrate. Utilizing a closed loop spray system, i.e., recirculating the spray water, avoided the potential problems associated with accumulating large volumes of water within the vessel. For the Phase 1 tests, a single Sprayco 1713 nozzle, 15 gpm flowrate, was mounted at the top of the test vessel. A manifold containing nine Sprayco 2163-7604 pinjet nozzles was mounted at the top of the test vessel for the Phase 2 tests. Depending on the pressure drop across the nozzles, the total spray flowrate for the Phase 2 tests varied from 1.1 to 1.4 gpm. The spray manifold was constructed so as to provide an even spray distribution throughout the test vessel.

An air-operated fan was mounted inside the test vessel to assure a well mixed vessel atmosphere prior to the quiescent tests. Use of an air-operated fan eliminated the potential of an electrical malfunction resulting in a spurious ignition. The fan's air exhaust was vented outside the test vessel to avoid diluting the vessel atmosphere.

Two 4 inch butterfly valves located at the top and near the bottom of the test vessel allowed the vessel to be purged following the completion of each test. A squirrel-cage blower attached to the lower butterfly valve provided the motive force for purging the vessel. The vessel contents were vented to the atmosphere through the upper butterfly valve. The vessel was not vented until post-test samples were obtained.

Vessel atmosphere sample taps were located near the top and near the bottom of the test vessel. A remotely operated solenoid valve isolated each of the two sample lines from the test vessel. When a solenoid valve was open, the vessel atmosphere sample was pumped through a cold trap to remove water. The sample then passed through a silica gel trap to remove any remaining moisture. The sample then flowed through a gas meter into a glass sample bottle. A sample was extracted from the sample bottle by a syringe and injected into a gas chromatograph. (A detailed discussion of the gas analysis methodology is presented in Appendix A).

Two ignitor assemblies supplied by Duke Power Company were mounted inside the test vessel. The ignitors were located on the vessel centerline at either the top, middle or near the bottom of the test vessel. Only two ignitor locations were occupied at one time. The top ignitor location was not used during the Phase 1 tests requiring sprays or during any of the Phase 2 tests since an ignitor assembly located at the top effectively created a significant spray/fog maldistribution within the test vessel.

2.2   INSTRUMENTATION

The test vessel was instrumented to provide the following information: vessel atmosphere temperature, vessel wall temperature, flame front propagation, and vessel pressure. Three mil Type K thermocouples were used to measure temperatures and detect flame front propagation. Strain gauge pressure transducers and piezoelectric pressure transducers were used to measure vessel pressures. A schematic of the test vessel instrumentation is presented in Figure 2-2.

As just mentioned, 3 mil thermocouples were used to measure temperatures and detect flame front propagation. Male Type K thermocouple jacks were used as attachment points for the 3 mil thermocouple junctions to increase the robustness of the thermocouple. The junctions were located between the jacks with the leads attached directly to the jacks. Vessel wall temperature thermocouples were welded directly to the vessel wall.

To determine the flame front propagation pattern within the vessel, a special electronic circuit was developed. This circuit used a high input impedance operational amplifier comparator to detect the temperature rise in the 3 mil Type K thermocouples located within the vessel. A schematic diagram of the flame front detector circuit is shown in Figure 2-3. Five circuits were used, each circuit monitoring seven thermocouples located in a vertical array within the vessel. The 5 x 7 grid was located vertically on a plane formed by the diameter and centerline of the test vessel as shown in Figure 2-2.

When one of the thermocouples in the grid was exposed to the flame front, the thermocouple output voltage would rise and trigger the comparator. This, in turn, placed a signal at one input point of the digital-to-analog converter. The output from the DAC was then recorded. Since the input signals from the thermocouples could be considered as binary bits, every voltage that was generated by the DAC corresponded to a discrete combination of hot thermocouples. Thus, by comparing the output voltage against time, the instant that the flame front arrived at each location could be determined, and a map derived showing flame front propagation.

Two types of pressure transducers were used. Bell and Howell CEC Model 1000 strain gauge pressure transducers were used for static and slow response conditions. These were powered by CEC 1-183 strain gauge signal conditioners located within a CEC 1-080 power supply chassis. To record high frequency transient pressure pulses, PCB Piezoelectronics Model 111A24 piezoelectric pressure transducers were used. These transducers were powered by a Model 484B10 power supply.

Two recording systems were used for data acquisition. A twenty eight channel FM tape recorder, EMI Model 7000C, was used to record all potentially fast response data. Frequency response of the unit was 10kHz or greater. An Autodata 9 datalogger recorded relatively slow response signals and served as a backup to the FM tape recorder.

FIGURE 2-1
TEST FACILITY MECHANICAL SCHEMATIC
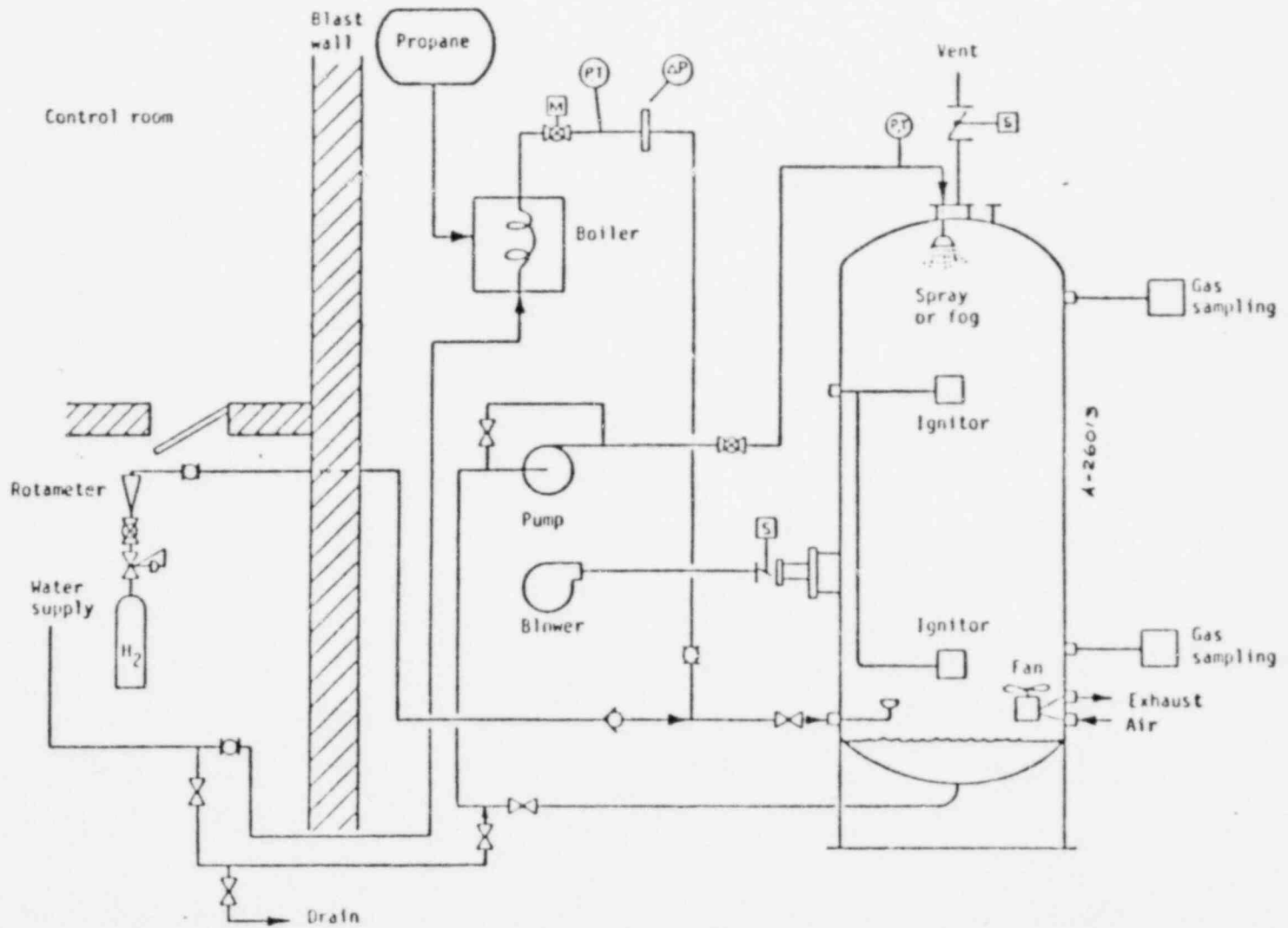
FIGURE 2-2
TEST FACILITY INSTRUMENTATION SCHEMATIC

F   Flame front gage
T   Thermocouple
WT   Wall thermocouple
SxD Strain gauge pressure transducer
PxD Piezoelectric pressure transducer
STG Strain gauge
SG   Silica gel water trap
DGM Dry gas meter
GB   Glass bottle
GC   Gas chromatograph

FIGURE 2-3
FLAME FRONT DETECTOR CIRCUIT

#7	#6	#5	#4	#3	#2	#1	V_{out}
0	0	0	0	0	0	1	0.078V
0	0	0	0	0	1	0	0.157V
0	0	0	0	1	0	0	0.314V
0	0	0	1	0	0	0	0.627V
0	0	1	0	0	0	0	1.255V
0	1	0	0	0	0	0	2.510V
1	0	0	0	0	0	0	5.020V
0	0	0	0	0	1	1	5.099V
			ETC				
1	1	1	1	1	1	1	10V

THERMOCOUPLE

+15V

30k
1k
LED
20

3290 #1
3290 #1
3290 #2
3290 #2
3290 #3
#3
3290 #4

Analog Devices AD558 DAC

Tape Deck
0-10V Output
+15V
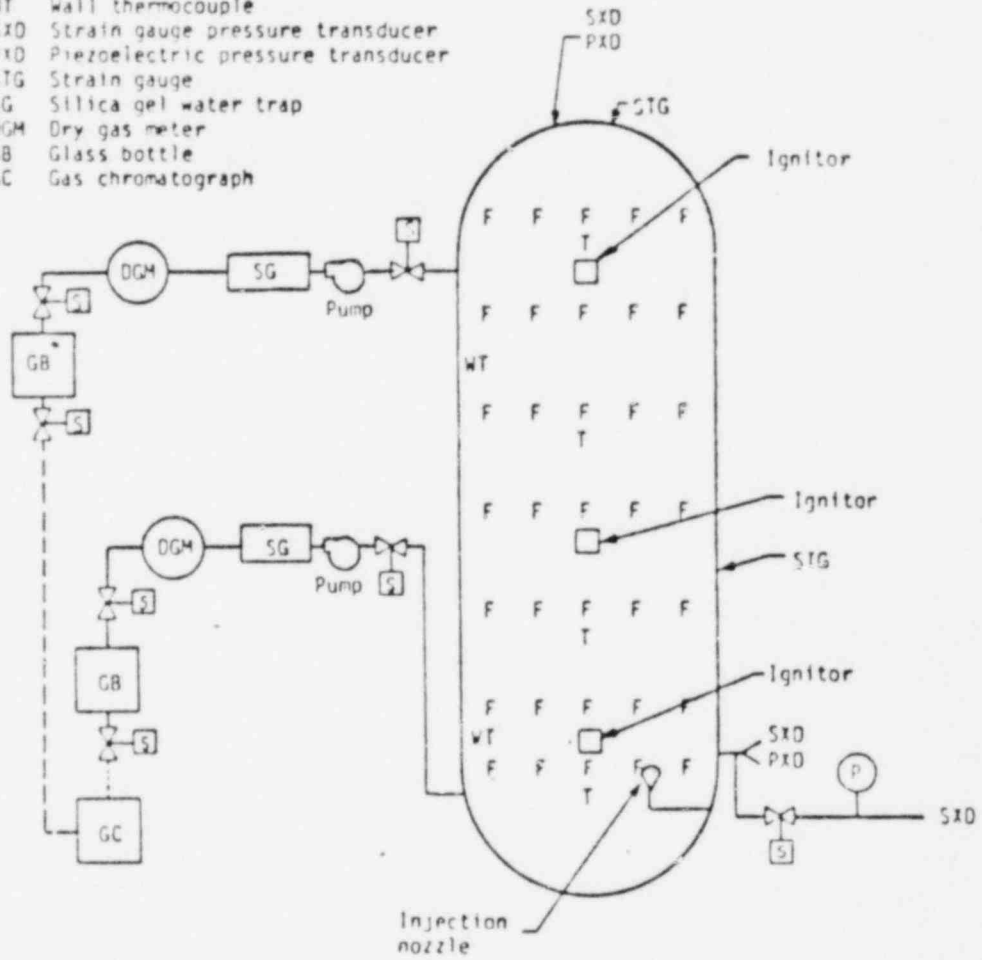
Section 3

Test Matrix and Procedures

3.1   TEST MATRIX

The test program was designed to investigate the effects of ignitor location and water fogs/sprays on hydrogen combustion. Test parameters were selected based on degraded core analyses conducted by American Electric Power, Duke Power Company, and TVA. Flowrates for steam and hydrogen were scaled by the ratio of test vessel volume to the combined lower compartment and deadended compartment volumes of an ice condenser containment. These scaled flowrates were derived from the average steam and maximum hydrogen release rates during the hydrogen generation portion of an $S_2 D$ accident sequence. Containment response analyses conducted by the aforementioned utilities indicated that 160°F was a maximum atmospheric temperature that would be encountered in the lower and deadended compartments at the onset of hydrogen generation. Hydrogen or hydrogen/steam mixtures were injected into the lower portion of the test vessel since many subcompartments within an ice condenser containment are accessed from the bottom.

Spray nozzle flowrates were determined by the desired mean droplet diameter. The Sprayco 1713 spray nozzle, a model used in containment spray systems, was operated at a ΔP of 40 psi. This provided a flowrate of 15 gpm and is the designed operating condition in a containment spray application. Vendor supplied information indicated that the number mean droplet diameter at this flowrate is 200μ. Based on studies conducted by Factory Mutual Research

Corporation, the Sprayco 2163-7604 nozzle was selected for use in the water fog tests. Measurements taken at Factory Mutual Research Corporation[1] indicated that when operated at ΔP's of 20 psi and 30 psi the resulting number mean droplet diameters were 11μ and 8μ, respectively. The total fog flowrates from the test vessel's nine nozzle manifold were 1.1 gpm and 1.4 gpm, respectively.

Tests outlined in Table 3-1 were intended to investigate the effect of ignitor location on combustion. Both hydrogen and hydrogen/steam mixtures were injected to account for the potential variation in the transient conditions within an ice condenser containment. Tests with sprays were included to account for the presence of subcompartment sprays in some containment designs. As mentioned earlier, the steam and hydrogen flowrates of 2.1 and 0.035 lbm/min were based on transient analyses. Tests 1.6 and 1.7 were conducted with the hydrogen flowrate arbitrarily increased by a factor of three. Test 1.11 was conducted to observe the effect of a lower preheat on combustion characteristics. The duration of tests was determined by the time required to obtain the same relative hydrogen mass injected in the test vessel as is calculated in the previously mentioned degraded core analyses. All tests were conducted with the test vessel atmosphere initially saturated.

[1]Zalosh, Robert G., "Water Fog Inerting of Hydrogen Air Mixtures," Factory Mutual Research Corporation, September, 1981.

The water fog test matrix is presented in Table 3-2. Quiescent tests were conducted as a basis of comparison to observed results of the dynamic tests. The basis for all remaining test parameters was discussed above.

3.2   TEST PROCEDURES

Two types of tests were conducted: quiescent and dynamic. A known amount of hydrogen was injected into the test vessel for the quiescent test prior to energizing the ignitor assembly. The dynamic tests consisted of injecting hydrogen or hydrogen/steam into the vessel with the ignitor assembly pre-energized. For all tests, the test vessel was pre-heated to the desired temperature and the instrumentation and data acquisition system was checked and calibrated. After the completion of each test, the test vessel fan was turned on and a post-test sample obtained. Subsequently, the test vessel was purged.

Test procedures varied slightly for the quiescent and dynamic tests. For the quiescent tests, the vessel fan was turned on after completing the pre-test activities mentioned above. A known amount of hydrogen was injected into the vessel and a pre-test sample was obtained. The vessel fan was then turned off and, if required, vessel sprays actuated. At this point, the data acquisition system and the ignitor assembly were energized. For the dynamic tests, the ignitor was energized after completion of pre-test activities. If necessary, vessel sprays were then actuated. The data acquisition system was energized prior to the initiation of hydrogen injection.

TABLE 3-1

Ignitor Location Test Matrix*

Test	Ignitor Location	Hydrogen Flow (lbm/min) 0.035	0.105	Steam Flow (lbm/min) 2.1	Spray Flow 15 gpm
1.1	Top	X		X	
1.2	Top	X			
1.3	Bottom	X		X	X
1.4	Bottom	X		X	
1.5	Bottom	X			
1.6	Bottom		X	X	
1.7	Bottom		X		
1.8	Center	X		X	X
1.9	Center	X		X	
1.10	Center	X			
1.11	Bottom	X		X	X

*Test vessel was preheated to 160°F for all tests except 1.11. Test 1.11 was performed with 120°F preheat.

TABLE 3-2

Water Fog Test Matrix*

Test #	Hydrogen v/o	Hydrogen Flow (lbm/min) 0.035	0.105	Steam Flow (lbm/min) 2.1	Fog Nozzle Pressure (psi) 20	30
2.1	5.0					
2.2	7.5					
2.3	10.7					
2.4	10.7					X
2.5	10.7				X	
2.6	7.5					X
2.7	7.5				X	
2.8		X			X	
2.9		X		X	X	
2.10**		X				X
2.11			X			X
2.12		X				X
2.13		X		X		X

*Test vessel was preheated to 160°F for all tests. Ignitor located near the bottom.
**Vessel mixing fan was operating.

Section 4

Test Results

4.1   DEFLAGRATION CHARACTERISTICS

Based primarily on pressure and flame front detector data, two distinct types
of deflagrations occurred. These deflagrations were termed "discrete" and
"intermittent". A "discrete" deflagration was characterized by a rapid pressure
and temperature rise. The duration of the burn appeared to be dependent on the
fraction of the vessel volume that could support a propagating hydrogen flame.
By comparison, an "intermittent" deflagration appeared as repeated burns
accompanied by much slower and lower pressure/temperature rises. Observed
deflagrations were further categorized as "major" or "minor". A "major"
deflagration, whether discrete or intermittent, occurred throughout the test
vessel. A "minor" deflagration, on the other hand, was localized in nature.

Pressure and temperature histories typical of a major-discrete deflagration are
presented in Figure 4-14. "CENTERLINE T1" and "CENTERLINE T4" are centerline
thermocouples located near the top and bottom of the test vessel. "VESSEL
PRESSURE 2" is a strain gauge pressure transducer located in the lower portion
of the test vessel. As seen in the figure, the test mixture ignited approxi-
mately twenty seconds into the test. The periodic disturbances in the two
temperature traces were caused by the datalogger scanning these channels. The
flame front detector output for the same test is presented in Figure 4-15. The
five data channels correspond to the five vertical columns of transducers shown

in the inset figure; each channel receiving the output of seven flame detectors. The size of each step is determined by the combination of detectors that triggered. A fullscale reading indicates that all seven detectors within a channel have triggered. Of the channel outputs presented in Figure 4-15, only channel 5 was not reading fullscale. The flame front detector data indicated that approximately 95% of the flame front detectors triggered. This, therefore, was classified a "major" and "discrete" deflagration.

Figures 4-5 and 4-6 present temperature, pressure, and flame front detector data typical of major intermittent deflagrations. The flame front detector data in Figure 4-6 indicate that all channels were triggered, signifying that a major deflagration occurred. Temperature data in Figure 4-5 shows a sharp, but not extremely large, temperature increase that remained relatively constant for several minutes before starting to slowly decay. This indicates that intermittent deflagrations were occurring. Note that near the end of this particular test, a major discrete burn occurred.

Minor intermittent burning is demonstrated by the temperature, pressure and flame front detector data presented in Figures 4-21 and 4-22. Flame front detector data, Figure 4-22, indicate that few flame detectors were triggered during this test. This characterizes a "minor" deflagration. The temperature and pressure data in Figure 4-21 show the small and gradual increases characteristic of intermittent burning. Figure 4-3 also provides temperature and pressure histories indicating minor intermittent deflagrations. Note that near the end of this test, several minor discrete deflagrations occurred.

4.2   INSTRUMENTATION UNCERTAINTY

Test data was primarily test vessel pressure/temperature histories and flame
front detector output. Additionally, vessel atmosphere constituents were deter-
mined via a gas chromatograph. To properly evaluate the test data, it was
necessary to know the errors associated with the instrumentation used.

Sources of error in the thermocouple data were: thermocouple material and
junction uncertainty, thermocouple amplifier error, test facility offset errors
due to electrical ground loops, tape recorder input and playback error, analog
to digital conversion errors and plotter inaccuracy. Standard Type K thermo-
couple error estimates were ±2.2°C from 0 to 278°C and ±3/4% above 278°C, ANSI
Standard C9C.1. The low temperature range error corresponded to approximately
±3% when peak temperatures were around 100°C. The estimated gain error for each
of the three signal amplifiers was ±1%. Errors associated with the analog to
digital conversion and plotter inaccuracies were considered negligible.
Therefore, using the root-mean-square method, the total random error for low
temperature cases was approximately,

$$[3^2 + 1^2 + 1^2 + 1^2]^{\frac{1}{2}} = 3.5\%$$

and for high temperature cases,

$$[(3/4)^2 + 1^2 + 1^2 + 1^2]^{\frac{1}{2}} = 1.9\%.$$

Pressure data were obtained from two strain gauge pressure transducers mounted at the top and near the bottom of the vessel. Although data from the piezoelectric pressure transducers were recorded, the observed pressure transients did not warrant use of the piezoelectric instead of the strain gauge pressure transducers. Sources of error in the pressure data were: transducer error, the transducer amplifier error, and the same tape recorder amplifier errors encountered in the thermocouple data. The manufacturer's estimated error for the transducer was ±.25% of full range. This corresponded to ±0.5% of the signal resulting from a large ΔP, i.e., a major deflagration, and ±2.5% for a small ΔP. Using the root-mean-square method, the total random error for high ΔP cases was approximately,

$$[(\tfrac{1}{2})^2 + 1^2 + 1^2 + 1^2]^{\frac{1}{2}} = 1.8\%$$

and for low ΔP cases,

$$[2.5^2 + 1^2 + 1^2 + 1^2]^{\frac{1}{2}} = 3.0\%.$$

Calibration and test gas chromatograms were analyzed using the peak height method. Water vapor corrections were made to convert dry gas sample analyses to actual test vessel conditions.

Uncertainty estimates for the resulting gas constituent volume percentages were based on the repeatability of sample analyses. Normalized mean peak heights were calculated from the analyses of each test run. The ratio of the largest deviation from the mean to the mean for each test run was used as an estimate

of the gas analysis uncertainty. The mean estimated uncertainties were
approximately ±10% for the hydrogen analysis and ±20% for the oxygen analysis.
Problems encountered with the gas chromatograph's thermal conductivity detector
were suspected as being a primary cause of scatter in the data. Discussions
with the manufacturer indicated that filament oxidation was hampering performance.

4.3   IGNITOR LOCATION TEST SERIES

Tests were conducted by varying the ignitor location in three test environments:
hydrogen injection, hydrogen/steam injection, and hydrogen/steam injection with
sprays. Two additional tests were conducted with the hydrogen flowrate arbitrarily
increased by a factor of three. The final test of this series was conducted
with a reduced vessel pre-heat. A summary of the results obtained from this
test series is presented in Tables 4-1 and 4-2.

Figures 4-2, 4-4, and 4-10 provide the pressure histories from ignitor location
tests without steam or spray (tests 1.2, 1.5, and 1.10). At lean hydrogen con-
centrations, flame propagation is only upwards. With this in mind, it was anti-
cipated that while localized burning was occurring in the vicinity of the
top ignitor, the hydrogen concentration would increase throughout the remainder
of the vessel. When the flammability limit for downward propagation was reached,
a major discrete deflagration would occur. This appeared to be the sequence of
events in test 1.2 with minor intermittent deflagrations beginning at 300 seconds
followed by a major discrete deflagration at 580 seconds. The maximum pressure
rise was expected to be smaller for the center ignitor location (test 1.10)
than the top location because of the increased vessel volume that would be

exposed to upward propagating flames at lean concentrations. Table 4-1 shows
that the pressure rise was lower by approximately a factor of three. Minor
intermittent deflagrations began around 220 seconds and continued throughout
the test. The lowest ignitor location was expected to produce an even milder
pressure rise since a substantial portion of the vessel would be exposed to
upward propagating flames. However, as Figure 4-4 shows, that was not the
case. Apparently, the relative locations of the injection port and the lowest
ignitor location precluded the ignitor from igniting hydrogen early in the test.
The major discrete deflagration that occurred at 450 seconds indicated that the
injection flow apparently bypassed the ignitor until most of the vessel contained
a flammable mixture. The resulting deflagration produced a higher pressure rise
than that attained by the top ignitor for two apparent reasons: 1) The top
ignition was preceeded by localized deflagrations; thus reducing the mass of
hydrogen within the vessel; 2) Flames propagate slower downward than upward;
thus allowing more time for heat transfer.

Figures 4-1, 4-3, and 4-9 show that results from the tests with hydrogen/steam
injection (tests 1.1, 1.4, 1.9) were similar to those obtained from the hydrogen
injection tests. It was anticipated that the hydrogen/steam injection tests
would yield milder pressure increases. This was due to steam impeding the
combustion process as well as acting as a diluent; thus reducing the flame
propagation velocity. This would result in increased heat transfer and decreased
temperatures/pressures. Additionally, adding steam increased the injection
velocity from approximately 0.7 ft./sec. to 5.7 ft./sec. This was believed to
increase mixing within the vessel and thus allow deflagrations to occur at leaner

hydrogen concentrations. Table 4-1 indicates that the peak pressures at the three ignitor locations were reduced with steam added to the injection flow. The most dramatic change was with the bottom ignitor location. Apparently, the increased mixing provided by the steam flow allowed the lowest ignitor to function as discussed previously. The top ignitor provided the largest pressure rise, with the center and bottom ignitors being approximately a factor of three less.

The addition of a water spray was expected to create some amount of turbulence within the vessel that would enhance mixing and allow combustion to occur at leaner hydrogen concentrations. It was also anticipated that a water spray would act as a dispersed heat sink; thus further reducing temperatures and pressures. Table 4-1 shows that the addition of water spray, tests 1.3 and 1.8, did reduce the maximum pressure. The bottom ignitor yielded only a very slight pressure rise with no corresponding flame front detector activity. However, post-test atmosphere analysis indicated that combustion had occurred. These deflagrations must have been very localized near the ignitor and apparently relied upon spray induced turbulence for a continual supply of lean hydrogen mixtures. Figure 4-8 shows that the center ignitor provided a series of minor discrete burns. The pressure rise was slightly higher than obtained from the bottom ignitor. Test vessel design did not allow a spray test to be conducted with the upper ignitor location.

Two tests were conducted with the hydrogen flowrate arbitrarily increased by a factor of three. One test was conducted with hydrogen injection, test 1.7, and the second with hydrogen/steam injection, test 1.6. The bottom ignitor was used

for both tests. Comparing tests 1.7 with 1.5 and 1.6 with 1.4 shows that the transients were similar to their low flow counterparts, with the exception of ignition occurring earlier in the transient. In test 1.7, ignition occurred slightly earlier than the 150 second ignition expected from a higher flow rate (see Figure 4.7). It is possible that the increased injection velocity had a slight effect on mixing within the vessel. This would allow an ignitable mixture to reach the ignitor earlier. This would also explain the slightly lower pressure rise from test 1.7 since less hydrogen would be present within the vessel at ignition. Note that the high flowrate pressure rise was 85% of the low flowrate pressure rise and that the high flowrate ignition time was 85% of the anticipated 150 second ignition time. Adding steam to the high hydrogen flowrate, test 1.6, yielded deflagrations similar to the low flowrate counterpart, test 1.4, but a pressure rise essentially identical to that obtained from test 1.7. Figure 4-5 shows that ignition occurred at approximately 100 seconds, one third of the 300 second ignition time for test 1.4. The ensuing intermittent deflagrations were more severe in test 1.6 because the higher hydrogen flowrate apparently resulted in a higher energy release rate. Why these intermittent deflagrations were not followed by repeated discrete deflagrations as seen in test 1.4 is uncertain. One possible explanation is that with vessel atmosphere temperatures in excess of 400°F for over one third the duration of test 1.6, a fraction of the water collected at the tank bottom from vessel pre-heating was vaporized during the intermittent burning. This could have caused the deflagrations to be very localized, similar to those obtained in test 1.3. Thus, hydrogen could have built up in the vessel while the steam was slowly condensing until an ignitable mixture was once again obtained. The result would be a lull in flame front detector activity followed by a major discrete deflagration.

Figures 4-5 and 4-6 show such characteristics. Some credence is lent to this possibility by noting that the post-test water concentration from test 1.6 was 50% larger than that obtained from test 1.4.

One test was conducted, 1.11, with the vessel pre-heat reduced to 120°F from 160°F. The results obtained were very similar to those obtained from 1.3, an identical test with a 160°F vessel pre-heat. A very slight pressure rise occurred with no corresponding flame front detector activity observed. This indicated that the burn, as in test 1.3, was very localized.

4.4   WATER FOG TEST SERIES

Tests were conducted to investigate the effects of a water fog on hydrogen combustion. The fog nozzle, Sprayco Model 2163-7604, created different fog characteristics depending on the pressure drop across the nozzle. Tests were conducted with two different fogs. Based on data obtained from Factory Mutual Research Corporation, a 20 psi ΔP yielded a fog with a number mean droplet diameter of 11u, while a 30 psi ΔP yielded a number mean droplet diameter of 8μ. Two types of tests were conducted: quiescent and dynamic. The dynamic tests were conducted with and without steam. All tests utilized the bottom ignitor. A summary of the results obtained from this series of test is presented in Tables 4-3 and 4-4.

4.4.1   QUIESCENT TEST SERIES

To provide a baseline of information for evaluating the dynamic fog tests, a
series of quiescent tests were conducted.   Nominal hydrogen concentrations of
5, 7.5, and 10% were selected.   Table 4-4 indicates that the completeness of
combustion for those tests without fogs (tests 2.1, 2.2, and 2.3) was approximately
30%, 90%, and 99%, respectively.   This data agrees reasonably well with published
data.   The temperature and pressure histories of these three tests are presented
in Figures 4-11, 4-12, and 4-13.   Further tests with 5% hydrogen were not con-
ducted.

Repeating these tests with fogs present, a significant decrease in pressure rise
was anticipated.   Due to the large surface area present within a fog, the fog
was expected to act as a dispersed heat sink; resulting in reduced temperatures
and pressures.   However, as Table 4-3 indicates for the 7.5% hydrogen tests, 2.6
and 2.7, the observed pressure rises were slightly higher.   Table 4-4 shows
that the completeness of combustion increased from approximately 90 to greater
than 99%.   This indicated that these particular fogs acted very much like sprays
for lean hydrogen concentrations.   The turbulence created by the fog flow
apparently enhanced the completeness of combustion; thus increasing the pressure
rise.   The heat sink effect of the fogs was evident from the slightly lower
temperatures (compare Figure 4-12 with Figures 4-17 and 4-18).   The fogs had no
apparent effect on the peak pressure rise in the 10% tests, 2.4 and 2.5.

4.4.2   DYNAMIC TEST SERIES

Hydrogen injection tests 2.8 and 2.12 were identical to test 1.5 except that fogs were included. Results from 2.8 and 2.12 indicated only minor intermittent deflagrations (see Figure 4-23). The observed pressure rise was an order of magnitude lower than that observed in test 1.5. It would be reasonable to assume that a great deal of the pressure reduction was due to fog flow induced mixing, which allowed a flammable mixture to reach the ignitor earlier. Note that the effect of adding steam to test 1.5 (test 1.4) was minor intermittent burning early in the transient with a pressure rise of 2.3 psi; the same effect observed in tests 2.8 and 2.12 (see Figure 4-3).

Figure 4-19 shows a pressure history typical of that obtained from hydrogen/steam injection tests with fog present, tests 2.9 and 2.13. The observed pressure rises were similar to that obtained in test 1.4, hydrogen/steam injection with no spray. In both cases, with and without fog present, ignition occurred at approximately 300 seconds. However, in test 1.4 the result was minor intermittent deflagrations eventually becoming minor discrete deflagrations. Tests 2.9 and 2.13 provided minor discrete burns immediately upon ignition. As a result, it appears that more hydrogen was consumed in the fog tests than in the non-fog tests. This would also appear to indicate that a major contribution from the generation of fog in this test series was to provide uniform mixing within the vessel.

One test was conducted with the hydrogen flowrate arbitrarily increased by a factor of three in the presence of a fog, test 2.11. Figures 4-21 and 4-22 show

the pressure history and flame front detector activity obtained from this test. This test provided an indication of the heat sink effect of a fog as well as its effect as a source of turbulence. Note on Figure 4-21 that ignition occurred approximately 20 seconds into the test, while in test 1.7, an identical test without fog, Figure 4-7 shows that ignition did not occur until 130 seconds into the test. This difference in ignition time could be accounted for by the mixing created by the fog. The heat sink effect was apparently demonstrated since the peak temperature of test 2.11 remained around 200°F, while the peak temperature in test 1.7 hovered around 400°F. In test 2.11, fog produced turbulence apparently prevented a major discrete burn by inducing intermittent deflagrations early, thus precluding the relatively high hydrogen concentrations needed for a major discrete deflagration. Additionally, the fog acted as a heat sink during the resultant intermittent deflagrations; thus minimizing pressure and temperature increases. Comparing test 2.11 with test 2.12, an identical test with the lower hydrogen flowrate, the deflagration character-istics were similar with the high flowrate test having an earlier ignition.

Finally, data on the effect of fan induced turbulence was obtained when the mixing fan was accidently actuated prior to test 2.10. The result was that ignition occurred earlier (see Figure 4-20) than in a similar test without the fan operating (see Figure 4-23). Other than the ignition time, the results of both tests were relatively similar; minor intermittent deflagrations with very slight pressure rises.

TABLE 4-1

Summary of Test Results: Ignitor Location Test Series

Test #	Test Characteristics	Ignitor Location	Max. ΔP (psi)	Deflagration Characteristics
1.1	Low H_2, steam	Top	13	Minor, major intermittent
1.2	Low H_2	Top	20	Minor intermittent, major discrete
1.3	Low H_2, steam, spray	Bottom	1	Minor intermittent
1.4	Low H_2, steam	Bottom	4.5	Minor intermittent, minor discrete
1.5	Low H_2	Bottom	28	Major discrete, minor intermittent
1.6	High H_2, steam	Bottom	24	Major intermittent, major discrete
1.7	High H_2	Bottom	23.5	Major discrete, minor intermittent
1.8	Low H_2, steam, spray	Center	2.7	Minor discrete
1.9	Low H_2, steam	Center	4	Minor intermittent
1.10	Low H_2	Center	6	Minor intermittent
1.11	Same as 1.3, lower preheat	Bottom	1	Minor intermittent

TABLE 4-2

Test Vessel Atmosphere Constituents: Ignitor Location Test Series

Test #	Post-Test		
	$H_2(v/o)$	$H_2O(v/o)$	$O_2(v/o)$
1.1	11.0	17.6	8.9
1.2	2.6	23.8	15.1
1.3	6.5	19.8	6.1
1.4	7.9	21.0	5.7
1.5	2.1	38.2	12.2
1.6	10.9	32.1	6.5
1.7	12.7	37.6	1.7
1.8	7.9	30.1	7.2
1.9	3.6	46.1	5.2
1.10	0.4	36.3	5.7
1.11	3.5	27.8	2.6

TABLE 4-3

Summary of Test Results: Water Fog Test Series

Test #	Test Characteristics	Max. ΔP (psi)	Deflagration Characteristics
2.1	Quiescent, 5 v/o H_2	8	Minor discrete
2.2	Quiescent, 7.5 v/o H_2	36	Major discrete
2.3	Quiescent, 10.7 v/o H_2	48	Major discrete
2.4	Quiescent, 10.7 v/o H_2, fog 30	47	Major discrete
2.5	Quiescent, 10.7 v/o H_2, fog 20	50	Major discrete
2.6	Quiescent, 7.5 v/o H_2, fog 20	40	Major discrete
2.7	Quiescent, 7.5 v/o H_2, fog 20	39	Major discrete
2.8	Dynamic, low H_2, fog 20	2	Minor intermittent
2.9	Dynamic, low H_2, fog 20, steam	5	Minor discrete
2.10	Dynamic, low H_2, fog 30, fan	1	Minor intermittent
2.11	Dynamic, high H_2, fog 30	2.9	Minor intermittent
2.12	Dynamic, low H_2, fog 30	1	Minor intermittent
2.13	Dynamic, low H_2, steam, fog 30	1.6	Minor discrete

TABLE 4-4

Test Vessel Atmosphere Constituents: Water Fog Test Series

Test #	Pre-Test			Post Test	
	$H_2(v/o)$	$H_2O\ (v/o)$	$H_2(v/o)$	$H_2O(v/o)$	$O_2(v/o)$
2.1	4.7	25.6	3.4	33.2	11.5
2.2	7.8	26.1	0.9	43.2	10.0
2.3	10.2	24.9	<0.1	40.4	10.9
2.4	9.7	23.8	<0.1	44.9	8.7
2.5	10.2	25.4	<0.1	40.4	9.2
2.6	7.2	32.9	<0.1	47.6	8.4
2.7	7.6	29.4	<0.1	41.6	11.4
2.8			3.3	30.1	6.8
2.9			6.2	45.5	5.1
2.10			2.8	49.2	2.7
2.11			13.5	35.1	<0.1
2.12			<0.1	37.0	9.2
2.13			3.7	45.4	3.7

FIGURE 4-1
TEST 1.1

VESSEL PRESSURE 1

TEMPERATURE (F)

PRESSURE (PSIG)

CENTERLINE T4

VESSEL PRESSURE 1

TEMPERATURE (C)

PRESSURE (KPA)
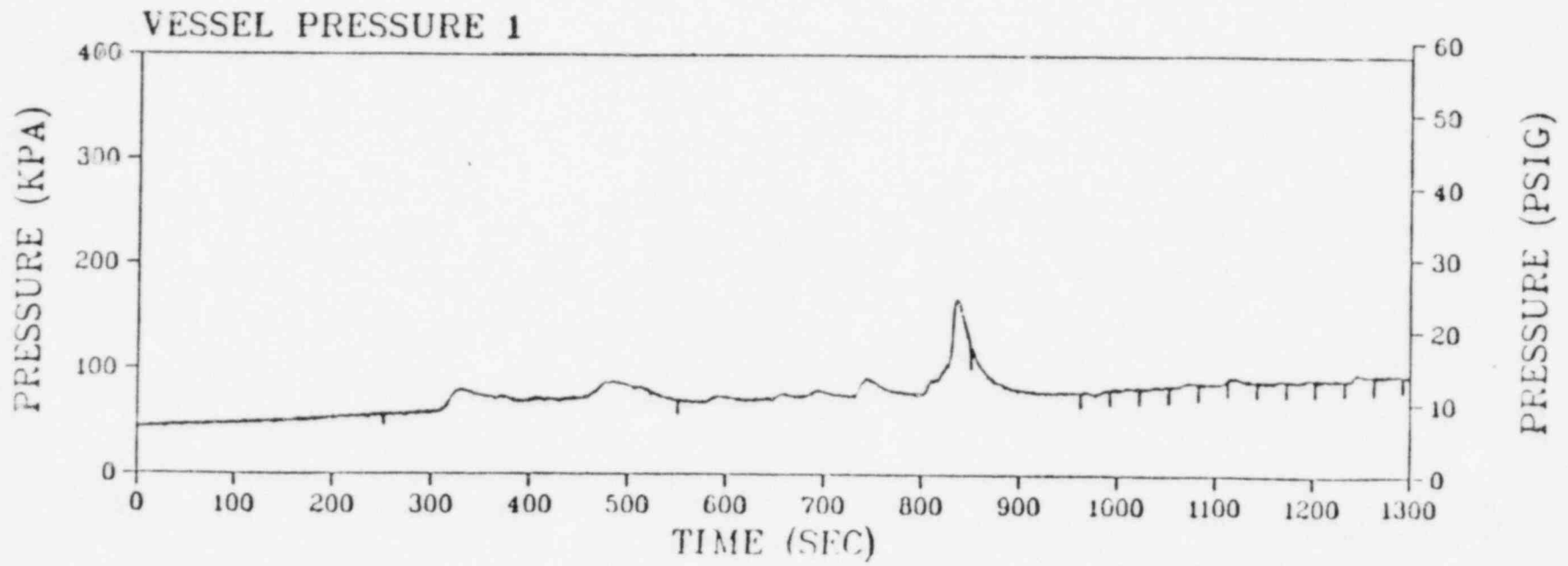
FIGURE 4-2
TEST 1.2

FIGURE 4-3
TEST 1.4

CENTERLINE T2

VESSEL PRESSURE 1
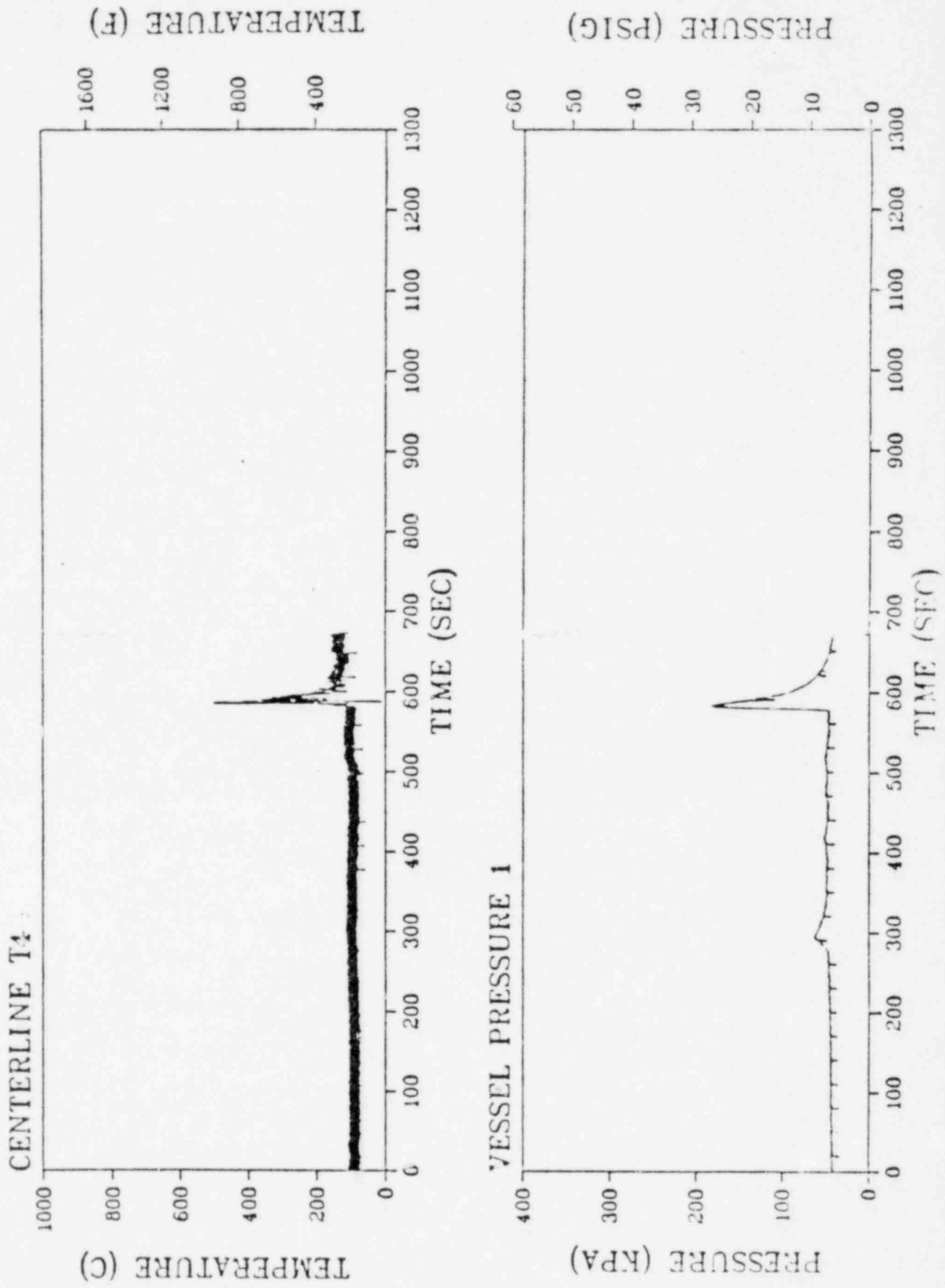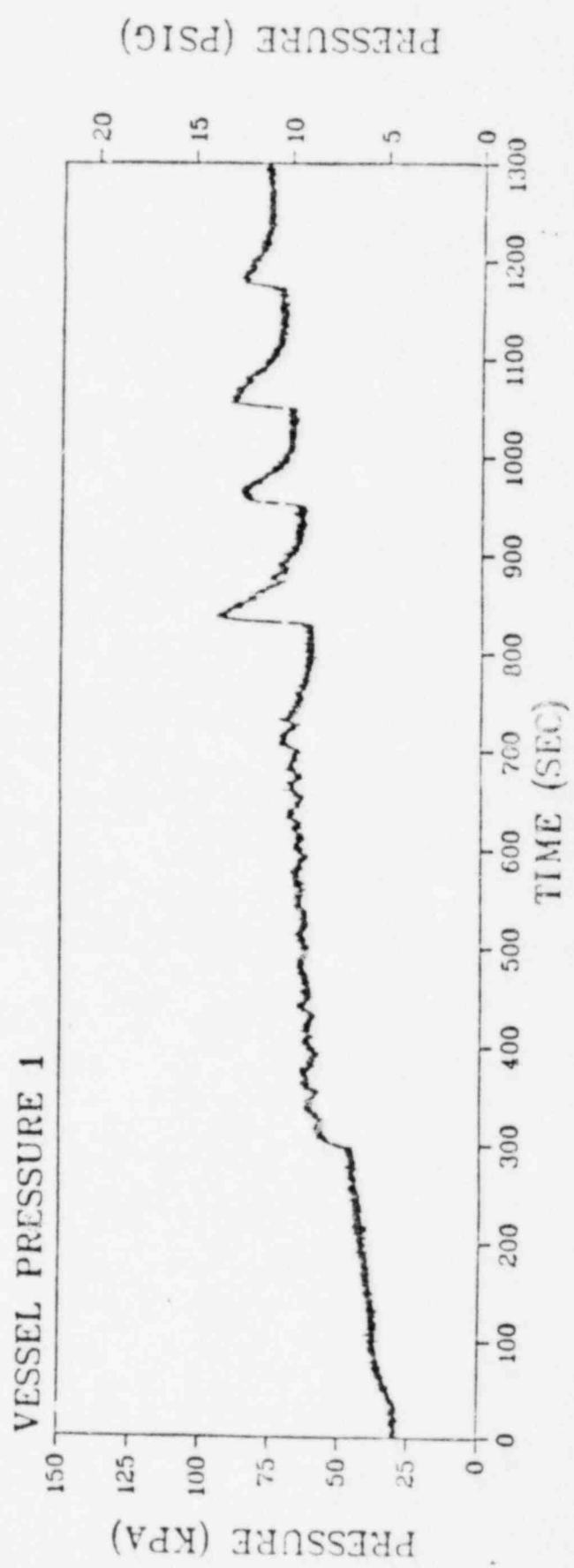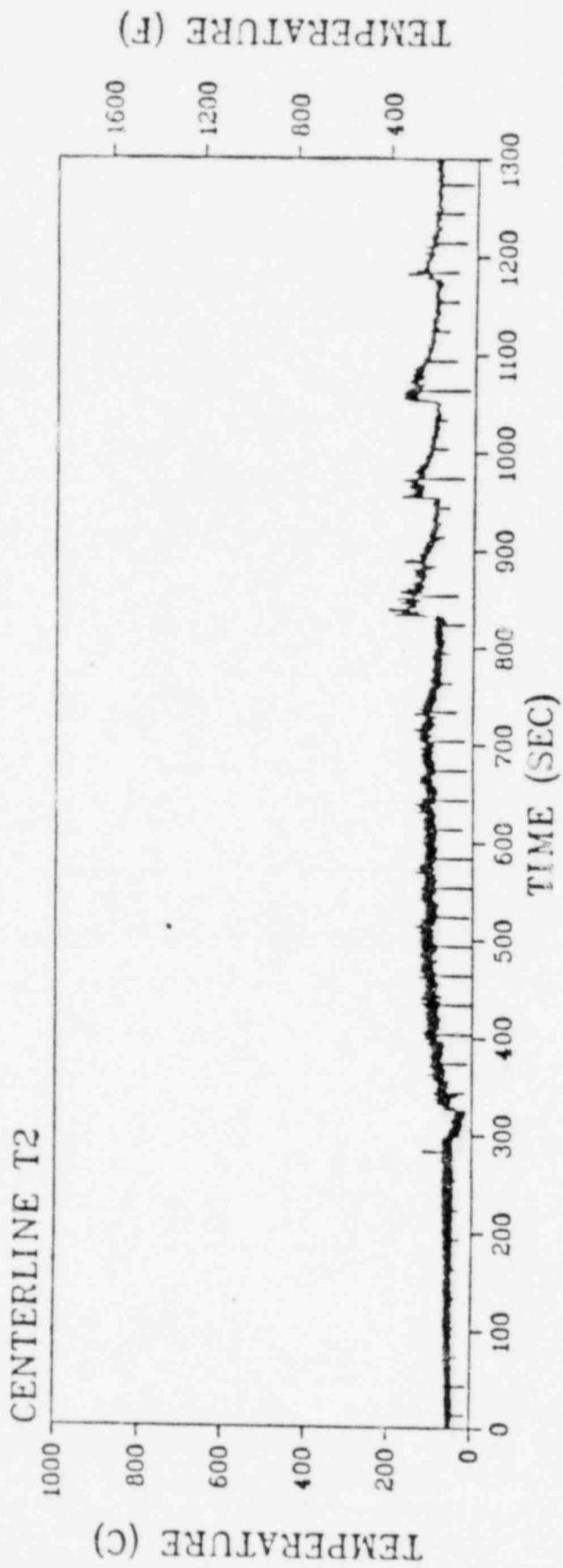
FIGURE 4-4
TEST 1.5

FIGURE 4-5
TEST 1.6

CENTERLINE T2

VESSEL PRESSURE 1
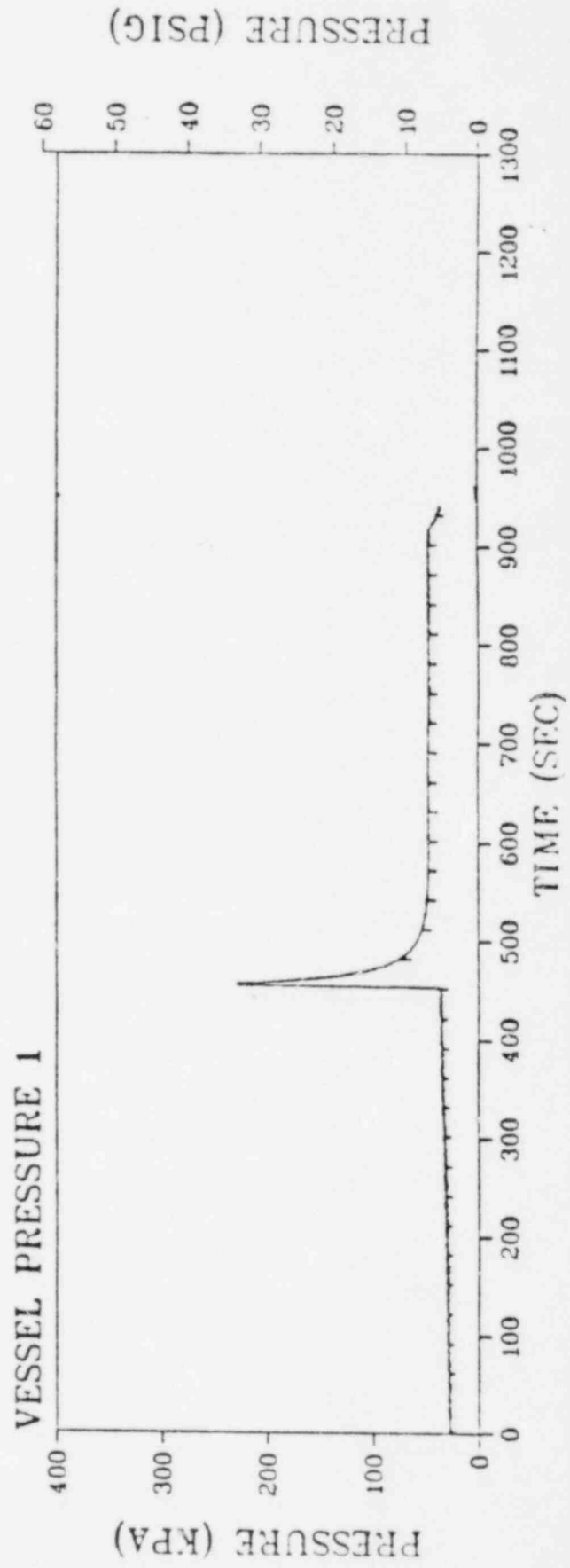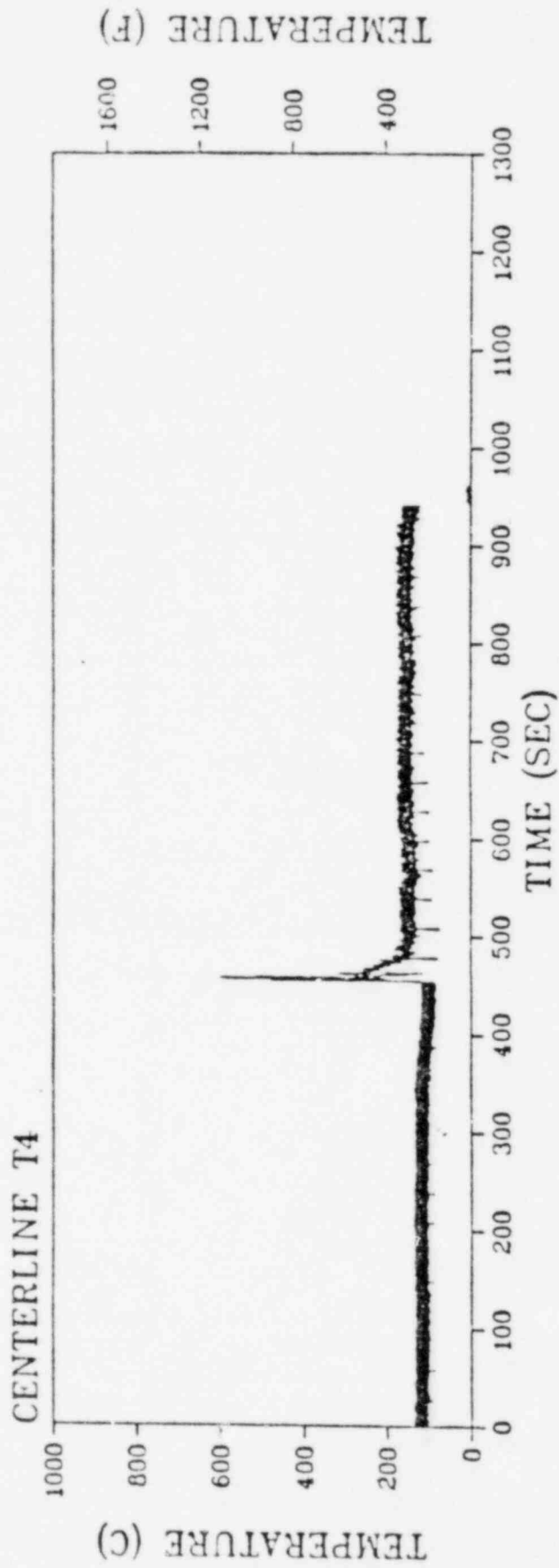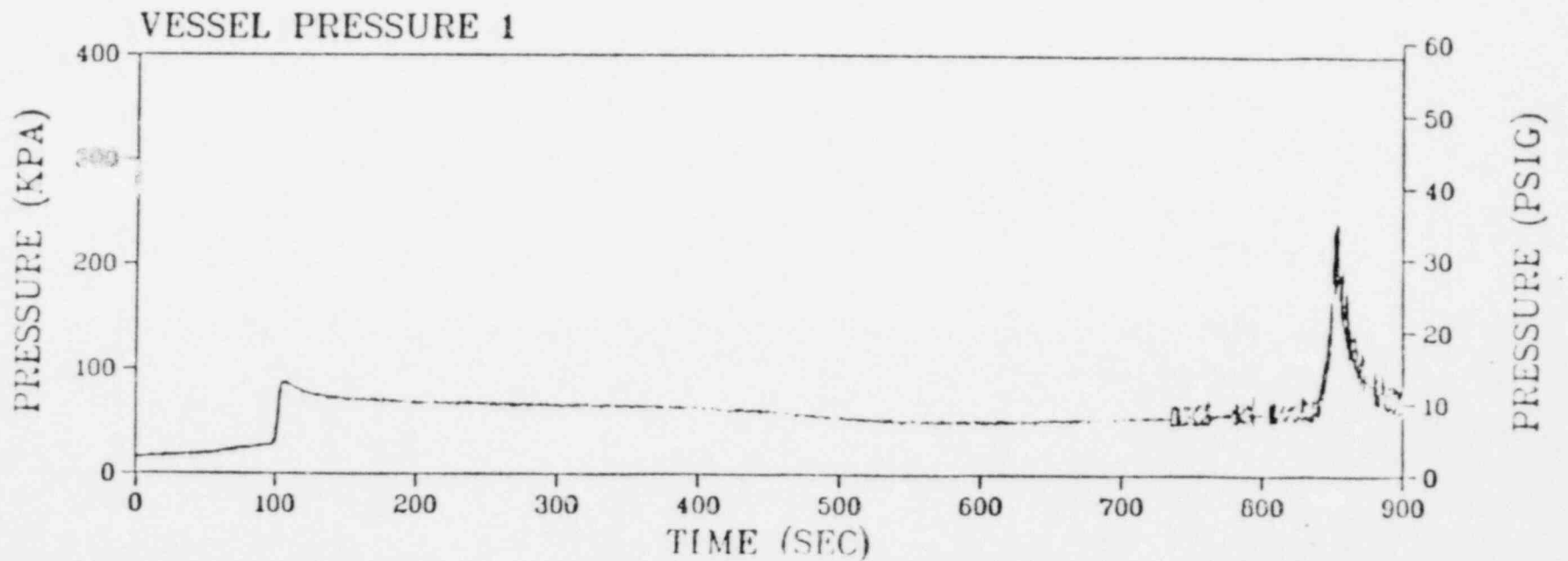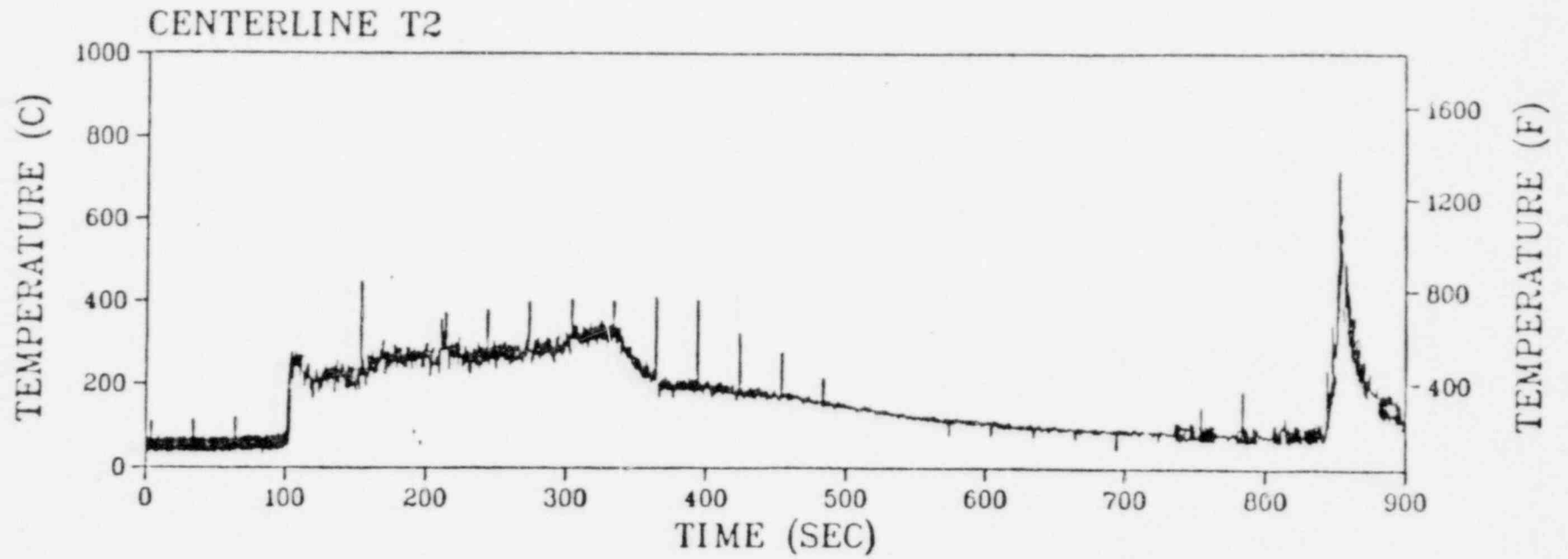
FIGURE 4-6
FLAME FRONT ACTIVITY
TEST 1.6
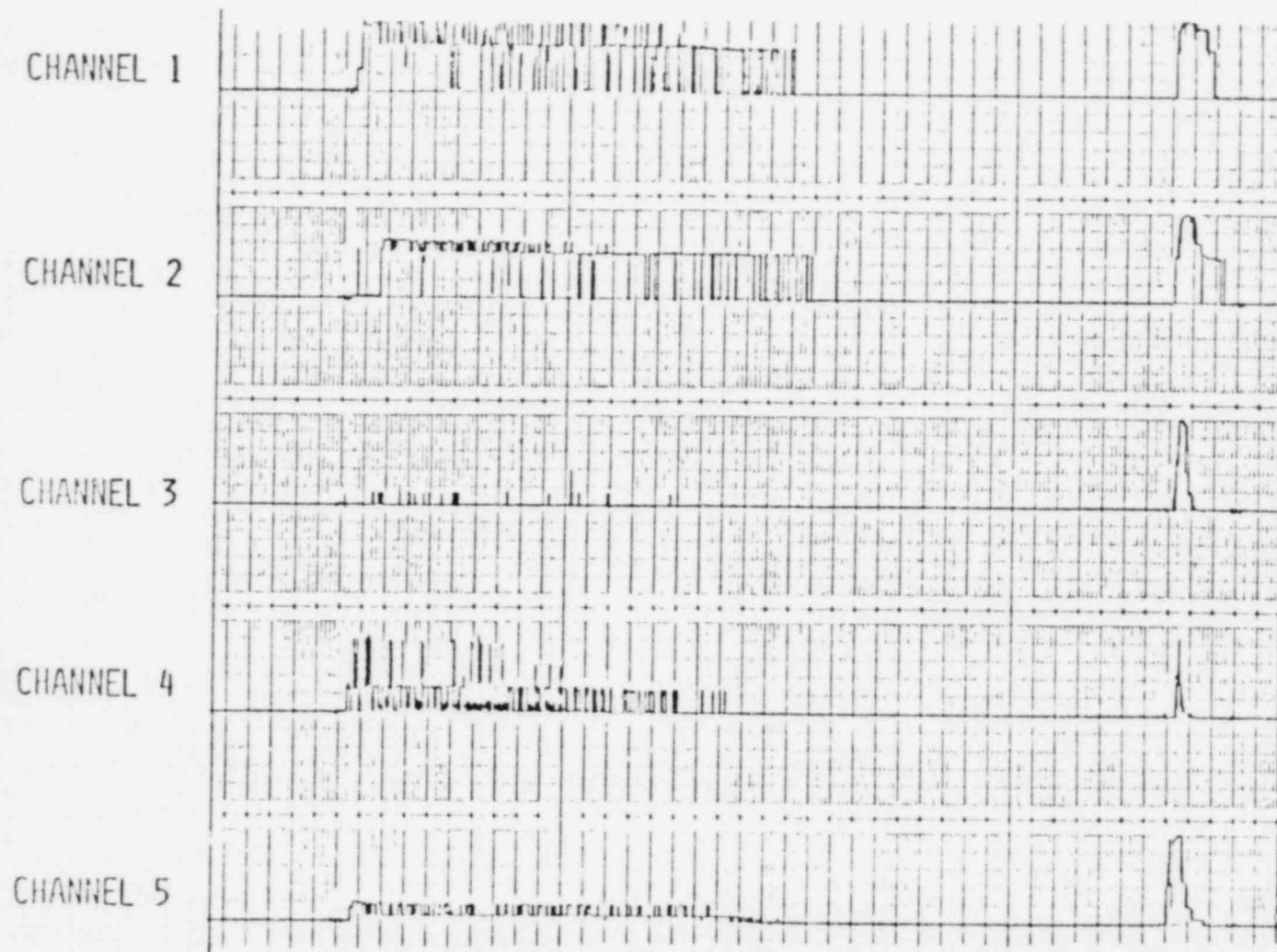
FIGURE 4-7
TEST 1.7

CENTERLINE T2

VESSEL PRESSURE 1

FIGURE 4-8
TEST 1.8

VESSEL PRESSURE 2

PRESSURE (PSIG)

PRESSURE (KPA)

TIME (SEC)

FIGURE 4-9
TEST 1.9

VESSEL PRESSURE 1

FIGURE 4-10
TEST 1.10

VESSEL PRESSURE 1

FIGURE 4-11
TEST 2.1

CENTERLINE T4
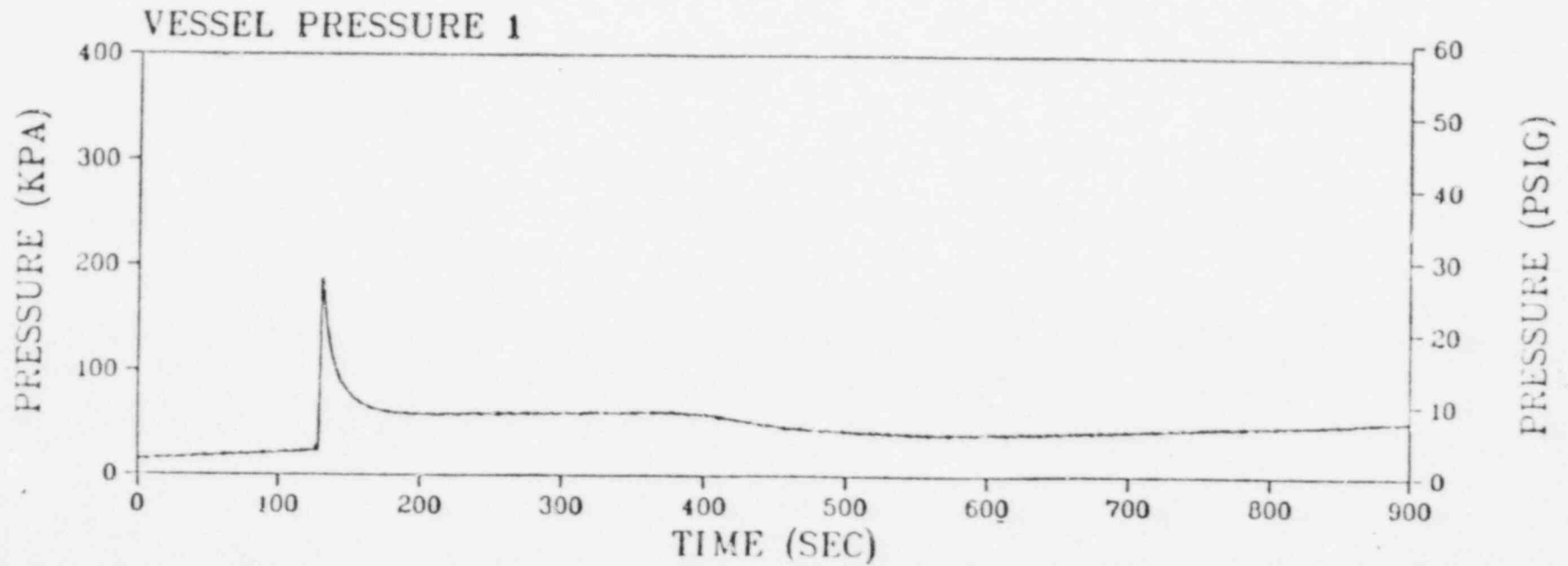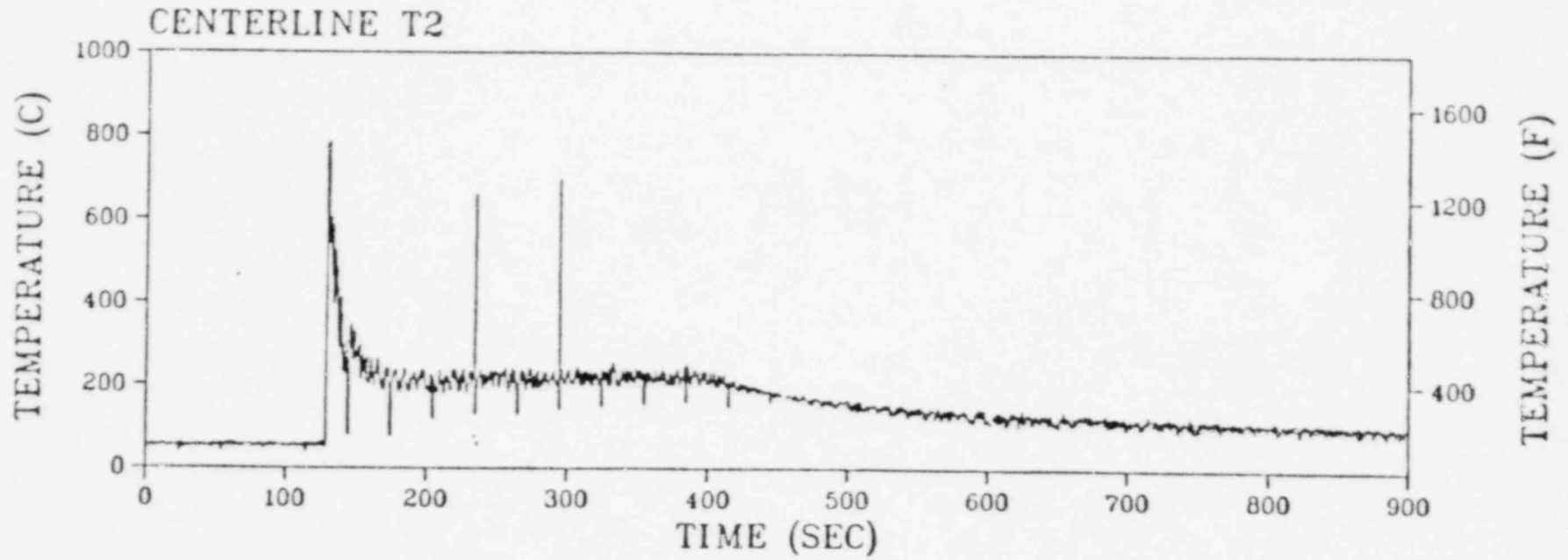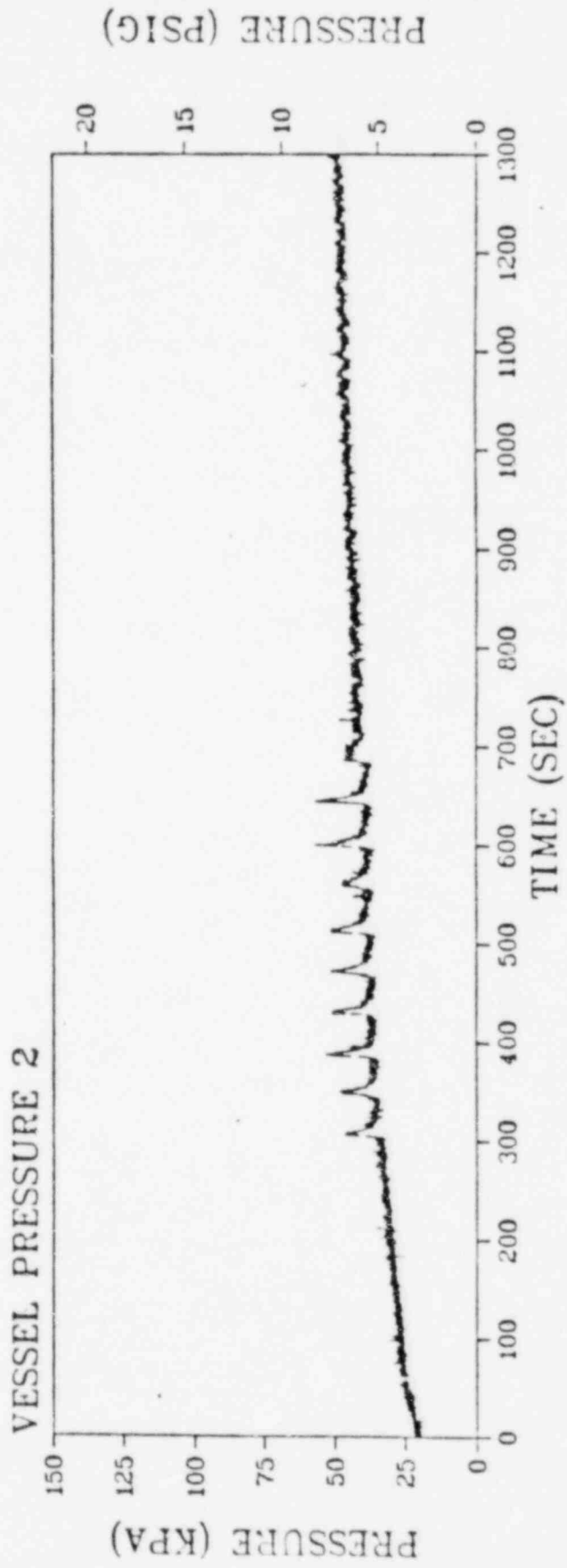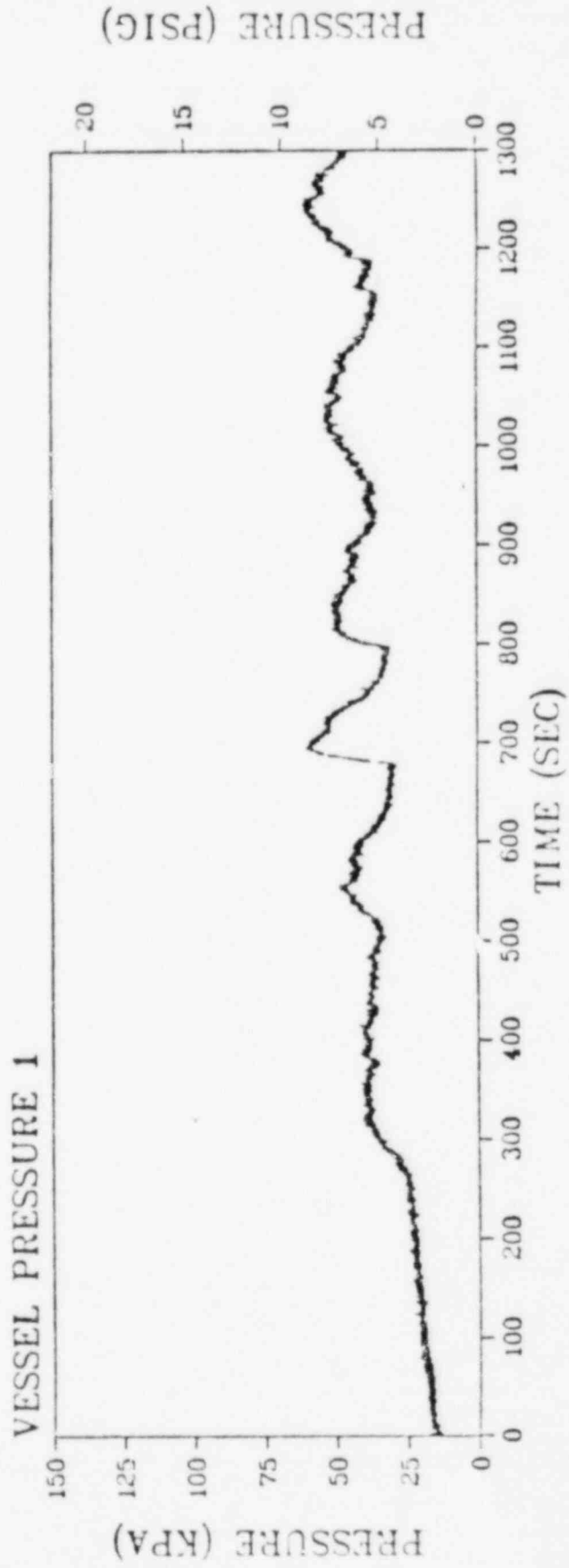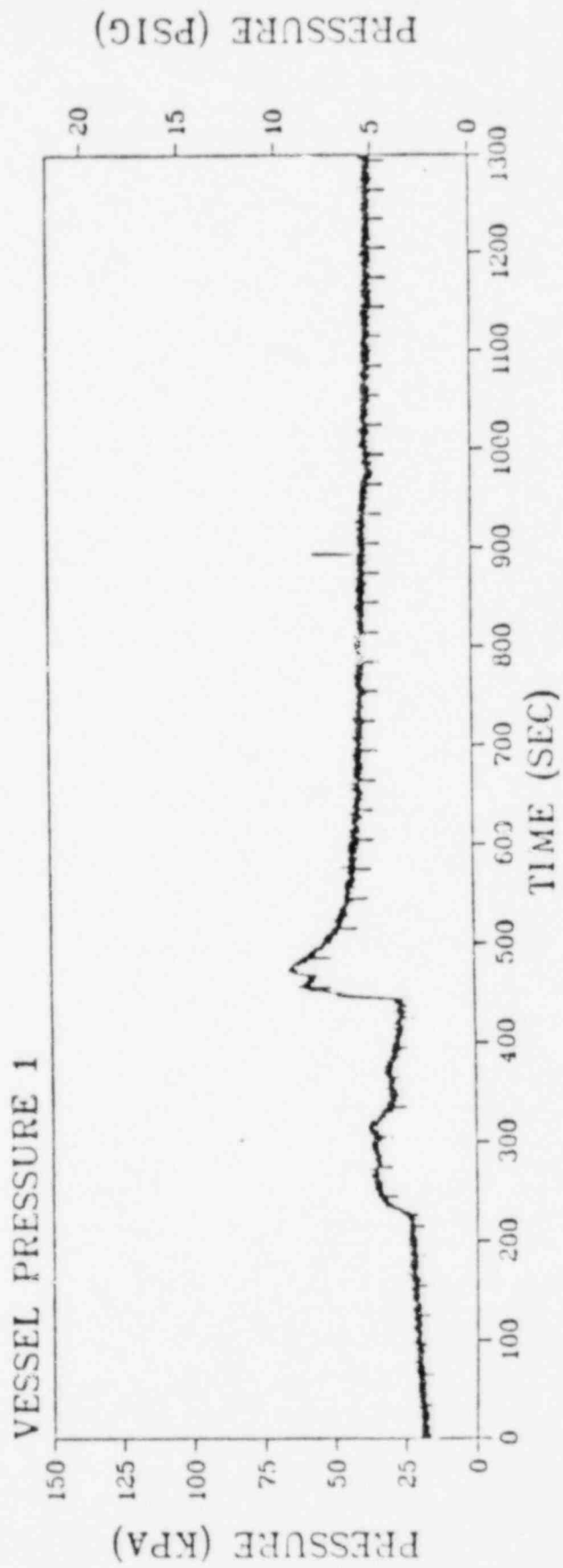
VESSEL PRESSURE 1
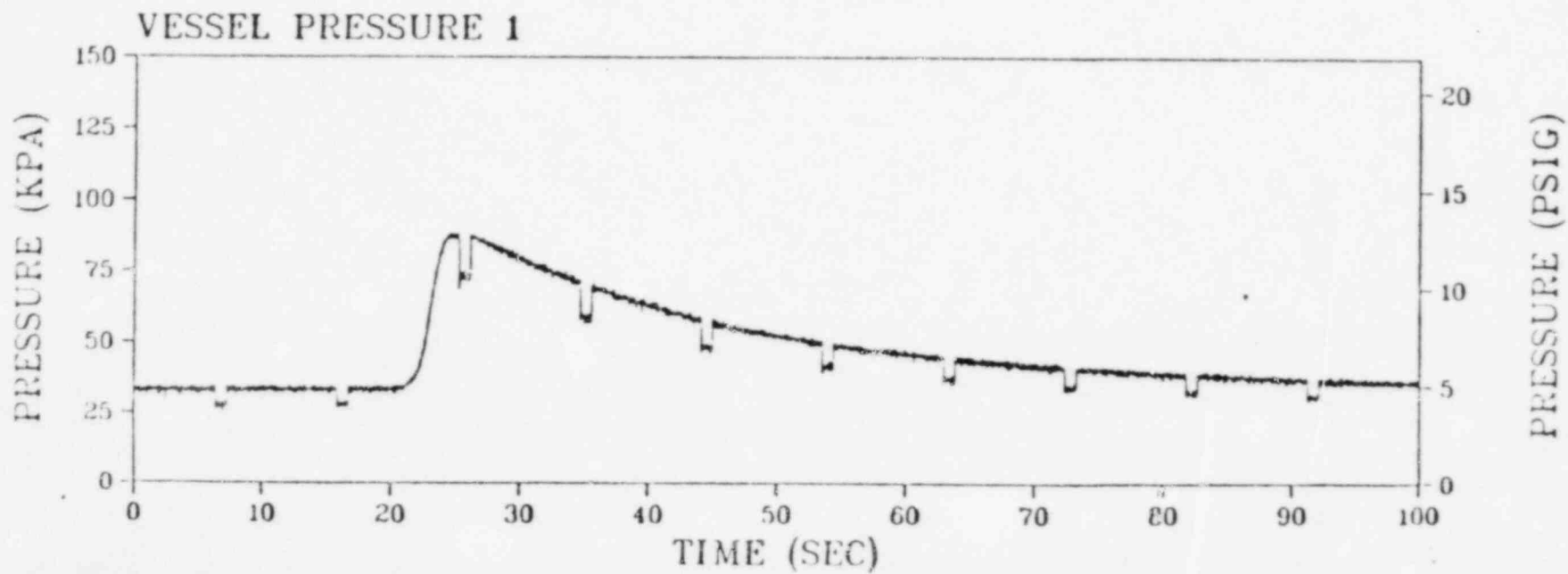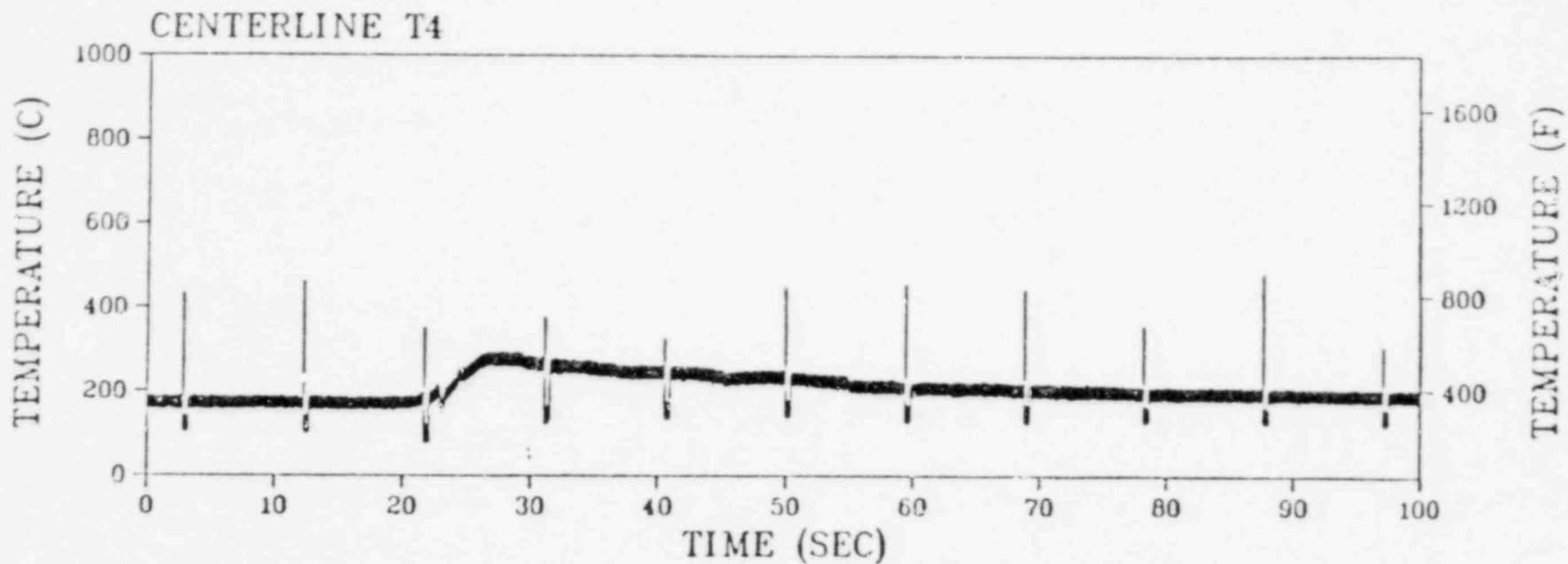
FIGURE 4-12
TEST 2.2

FIGURE 4-13
TEST 2.3

CENTERLINE T2

CENTERLINE T4

VESSEL PRESSURE 2

FIGURE 4-14
TEST 2.4

CENTERLINE T1

CENTERLINE T4

VESSEL PRESSURE 2
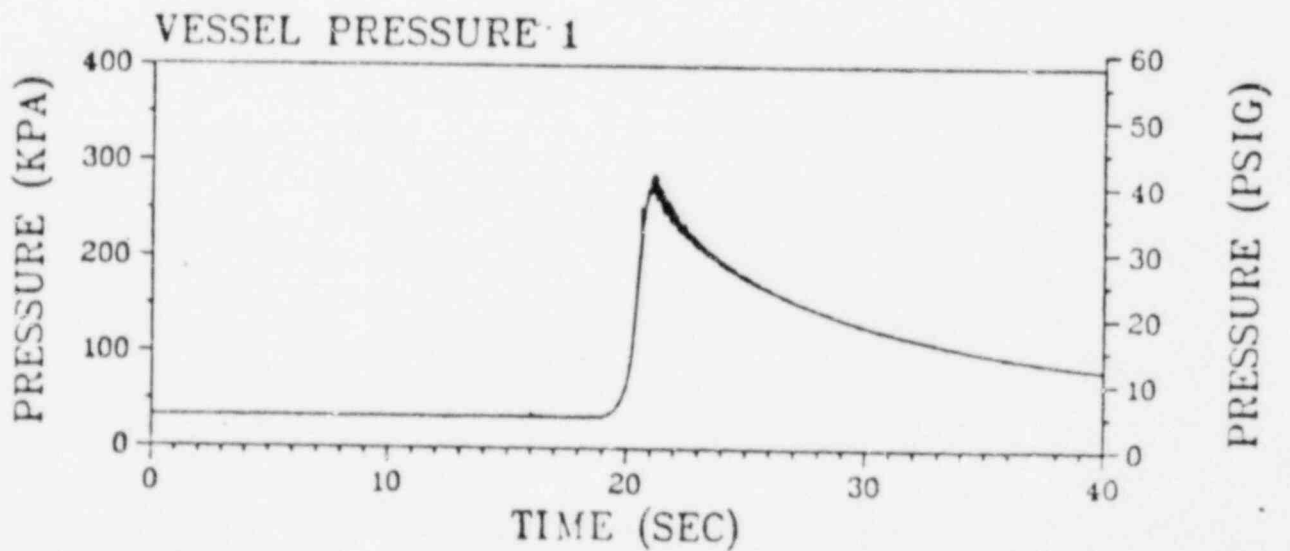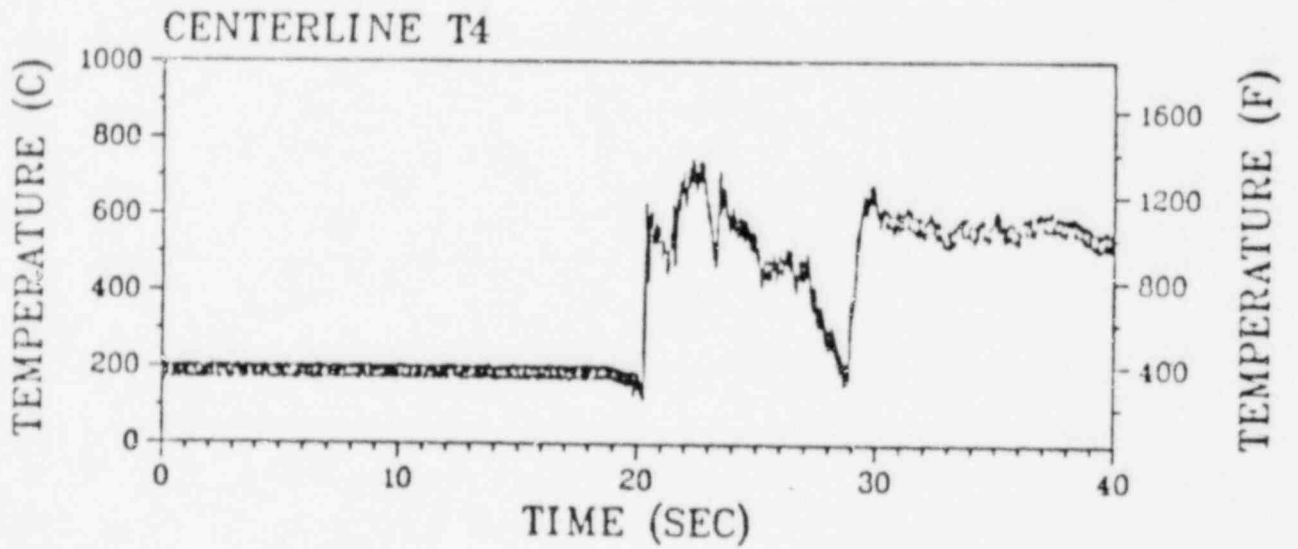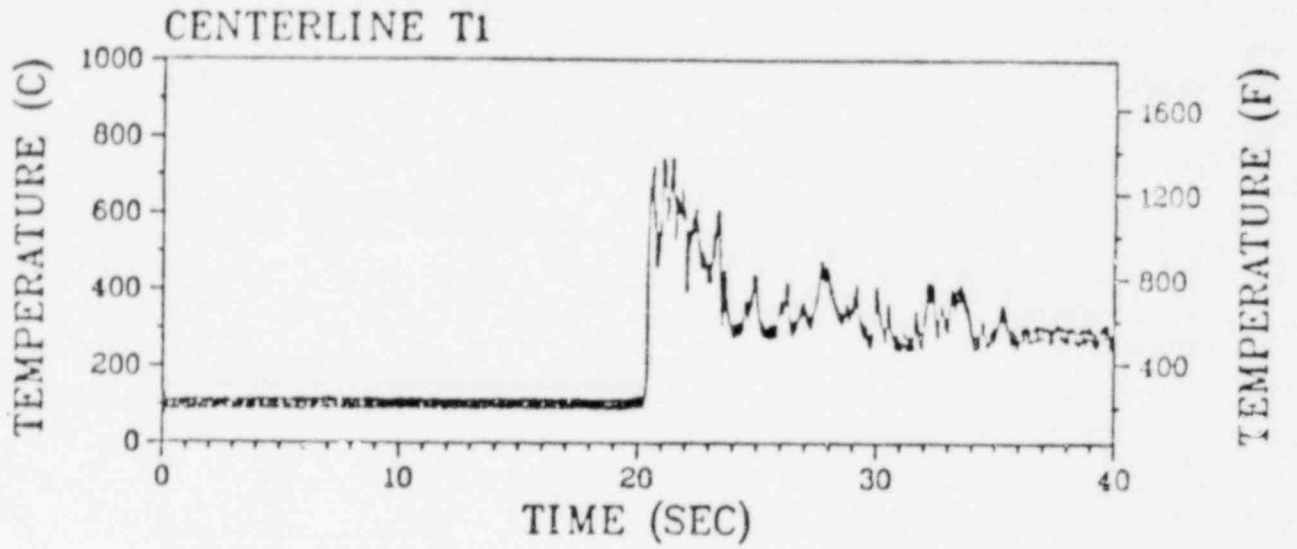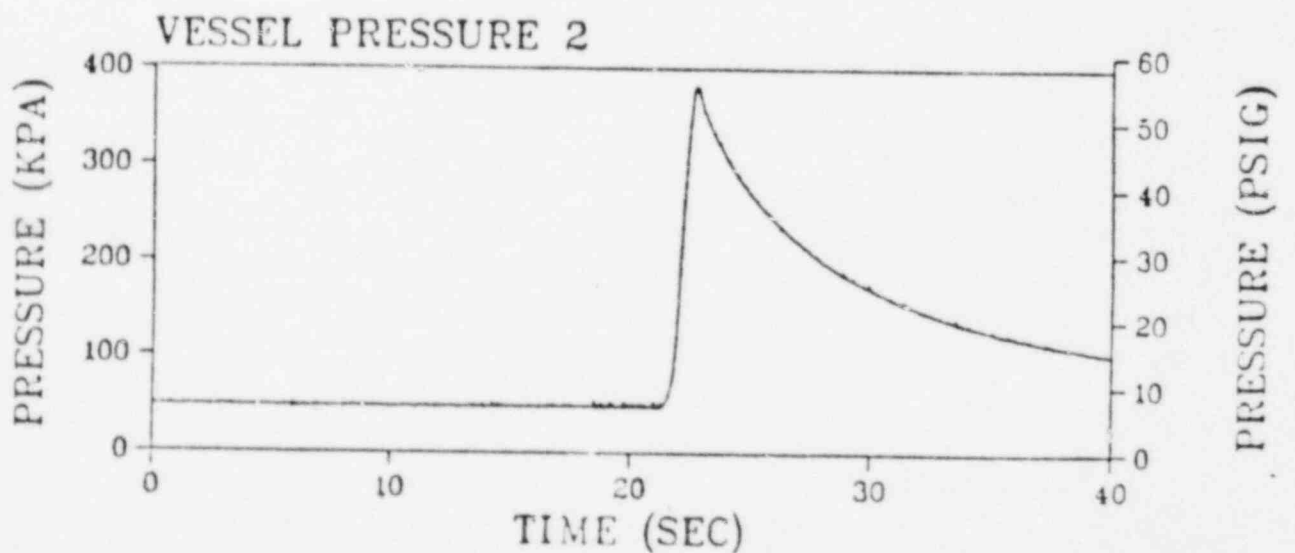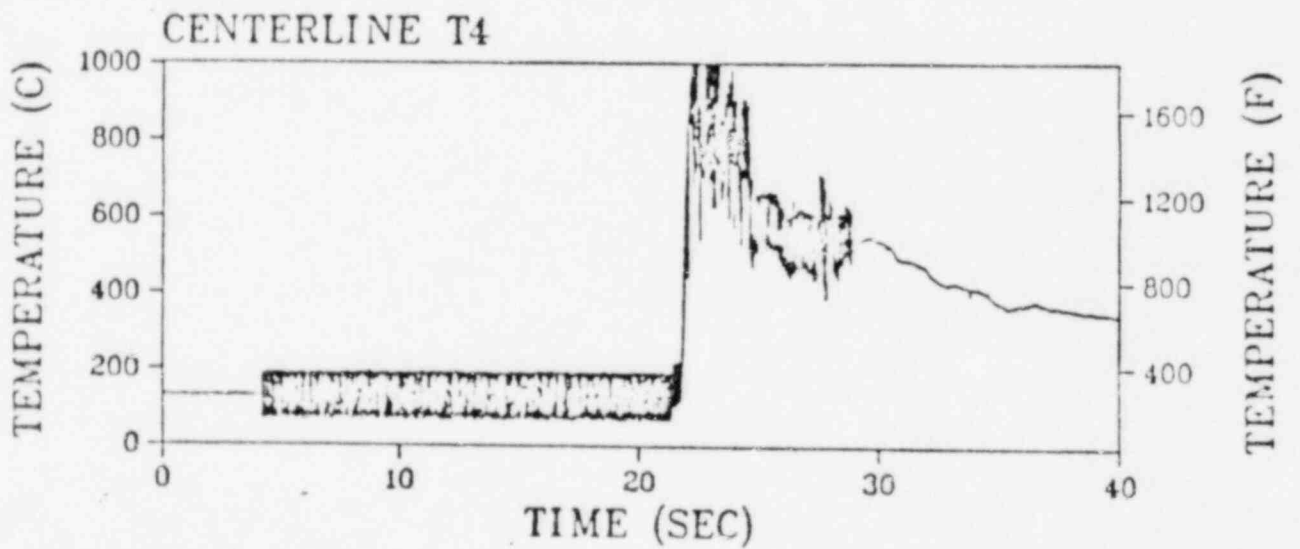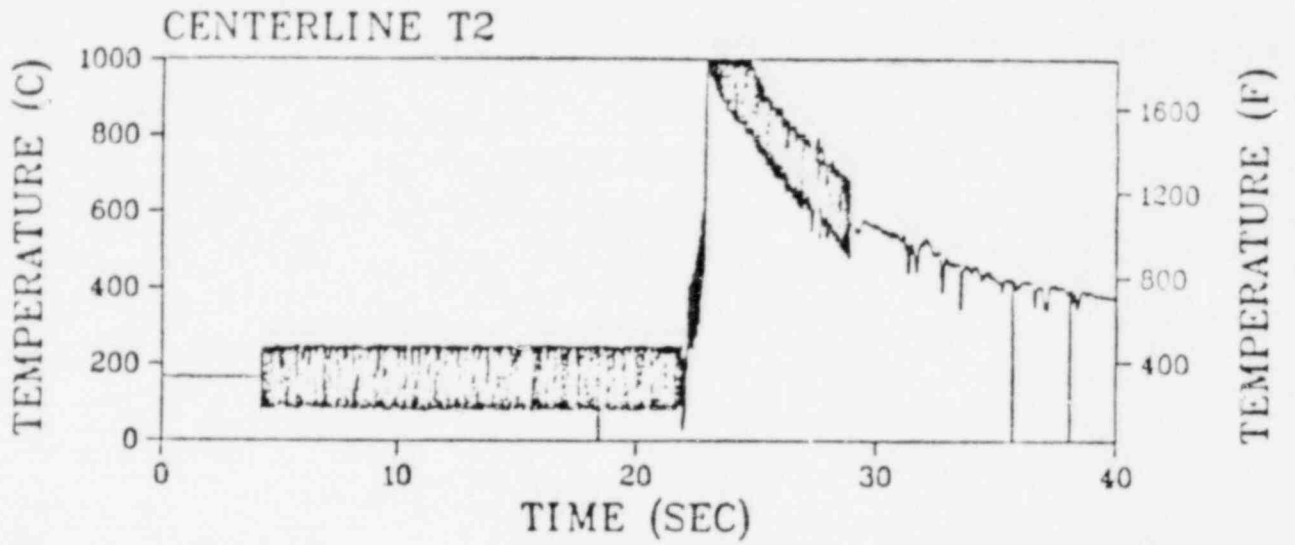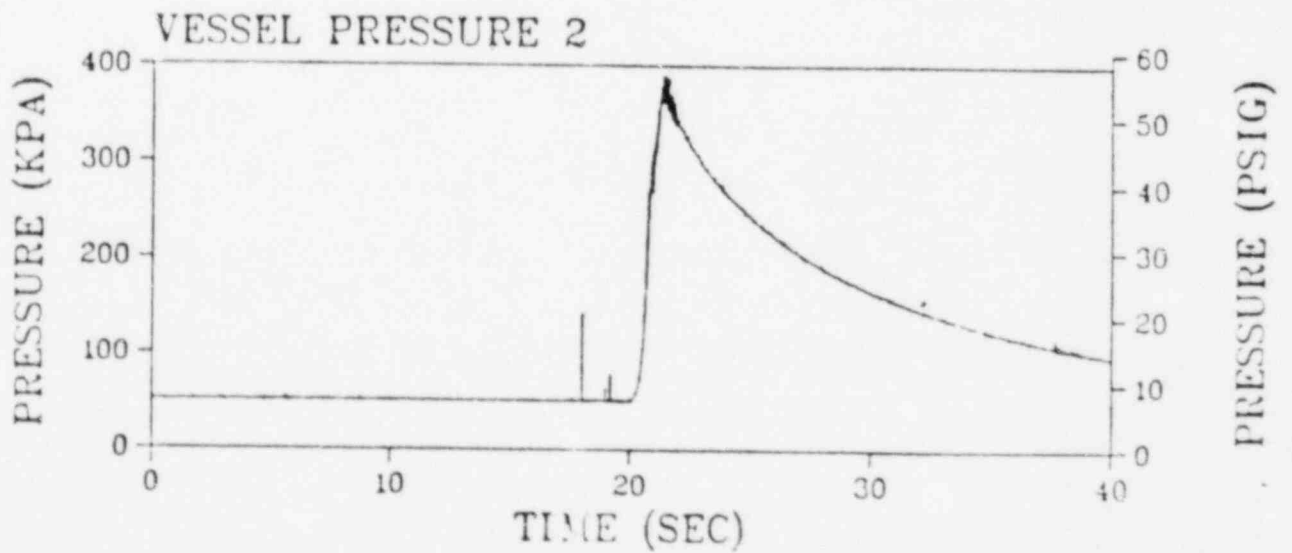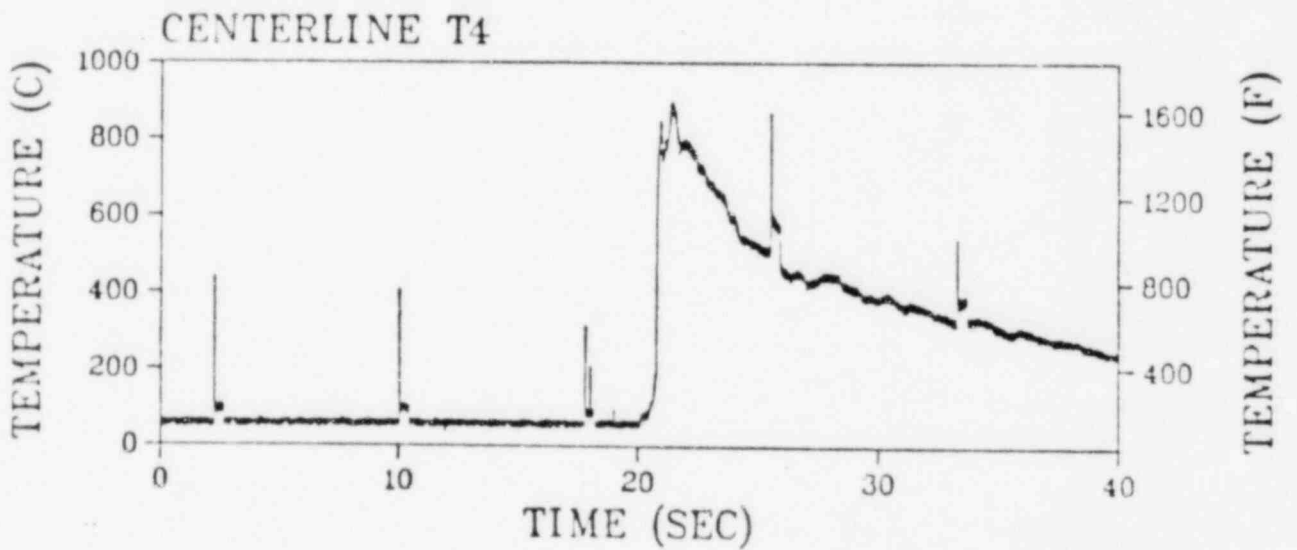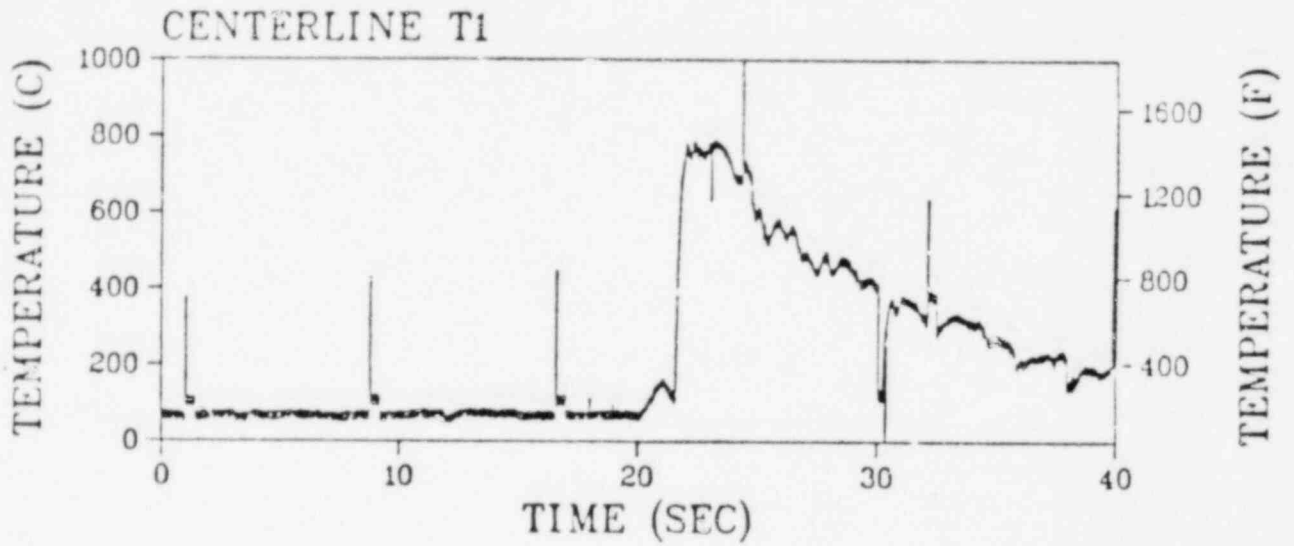
FIGURE 4-15
FLAME FRONT ACTIVITY
TEST 2.4

FIGURE 4-16
TEST 2.5

CENTERLINE T1

CENTERLINE T4

VESSEL PRESSURE 2
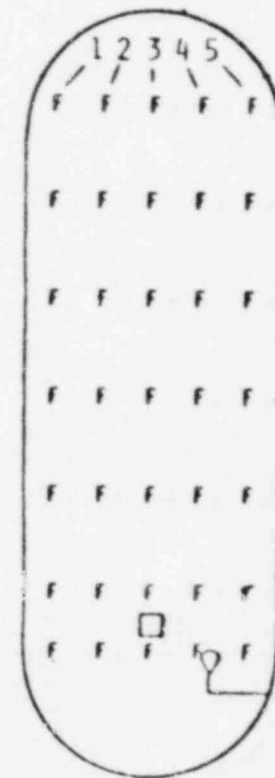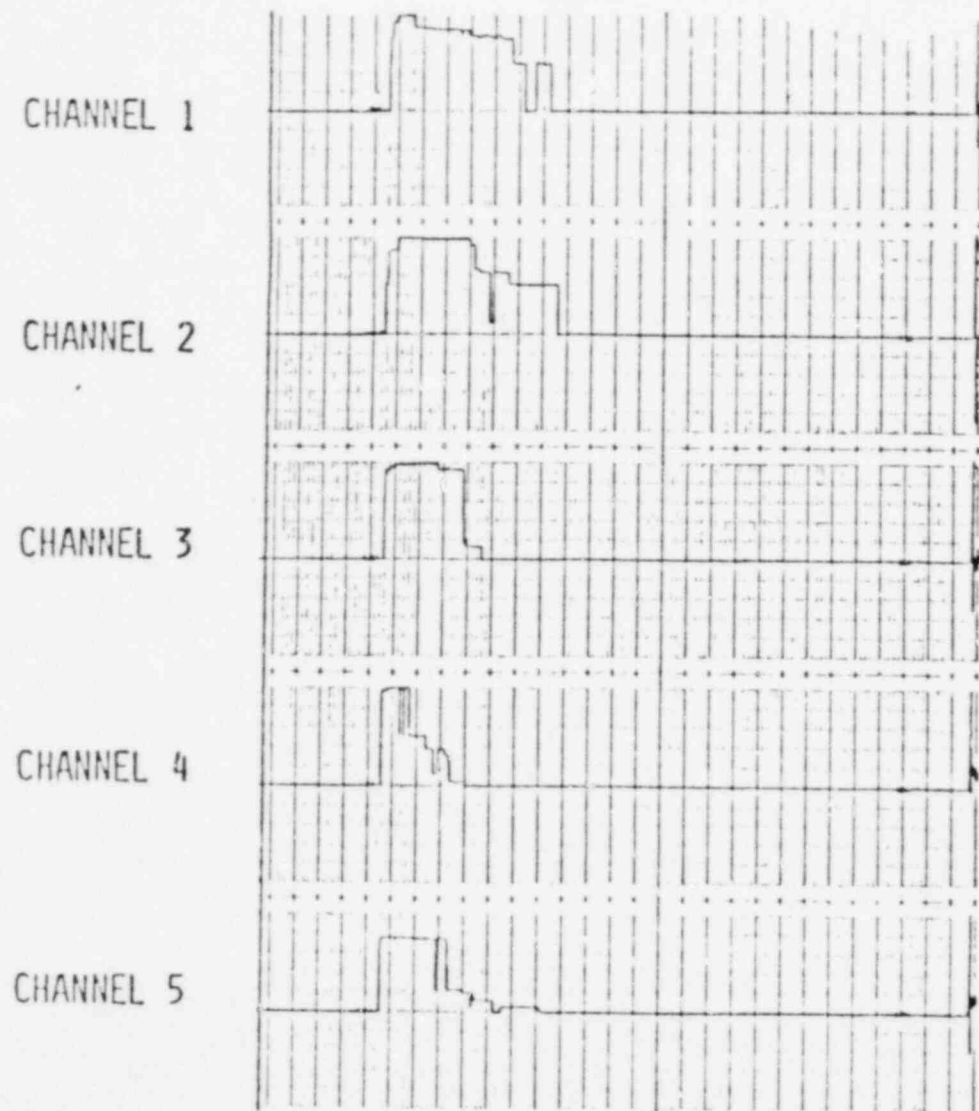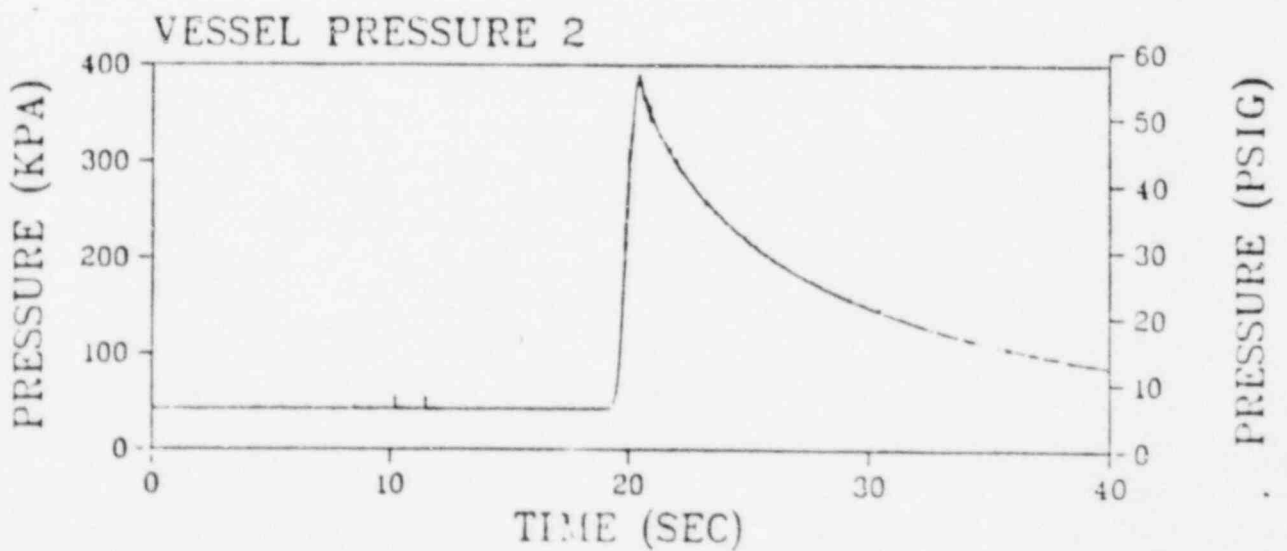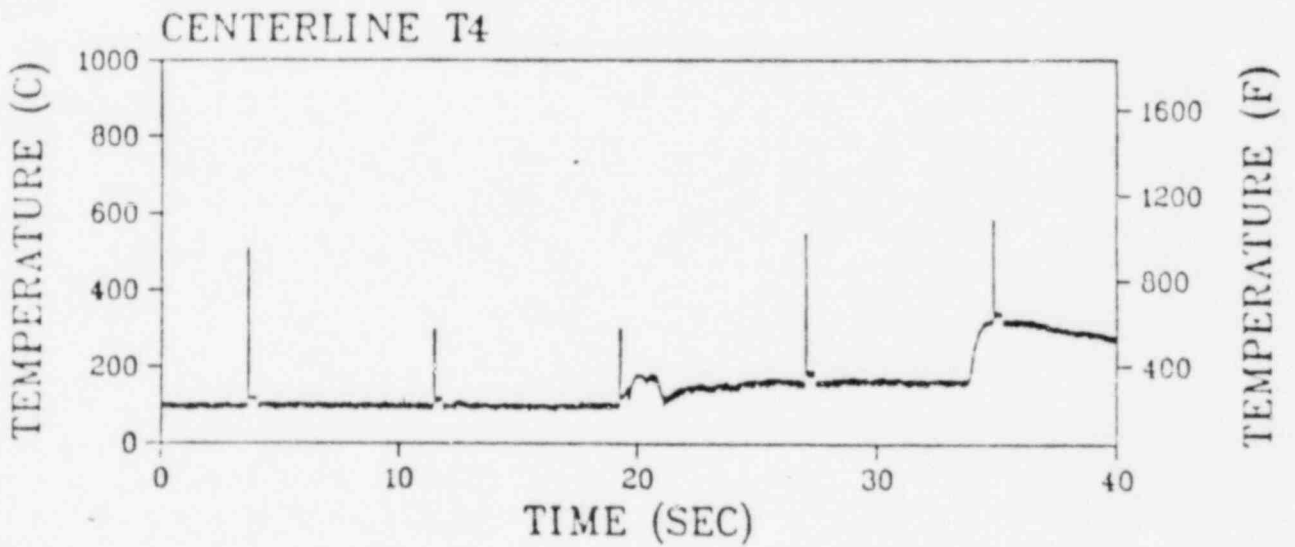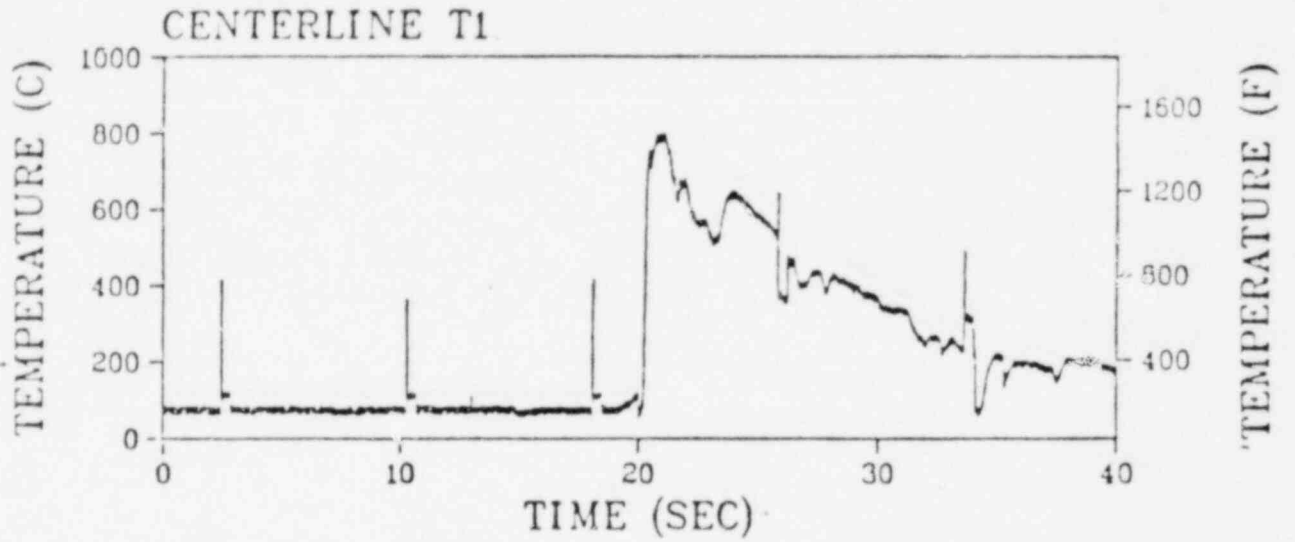
FIGURE 4-17
TEST 2.6

FIGURE 4-18
TEST 2.7

CENTERLINE T1

CENTERLINE T4

VESSEL PRESSURE 2

FIGURE 4-19
TEST 2.9

VESSEL PRESSURE 2
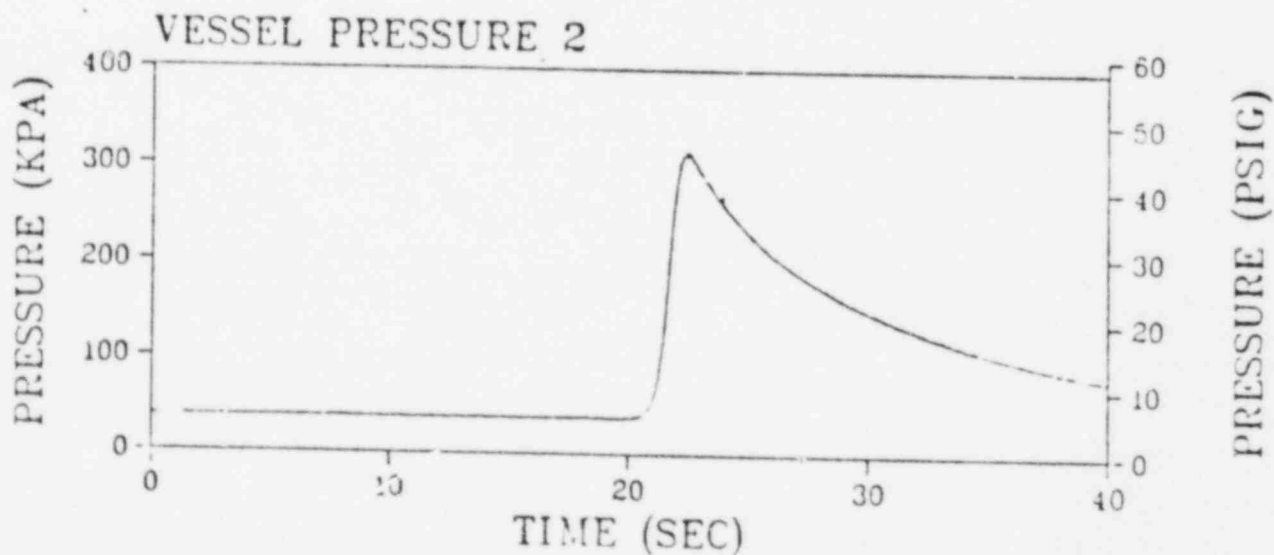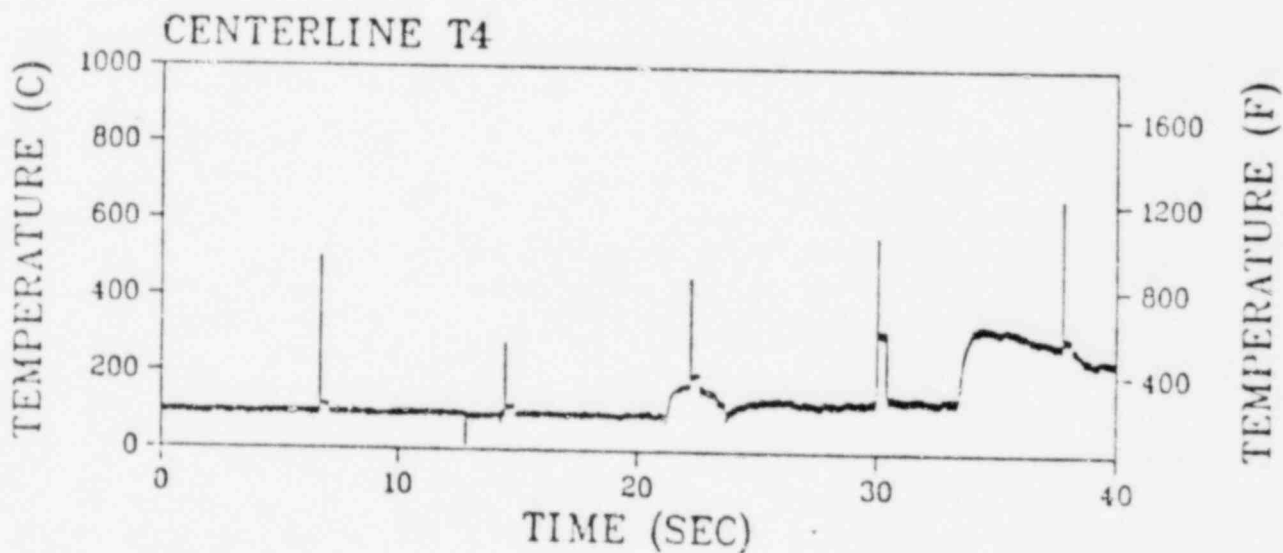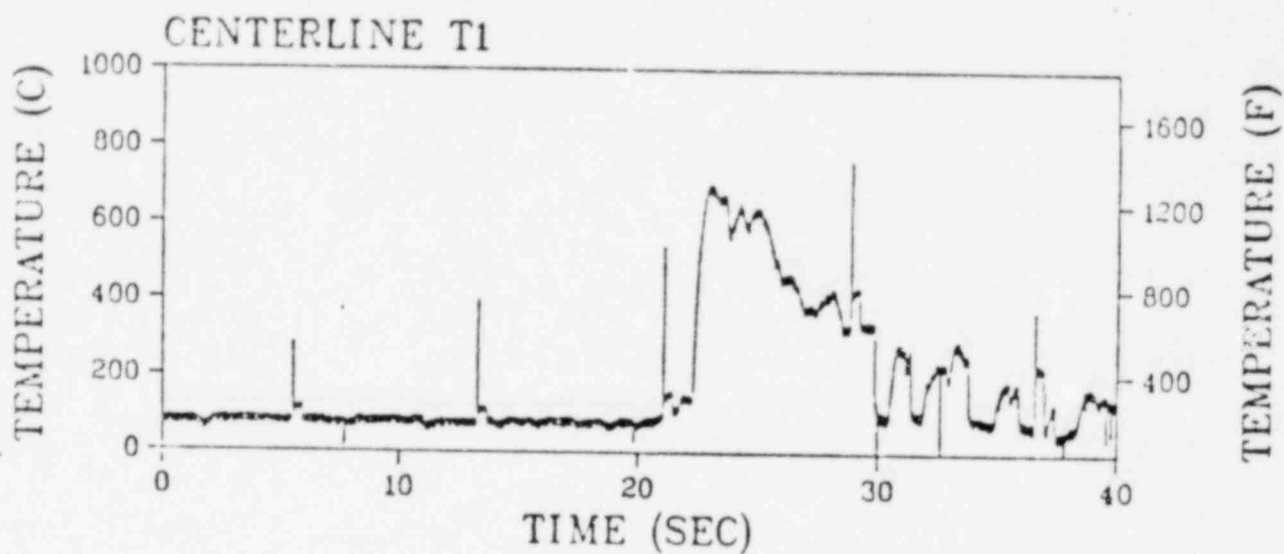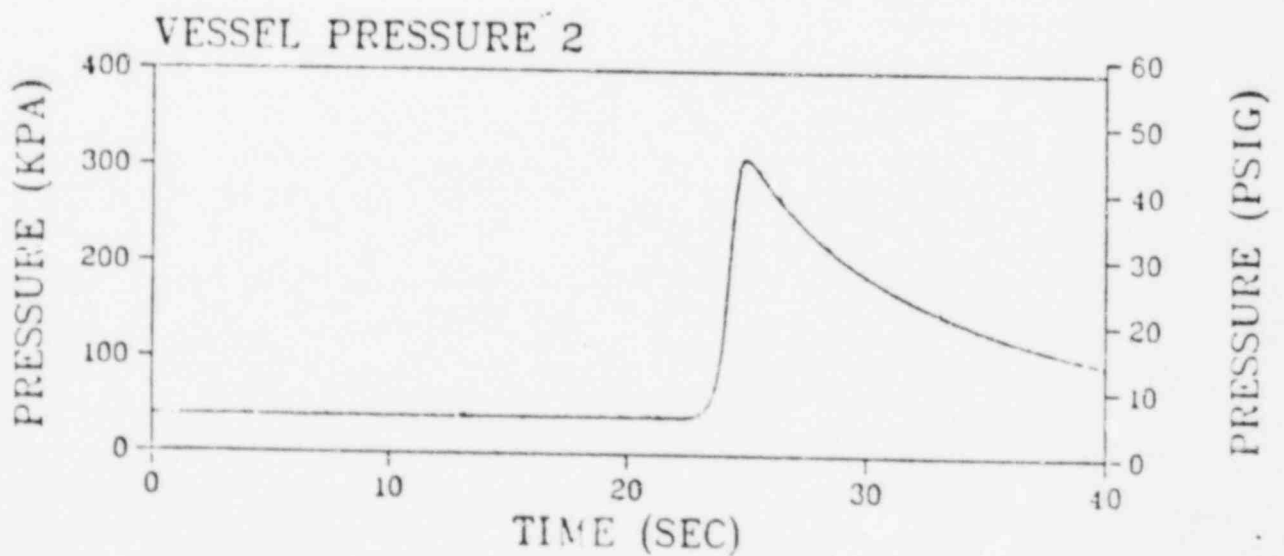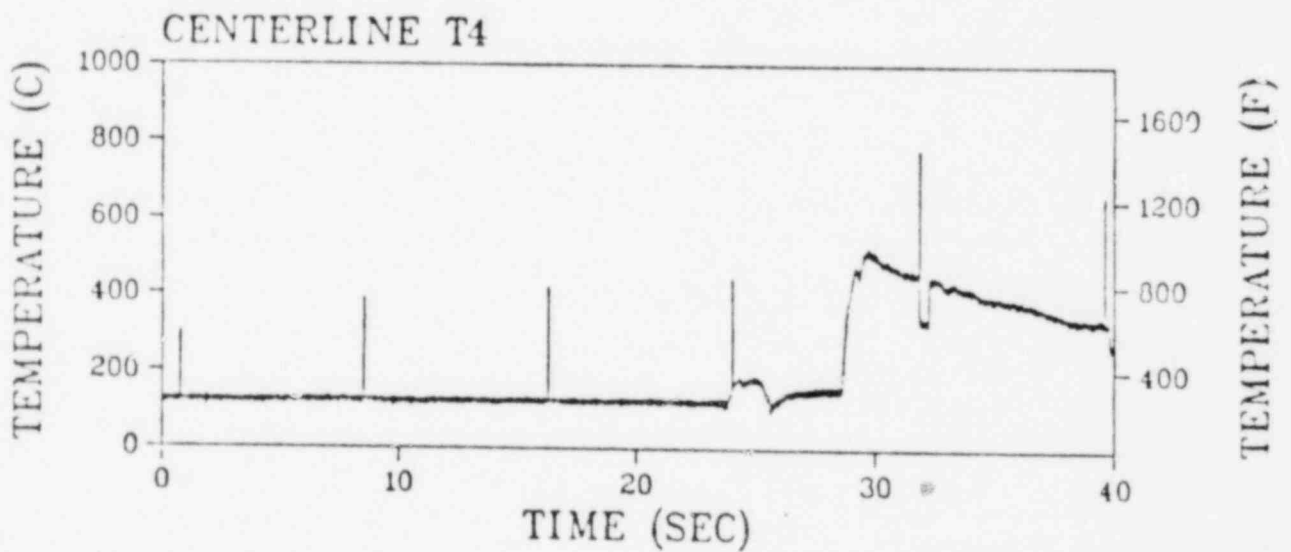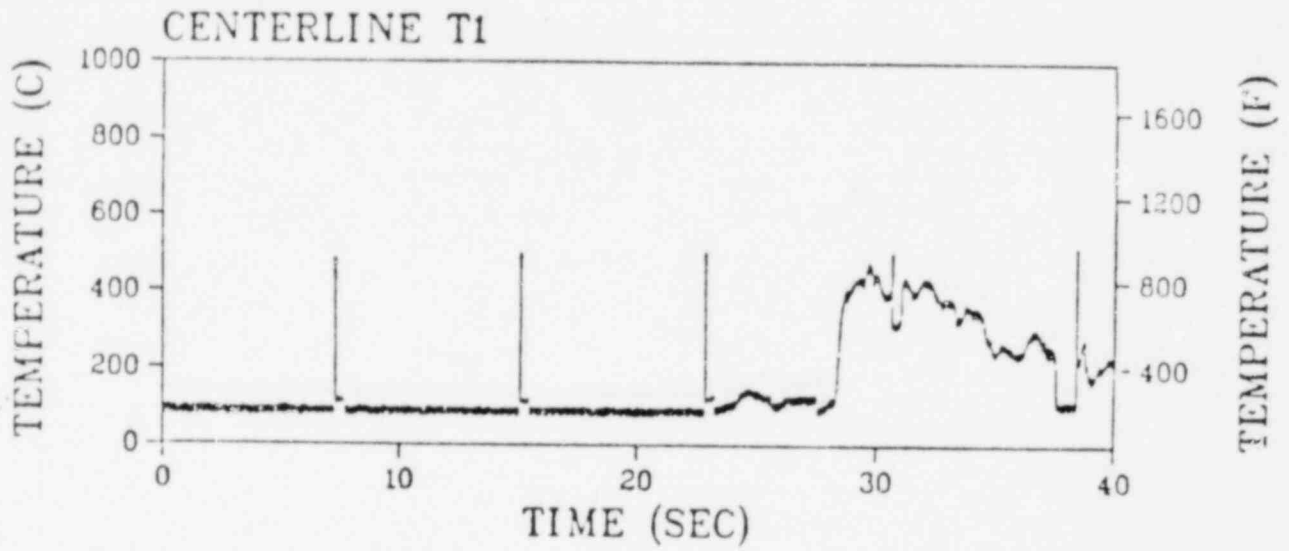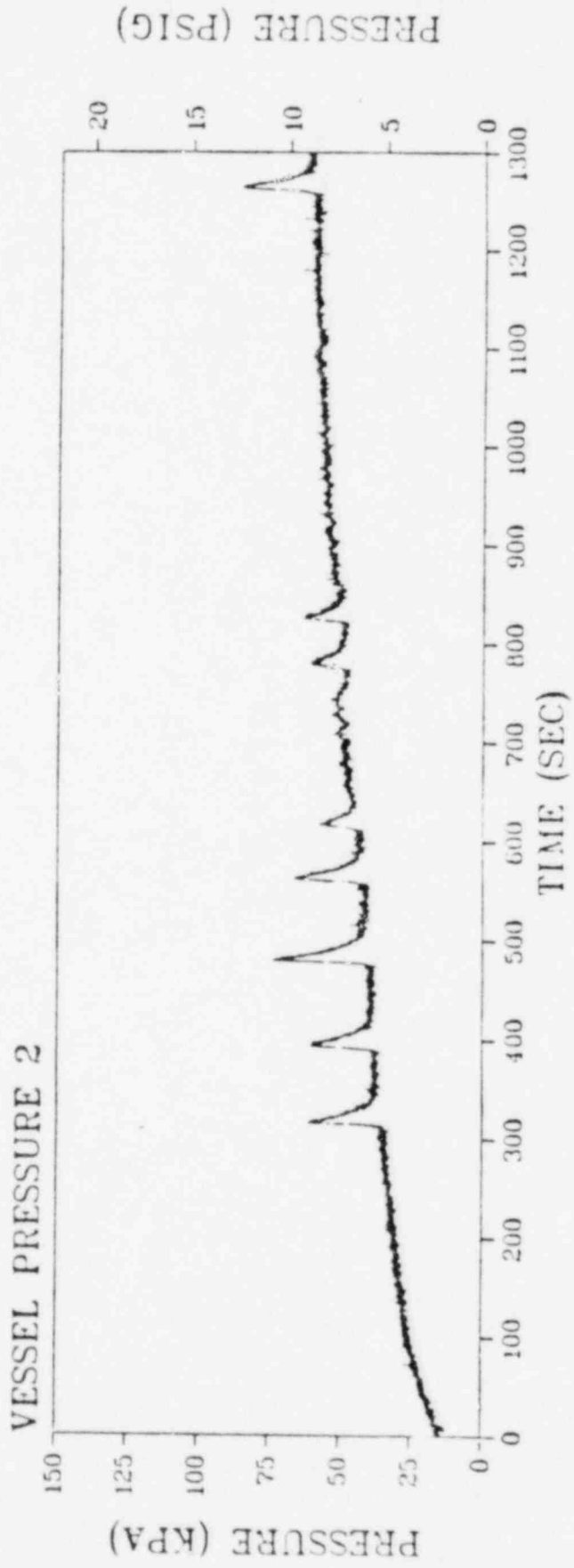
FIGURE 4-20
FLAME FRONT ACTIVITY
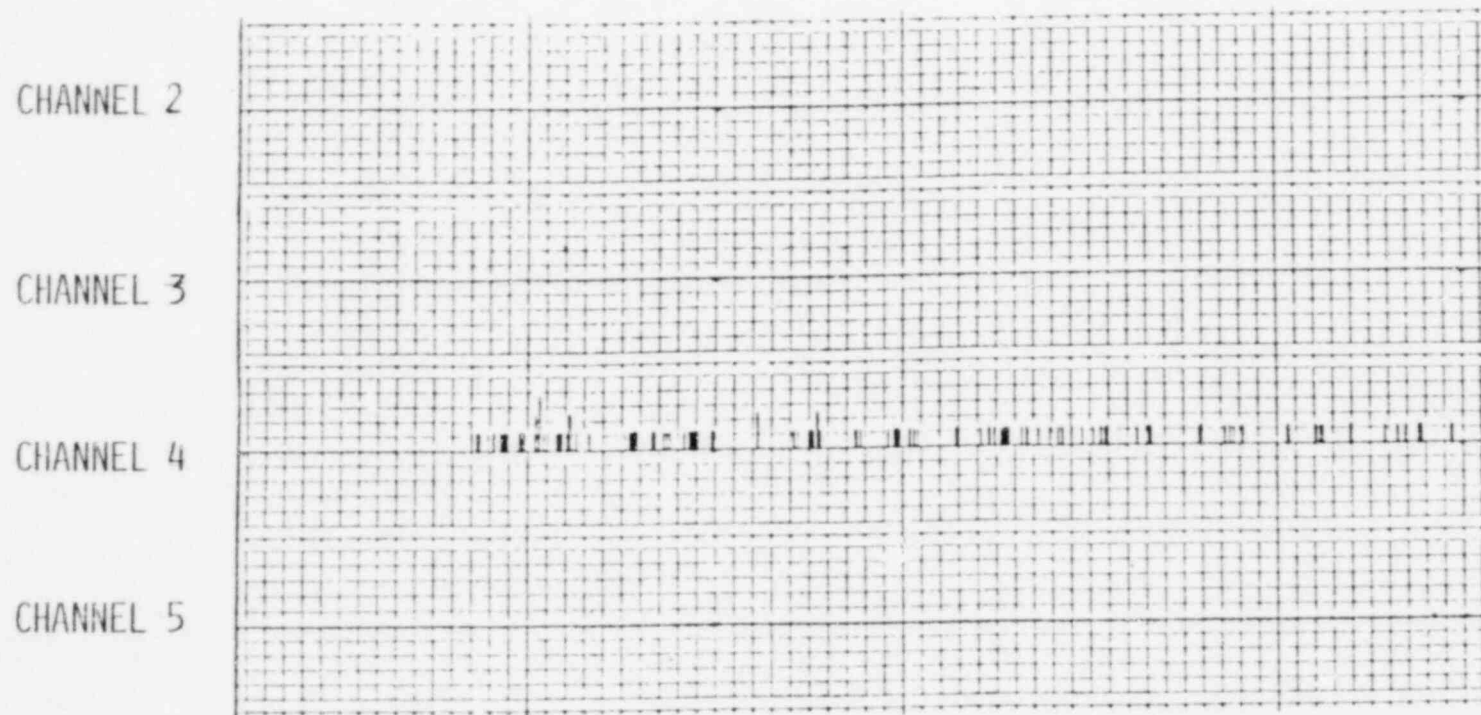TEST 2.10

FIGURE 4-21
TEST 2.11
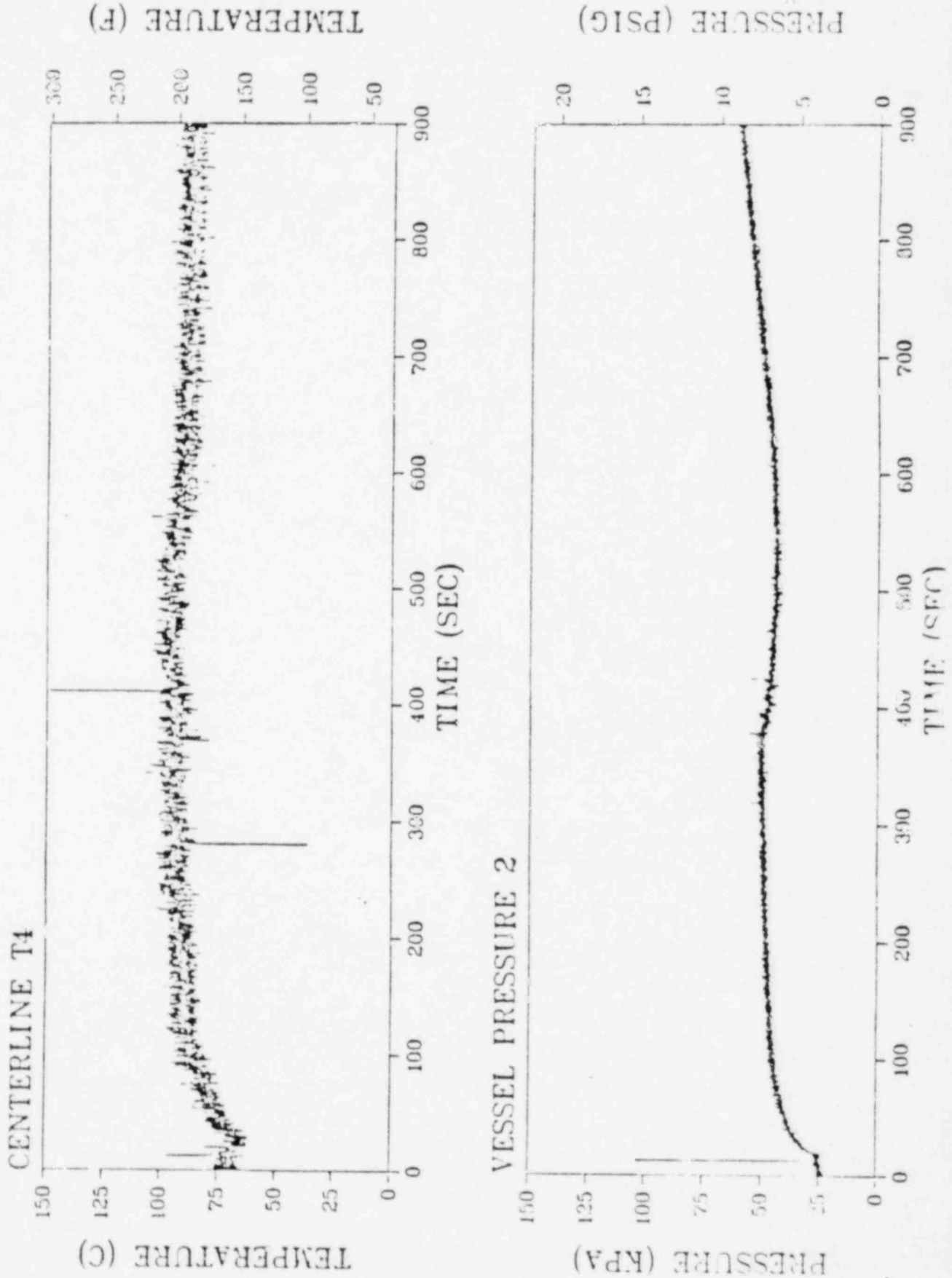
FIGURE 4-22
FLAME FRONT ACTIVITY
TEST 2.11
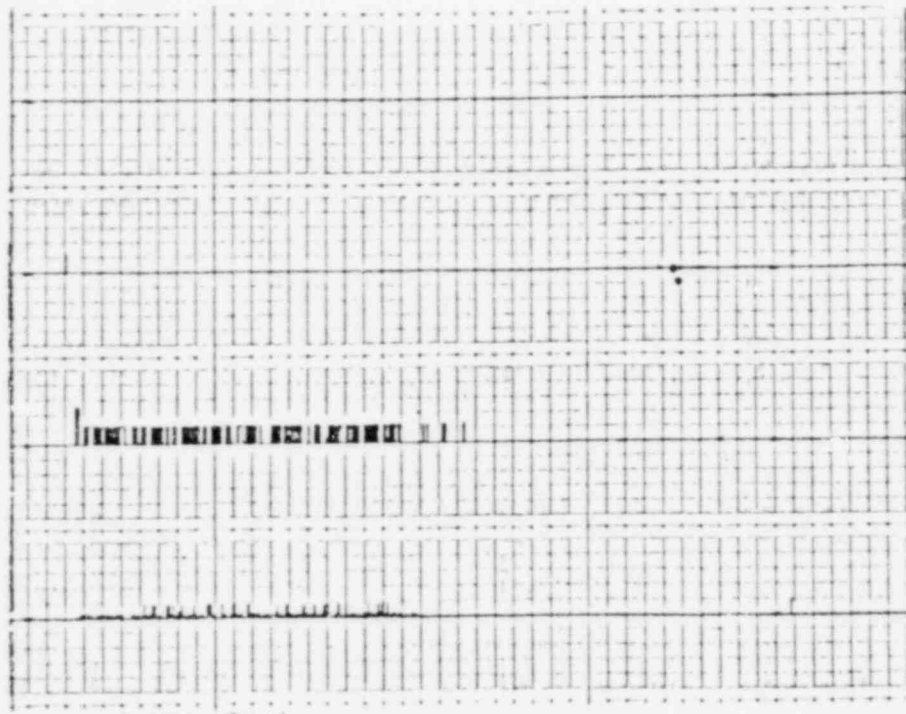
FIGURE 4-23
FLAME FRONT ACTIVITY
TEST 2.12

Section 5

Conclusions

1. Location of an ignitor within the test vessel does affect the characteristics of hydrogen deflagrations. Lowering the ignitor location produces milder pressures during hydrogen combustion. This appears to be a result of increasing the fraction of the vessel volume exposed to upward propagating flames in lean hydrogen concentrations. The addition of steam and water sprays also reduced the pressure rise. However, the lower ignitor locations still produced milder pressures than the top location.

2. Fogs were thought to reduce the pressure rise resulting from hydrogen combustion. This was the case for dynamic tests, but not for quiescent tests. Water fogs apparently enhance the rate of combustion. Thus, heat transfer is not as significant in quiescent tests causing the deflagration to be more like an adiabatic deflagration. For dynamic tests, water fogs promote mixing and allow ignition to occur earlier, resulting in lower energy release rates.

APPENDIX A

Gas Chromatography Analysis

Test vessel samples were obtained through nonheated ¼ inch stainless steel probes located near the top and bottom of the vessel (See Figure 2-1.). Each probe was connected to the inlet of a Thomas diaphragm pump. Vessel isolation was provided by solenoid valves. A ¼ inch stainless steel line connected the discharge of each pump to a stainless steel condenser coil submerged in an ice bath. Tarred silica gel columns were located at the outlet of the condenser coil to remove any remaining moisture. ¼ inch stainless steel tubing carried the sample from the silica gel columns, through a dry gas meter, and into a 250 mil glass bulb. Thermocouples monitored the inlet and outlet pressures of the gas meter. Solenoid valves isolated the sample bulb. When the sample was collected, the sample lines were purged.

Sample analysis was conducted by using a Carle Model 8700 gas chromatograph. Instrument specifications are presented in Table A-1. This unit was equipped with a thermal conductivity device. The output was recorded with a Linear Instruments Model 252 dual pin recorder. All samples and calibration standards were analyzed using repeat injections. A ten foot by 1/8 inch O. D. stainless steel column packed with Molecular Seive 13x, 80/100 mesh operating at 195°F, was used to separate the component gases. The gas chromatograph operating conditions are presented in Table A-2. Calibration standards consisted of several known concentrations of hydrogen (0.595%, 5.12%, 13.19%, 18.27%,

balance nitrogen) and oxygen (5.0%, 18.1%, balance nitrogen). These standards
were analyzed at the beginning and end of each sampling day.

TABLE A-1

GAS CHROMATOGRAPHY SPECIFICATIONS

Sensitivity	Variable, two level detector sensitivity switch
Attenuator	Eleven step binary type, 1024 to 1
Detectors	Dual chamber, 100 l volume with 8-10K, 0.013 dia. matched thermistors
Power Requirements	115V, 60 Hz
Temperature Control	Ambient to 200°C

TABLE A-2

GAS CHROMATOGRAPHY OPERATING CONDITONS

Argon Carrier Gas Flow	20 ml/min @ 25 psi
Oven Temperature	90°C
Column	10' SS tubing with molecular sieve 13x, 80/100 mesh
Detector Temperature	Low Position
Attenuation	Variable

APPENDIX 2I

IGNITOR PERFORMANCE

INTERIM PROJECT REPORT

COMBUSTION BEHAVIOR STUDY OF GLOW PLUG IGNITOR

IN HYDROGEN-AIR-STEAM MIXTURES

INTERIM PROJECT REPORT

December 1981

Prepared by:

K. K. Shiu, American Electric Power
F. G. Hudson, Duke Power Company
J. J.Wilder, Tennessee Valley Authority

Project conducted by:

Whiteshell Nuclear Research Establishment

Project Sponsors:

American Electric Power Service Corporation
Atomic Energy of Canada Limited
Duke Power Company
Electric Power Research Institute
Ontario Hydro
Tennessee Valley Authority

TABLE OF CONTENTS

1.0 INTRODUCTION

One of the research efforts undertaken at Whiteshell Nuclear Research Establishment pertains to investigating the effectiveness of the glow plug igniter in a more detailed and comprehensive manner and of other potential igniter types. This report presents the GM AC Model 7G glow plug igniter test results observed to date.

2.0 EXPERIMENTAL SETUP

A 17-litre quasi-spherical vessel with a pressure rating of 600 lb/in^2 (4 MPa) was used in this study. Figure 1 shows schematically the vessel and the components used in these experiments. The vessel has a pair of 3.9-in. (100 mm) diameter viewports on a horizontal axis for flame visualization and photography.

There are two 3/4-in. (1.9 cm) pipes welded to one of the convex walls. One of these is used for gas injection and sampling. A branch from this pipe is connected to a strain gauge (Data Instruments, Incorporated Model RS-101) for measuring the static pressure before and after ignition tests. The other 3/4-inch pipe is not used in these experiments and was capped. The other convex wall has a 600 lb/in^2 (4 MPa) safety rupture disk.

Figure 2 shows a schematic of the gas supply system. All lines are standard 1/4-in. (6 mm) stainless steel tubing. Steam is provided from distilled water in a 100 ml flask heated by a hot water bath.

The vessel and gas piping are electrically trace heated to 176-212°F (80-100°C) to prevent steam condensation inside. Eight

chromel-alumel (type K) thermocouples attached to the outside vessel and pipe surfaces are used to monitor this temperature.

3.0 INSTRUMENTATION

The instrumentation is shown in Figure 1. Specific components described below are numbered in the figure for clarity.

An ionization gap probe (No. 1) coated with sodium bicarbonate ($NaHCO_3$) is supported by a 1/8 in. (3 mm) steel rod (No. 2) at about 1.58 in. (4 cm) below the upper wall for detecting flame arrival. The support rod is mounted on the bottom flange.

A similar rod (No. 2A) screwed to a strong magnet (No. 7) is used to support the following: a .010 in. sheathed K-type thermocouple (No. 3) to measure gas temperature, an ionization gap probe (No. 4) to determine ignition and the GM AC Model 7G glow plug (No. 5). The ion probe and thermocouple are located approximately .32 in. (8 mm) above the glow plug and at an angle of 45° away from the central axis. Two type K thermocouples (No. 3A) have been spot welded to the bottom surface of the glow plug to determine its temperature history. As seen from Figure 3, this assembly is bound with high temperature tape and inserted into the vessel such that the glow plug is horizontal, about .39 in. (1 cm) above the lower edge of the viewport to permit flame photography.

A small fan (No. 6) with aluminum blades 2.76-in. diameter (70 mm) mounted on a magnet (No. 7) is available for forced convective flow experiments. All of the electrical wires (No. 8) penetrate the flange

via Conax fittings (No. 9). A Kistler 603B1 piezoelectric transducer (No. 10) is flush-mounted on the flange to measure the pressure transients. A slow response 1/16" type K thermocouple (not shown in figure 1) located near the lower vessel wall level is used to measure initial and final gas temperatures.

Although the two thermocouples, which are spot welded to the bottom surface of the glow plug, are similar, they do show a somewhat different response time, as shown in Figures 4 and 5. The higher of the two glow plug temperatures is consistently used for glow plug surface temperature evaluations.

The thermocouple for gas temperature is clearly too slow to properly determine the peak temperature. However it does provide clear indication of ignition. Maximum gas temperature is more reliably obtained from the application of the ideal gas law based on the more accurate pressure measurement of the strain gauge pressure tranducers.

3.1 Pressure Measurements

A Data Instrument, Incorporated, Model 101-25 strain gauge transducer is used to measure the initial partial pressures and the final pressure. This transducer is connected to a Data Instrument Model (RS-100) digital readout system calibrated to better than $\pm.02$ lb/in^2 (0.133 kPa).

Since the strain gauge transducer will record up to 25 lb/in^2 absolute (170 kPa), it also serves as added confirmation of pressure history measurement.

For fast pressure transients, a Kistler 603B1 piezoelectric pressure transducer, flush-mounted on the flange and connected through a Kistler 504E charge amplifier to the recorder, is used for pressure measurements.

3.2 Flame Arrival Detection

The two ionization gap probes, used to detect flame arrival, are connected directly to the recorder. Although in principle they can be used for flame speed determination, the slow recorder speed limited their use to confirming combustion.

The gap probes are operated at 200V dc. Each probe has a single RC coupling circuit. Since hydrogen flames produce few ions, the probes are coated with sodium bicarbonate to provide detectable signals.

The central probe tends to pick up 60 Hz noise more readily than the upper probe as a result of its close location to the 60 Hz power source for the glow plug. However, the combustion wave signals were still strong enough, even for lean mixtures, to determine flame arrival.

3.3 Chemical Analysis

Partial pressure data have been used as the principle method in determining initial concentrations due to its reliability and consistency. Also, when available, the mass spectrometer has been used to measure gas concentrations before and after ignition. Like most commercial systems, this device does not measure steam concentration. Nonetheless, the extent of combustion can be readily evaluated by comparing the hydrogen/nitrogen ratios before and after ignition.

4.0 EXPERIMENTAL RESULTS

Most tests were performed with quiescent hydrogen-air-steam mixtures using a 14V ac supply to the glow plug. A limited number of tests have also been done with a 12V ac supply and with the fan on.

Typical measurements made in each test are presented in Figure 6. They include the two-time traces of the ionization probes, glow plug surface temperature, and the pressure data.

The extent of reaction can be estimated from three different measurements: (a) mass spectrometry analyses before and after reaction, (b) static pressure measurements before and after ignition, and (c) peak pressure measurements. From the mass spectrometer measurements, the extent of reaction is defined as follows:

$$\text{extent of reaction} = \frac{1 - (H_2/N_2) \text{ final}}{(H_2/N_2) \text{ initial}}$$

The estimate of extent of reaction from static pressure is based on the fact that there are two moles of gas after combustion for every three moles of fuel and oxidizer reacted. The following formula for the extent of reaction can be derived:

$$\text{extent of reaction} = \frac{2(P_{initial}/P_{final}) - 1}{H_2 \times (P_{initial}/P_{final})}$$

Where H is the volume faction of hydrogen prior to combustion.

Because the differences in pressure are small, the calculated results are very sensitive to the measured pressures.

Figure 7 summarizes the results of the experiments. Ignition criterion is defined as detection of flame arrival by the upper ionization probe. For marginal ignition, the pressure and temperature rise were small and often barely recorded. For a pressure rise less than 1.8 lb/in^2 (12 kPa) but with a detection of flame arrival by the upper ionization, ignition is defined as marginal. It can be seen that the ignition region limit is similar to flammability limit curves.

Figure 7 depicts the ignition limits of hydrogen air mixtures in various steam concentrations. Majority of the data points are for static mixtures; turbulent mixture tests are still being conducted. The range of steam concentration investigated varies from 0 to about

60 percent. At about 55-percent steam concentration, only marginal ignition was observed for a hydrogen mixture of 20 percent. The initial pressure for these tests was essentially atmospheric, and the maximum pressure observed was about 54.7 lb/in^{2}g (372 kPa).

The surface temperature of the ignitor at which ignition occurred was recorded for each test. The results are presented in Figure 8. It is obvious that as the steam concentration increases, so does the ignition surface temperature. The maximum temperature observed was about 1560°F (850°C).

Preliminary evaluation of the experimental data indicates that results obtained:

(a) are consistent with glow plug data from Fenwal and

(b) are consistent with other hydrogen-air-steam mixture data with other ignition sources.
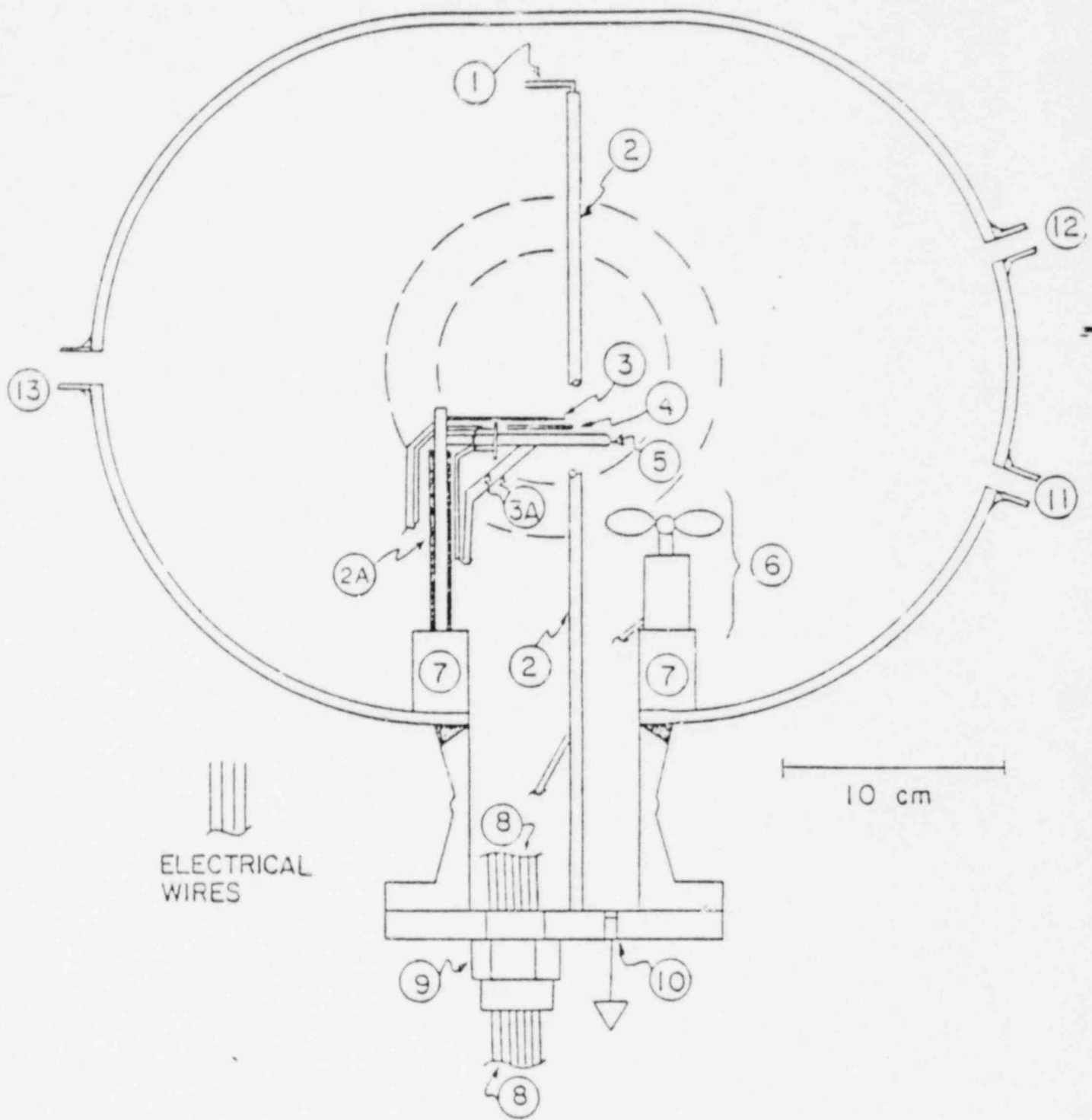
THE SCHEMATICS OF THE INSTRUMENTATION FOR THE
IGNITION EFFICIENCY TEST USING A GM AC NO. 7
GLOW PLUG IN A 17-LITRE VESSEL.

FIGURE 1

VESSEL

steam

strain
gauge

sample

mercury
vaccum
guage

H₂

air

vacuum
pump
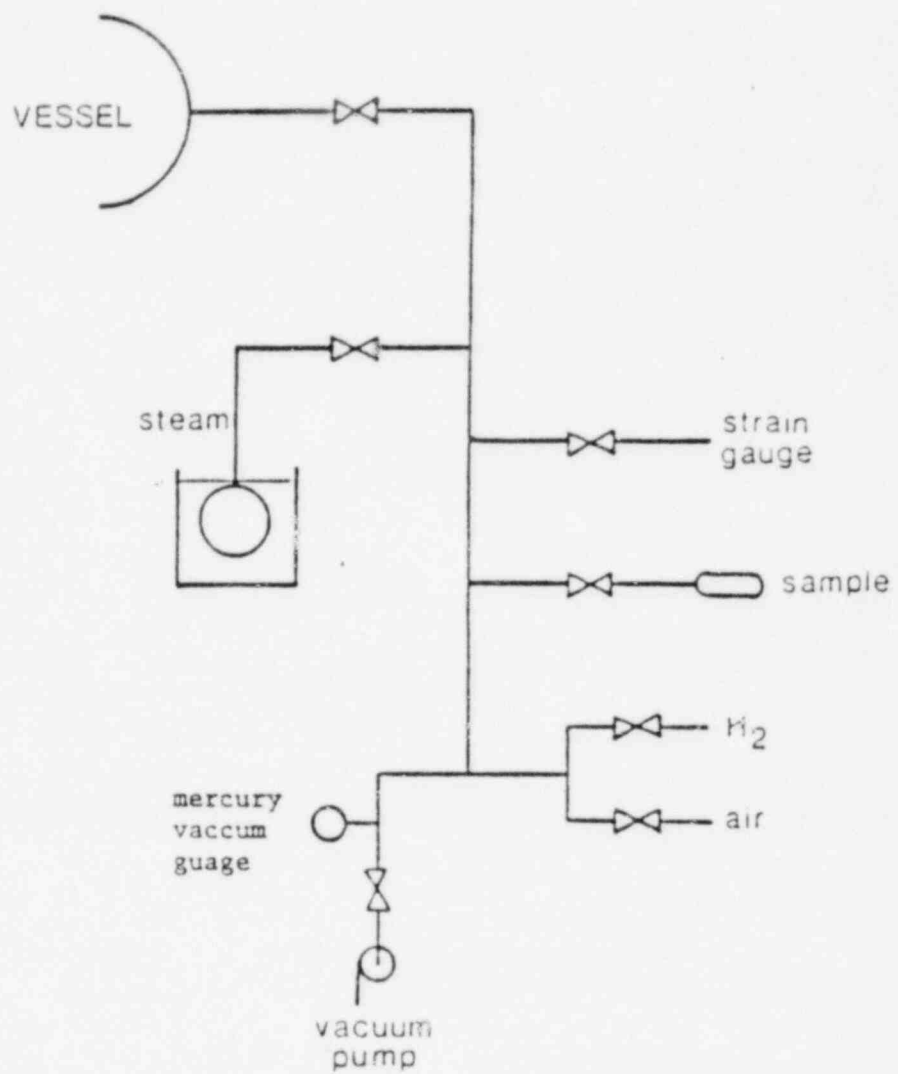
GAS SUPPLY SYSTEM

FIGURE   2
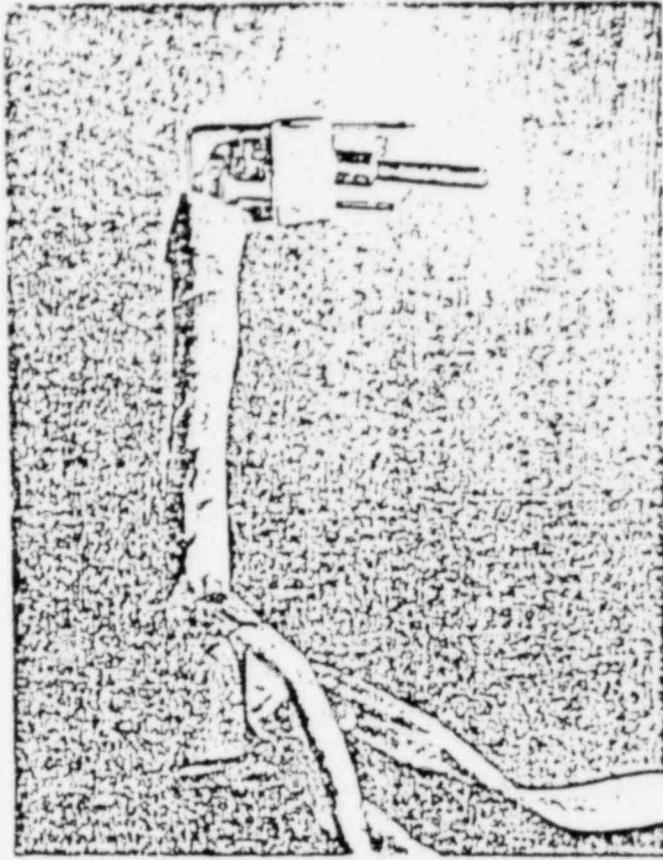
> THE GM AC No. 7 THERMAL GLOW PLUG
EQUIPPED WITH DETECTORS FOR TESTING
THE IGNITION EFFECTIVENESS AND
RELIABILITY.

FIGURE   3

GLOW PLUG RESPONSE CURVE
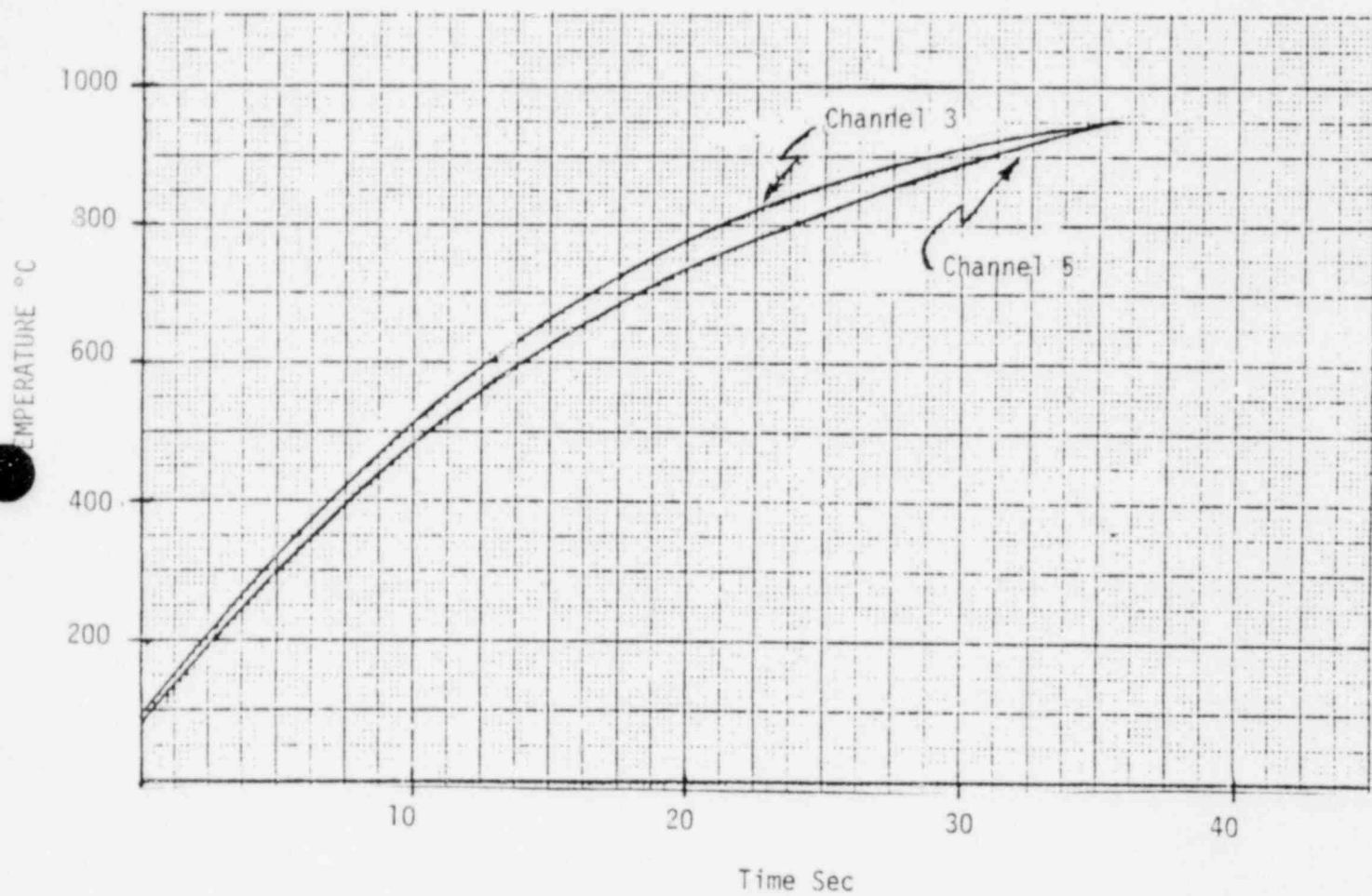
CASE #18

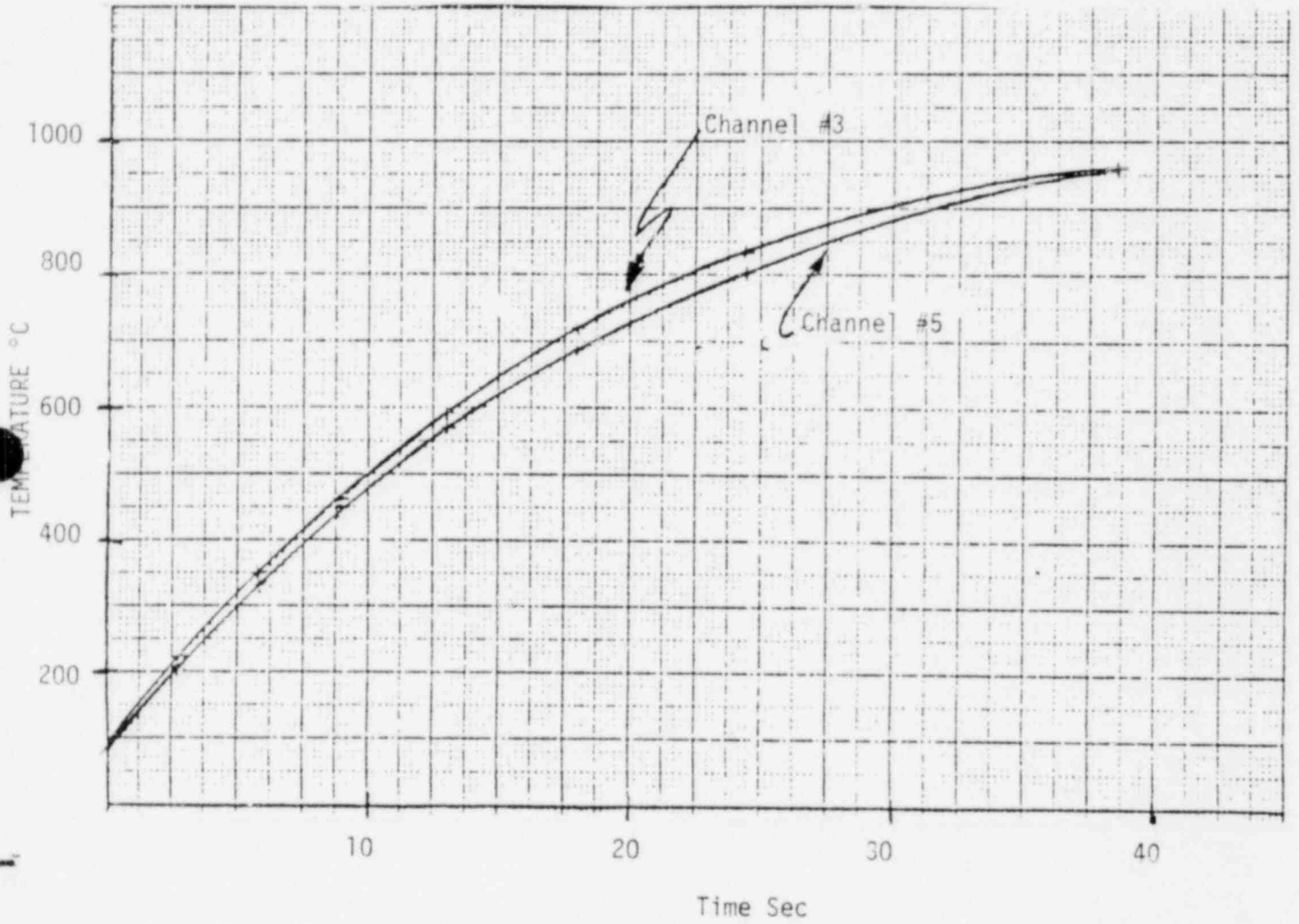## AIR ONLY

NO FAN

FIGURE 4

GLOW PLUG RESPONSE CURVE

CASE #19

AIR AND STEAM

NO FAN

FIGURE 5
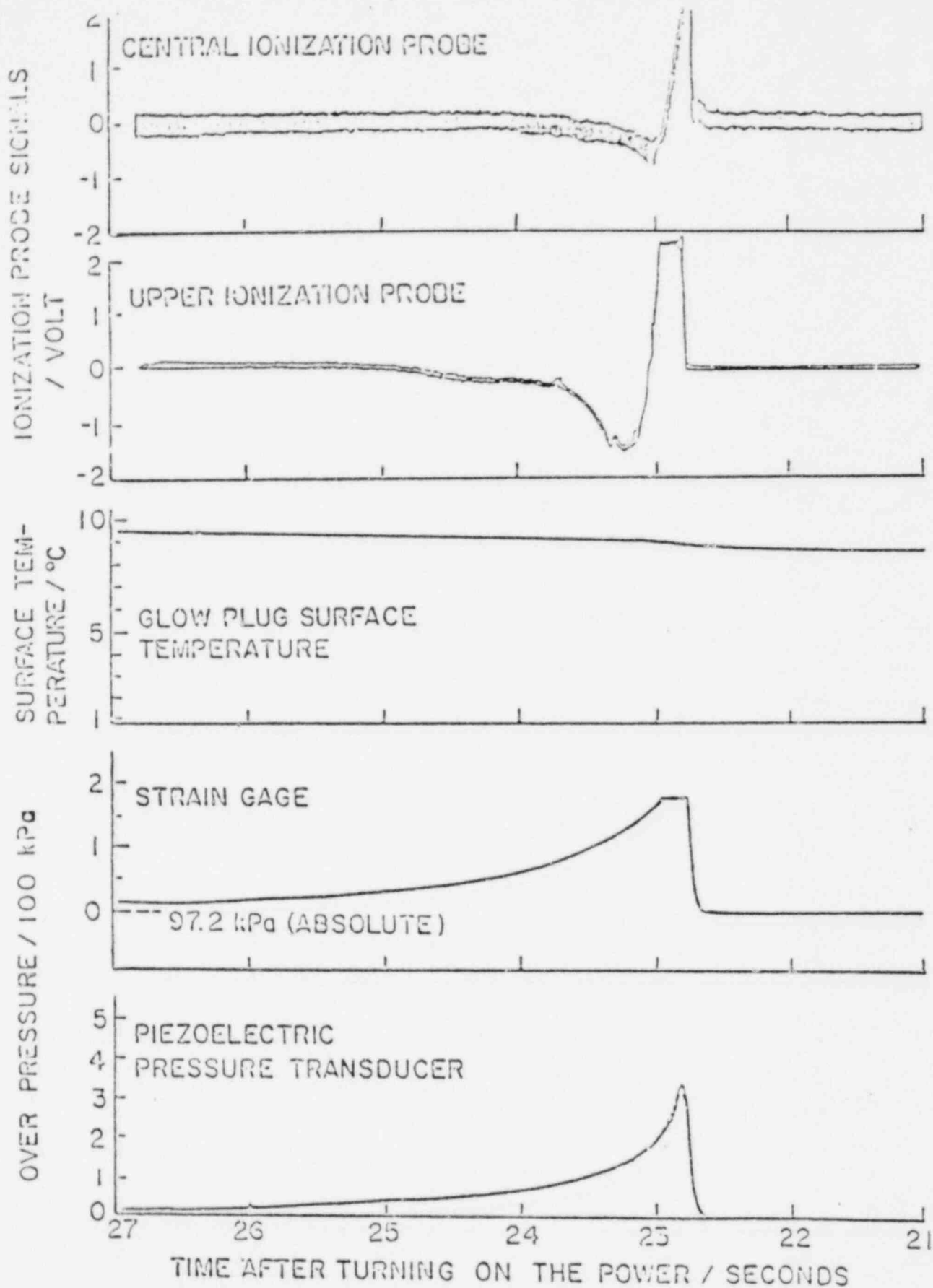
FIGURE 6

OBSERVED TRANSIENTS IN THE IGNITER EFFICIENCY TEST. A GM AC NO. 7 GLOW PLUG OPERATED AT 14 VAC IN A 12.6%-HYDROGEN/20.5%-STEAM MIXTURE IN A 17-LITRE VESSEL.
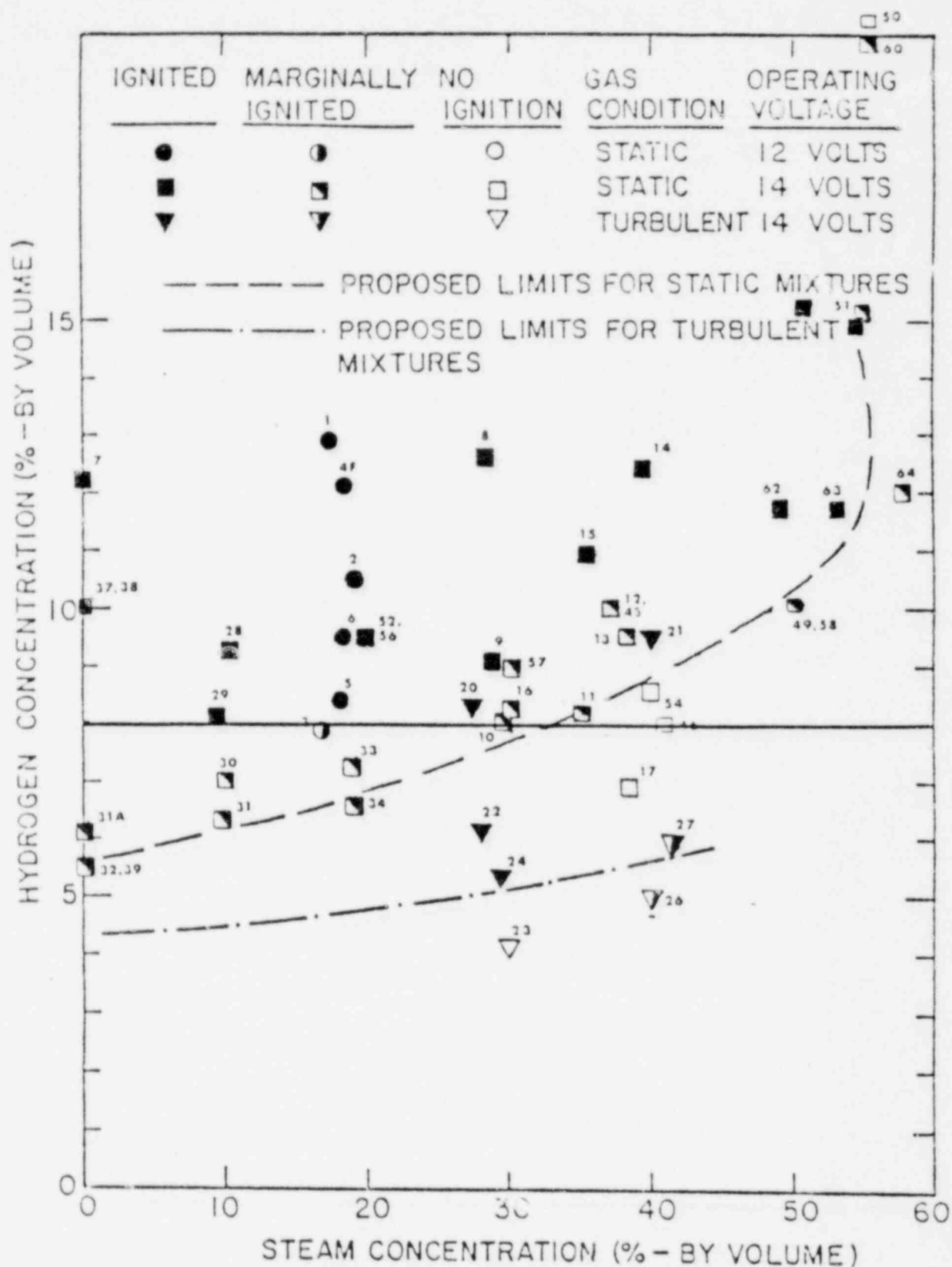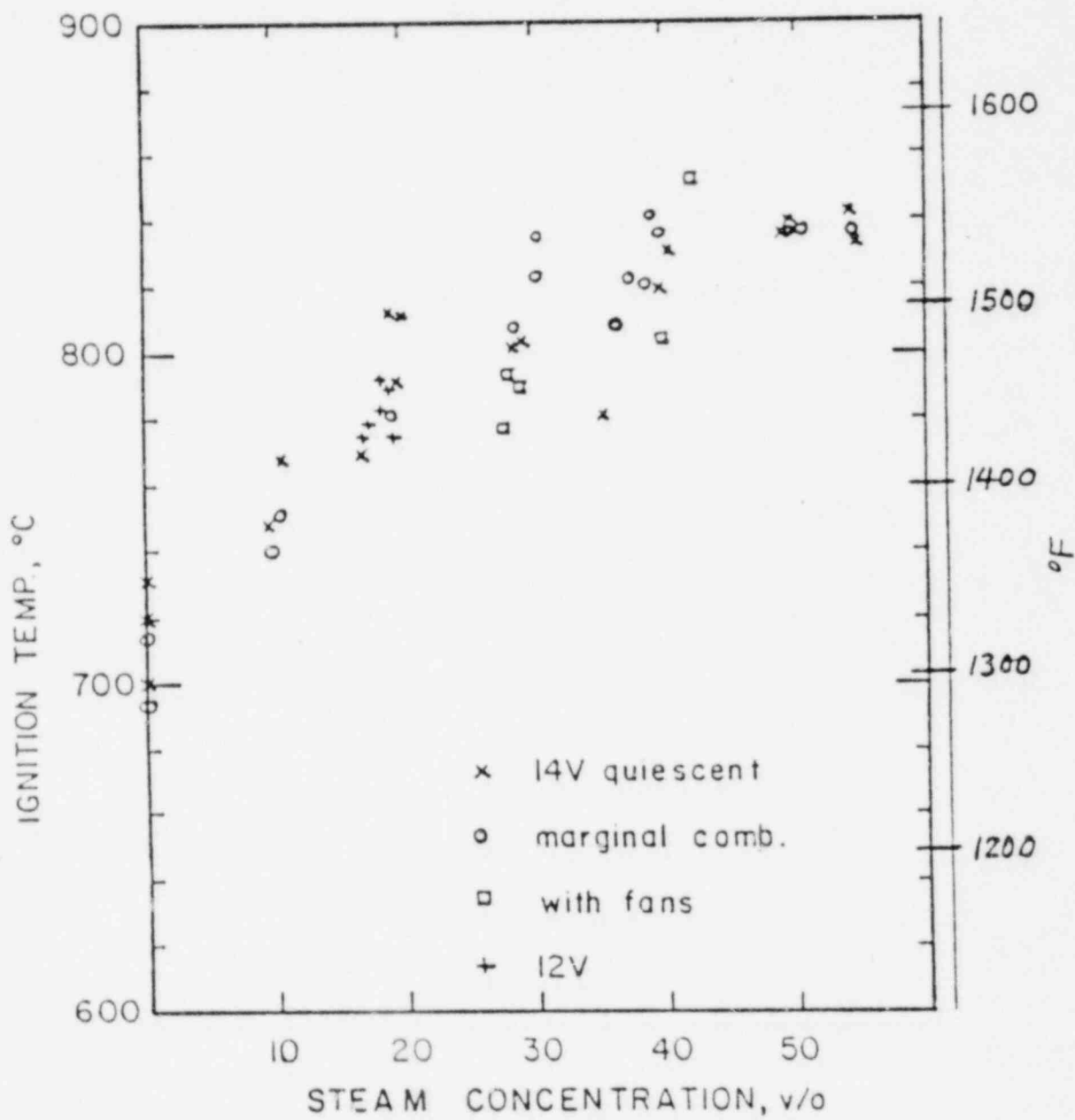
FIGURE 7

THE IGNITION LIMITS OF HYDROGEN / AIR / STEAM MIXTURES
USING A GM AC MODEL NO. 7 THERMAL GLOW PLUG LOCATED
AT THE CENTRE OF A 17-LITRE QUASI-SPHERICAL VESSEL.

FIGURE   8

APPENDIX 2J

COMBUSTION PHENOMENA

INTERIM PROJECT REPORT

STUDY OF HYDROGEN COMBUSTION
NEAR LOWER FLAMMABILITY LIMITS

INTERIM PROJECT REPORT
DECEMBER, 1981

Prepared by:

K. K. Shiu, American Electric Power
F. G. Hudson, Duke Power Company
J. J. Wilder, Tennessee Valley Authority

Project Conducted at:

Whiteshell Nuclear Research Establishment

Project Sponsors:

American Electric Power Service Corporation
Atomic Energy of Canada Limited
Duke Power Company
Electric Power Research Institute
Tennessee Valley Authority
Ontario Hydro

CONTENTS

1.   INTRODUCTION

This report provides preliminary information on the
Whiteshell combustion study currently underway at the
Containment Test Facility at Whiteshell Nuclear Research
Establishment. Included in this report are static and
turbulent test results obtained for varying pre-mixed
hydrogen mixtures. Data on the effects of turbulence are
also presented.

2.   DESCRIPTION AND INSTRUMENTATION OF THE TEST FACILITY

2.1   DESCRIPTION OF THE TEST FACILITY

The test configuration consists of two test volumes: a
sphere and a pipe which may be interconnected. The
dimensions of the two vessels are shown in Table 1.
For the series of experiments reported here only the
sphere is used, Figure 1. The pipe/sphere geometry
experiments are being conducted at the test facility.

The sphere has three large openings and several small
ones. The smaller openings are used for mounting
instruments and measurement probes. The sphere is
insulated and trace heated with steam. The temperature
of the sphere can be maintained at any desired value up
to about 275° F (135° C). Steam is injected into the
sphere through one of the ports when it is required. A
view of the sphere is shown in Figure 1. Two fans
driven by air motors are mounted diametrically opposite
to each other as shown in Figure 2. Some of the fan
characteristics are shown in Table 2.

2.2   INSTRUMENTATION

A schematic of the instrumentation within the sphere is
shown in Figure 3. The transient pressures during
combustion were measured by three piezoelectric type
transducers with a rise time of 2 microseconds and a
Rosemount capacitance transducer with a response time
of 0.2 seconds. The piezo-transducers were mounted
flush with the inner surface of the flanges. A
resistance temperature detector was employed to monitor
the steady state temperature of the gases. It was not
intended for fast transient measurements.

A spark ignition source was used for all the tests
performed in this facility. The use of a spark made it
easier to instrument these experiments.

The passage of the flame front was detected by two
seven point ion probes mounted approximately in the
radial direction opposite to each other as shown in
Figure 3. The departure from the radial direction was

slight, so for all practical purposes the orientation of the probes can be assumed radial. Each of the seven points consisted of two electrodes of .04 inches (1 mm) diameter bare wires separated by .08 inches (2 mm) gap. The ion probes for these experiments were developed by Liu et. al. and details are presented in reference (1).

The signals from the piezoelectric transducers and ion probes were processed by an analog to digital convertor with a scan time of 1.5 millisecond per scan. For low hydrogen concentration experiments this was considered adequate. A two channel transient recorder was available for any selected two channels, if required.

All the transducer and probe amplifiers were mounted as close to the vessel as practically possible in purge boxes and explosion proof casing so that the cables connecting the transducers and the amplifiers were not excessively long.

The gases in the sphere before and after combustion were measured using a gas chromatograph employing a Hydrogen Transfer System (HTS). The details of the chromatograph, its calibration, and sampling technique are given in reference (2). A schematic of the sampling loop is shown in Figure 4.

3.   EXPERIMENTAL PROCEDURE

3.1 PREPARATION OF THE MIXTURE

First, the vessel was evacuated to a sufficiently low pressure, 0.73 lb/in^2 (5 kPa absolute). Next, hydrogen was introduced to the appropriate partial pressure, followed by the introduction of steam and air to their partial pressures. The gases were further mixed by turning on the fans for about 30 seconds prior to the initiation of any test.

3.2 SAMPLING

Before any sampling was initiated at least two calibration mixtures were run through the gas chromatograph (GC) several times to ensure the proper performance of the GC. Only when the GC measurements were repeatable, was the sampling loop activated. The sampling lines run from the sphere to the control room and are steam trace heated all the way to the injection port.

The sampling line was thoroughly flushed by the mixture in the sphere for at least 5 minutes to ensure that the sample passing through the GC was the same as that in the sphere. Two samples were normally taken and, if the two GC measurements agreed with each other and also with the amount of hydrogen introduced by the partial pressure method within the limits of accuracy, it was assumed that the constituents were in the right amount to carry out the test. The same procedure was repeated for sampling the combustion products. The products were mixed by turning on the fans before sampling. Table 3 shows the precision of the gas chromatograph. The accuracy shown represent the upper limits. However, the measurements tended to be much more accurate than what the numbers indicate. For example, a calibration mixture with 9.62% hydrogen was measured by the partial pressure method and by the GC within ±0.2%.

3.3 TURBULENT COMBUSTION EXPERIMENTS

In this case the fans were turned on for a short time (~ 1 minute) before ignition and were kept operating during the test. Though the fan speed can be varied, the present series of experiments have been done at a constant fan speed of about 1500 rpm.

Measurements of the turbulence created by the fan have been made in the open atmosphere simulating conditions prototypic of those in the sphere. The results are shown in Figure 8. The turbulent intensities, which can be represented by the root mean square of the difference between the local velocity squared and the mean velocity squared, indicate the degree of local fluctuations in the velocity components at that particular location. For instance, at a location ten inches away from the fan in the axial direction and zero inches away from the central axis, the RMS velocity is about 9.5 feet per second, whereas at the same axial distance, but at a radial location four inches away, the RMS velocity increases to 10.5 feet per second, which indicates an increase in the degree of turbulence of the second location.

4. RESULTS AND DISCUSSION

4.1 COMBUSTION AT LOW CONCENTRATIONS

Combustion of hydrogen at low concentrations of
around 5% hydrogen by volume is characterized by
low burning velocities and a low degree of burn
completeness. Only about 20% of hydrogen is
burned. Figure 5 shows the pressure time history
for a 5% H_2 in air and steam-air mixtures. In
In this case, it appears that combustion is
dominated by buoyancy effects. The fireball
initiated at the bottom moves upward at a speed
greater than the burning velocities of the mixture
and no downward propagation is possible. Thus for
low initial hydrogen concentrations only a small
fraction is burned. Larger concentrations result
in correspondingly increased amounts of hydrogen
burned and higher peak pressures. Once the
fireball reaches the top, it is quenched and the
pressure in the system decays.

The middle curve of Figure 5 shows the pressure
time history of 5% hydrogen with 15% steam added.
The behavior seems to be similar to the dry case
except that the peak pressure in the system is
lower. The extent of combustion is virtually the
same and the reduced pressure can be attributed to
the increased heat capacity of the mixture due to
the presence of steam. This results in reduced
flame temperatures and thus in reduced peak
pressures. The behavior of a 30% steam case is
similar to that of a 15%.

4.2 COMBUSTION AT RELATIVELY HIGH H_2 CONCENTRATIONS

The extent of combustion at higher hydrogen
concentrations, around 8% by volume, is
characterized by 100% burning. The pressure peaks
are much higher than the 5% tests depicted in
Figure 5 as can be expected. Figure 6 shows
combustion at 8% H_2. Addition of 15% steam has
not altered the shape of the curve very much. The
reduction in peak pressure, as explained earlier,
is due to increased heat capacity of the mixture
yielding lower flame temperatures. Combustion in
both dry and 15% steam case resulted in 100%
hydrogen consumption.

The bottom curve of Figure 6 is for 30% steam addition. In this case only about 38% H_2 was burned and the peak pressure is about 25% that of the fully burned case. Larger quantities of steam appear to reduce the burning velocity of the mixture by decreasing the flame temperature and increasing the radiation loss from flame to steam. As the burning velocity is reduced, the combustion is again governed by buoyancy effects and downward flame propagation is negligible.

These findings agree with the findings of Liu et al (3) that moderate (0-15%) steam additions do not affect significantly the degree of combustion for bottom ignition.

4.3 EFFECT OF TURBULENCE

It has been well established that turbulence enhances the rate and degree of combustion. Recent investigations of Abdel-Gayed et al (4) have shown that turbulence effects are large even for hydrogen. Preliminary results from these tests appear to confirm their conclusion. This is illustrated in Figure 7 by plotting pressure as a function of time for the combustion of 5.5% hydrogen-air mixture with and without fan. The dashed curve is for the quiescent mixture. The degree of burn is only 26%, showing the dominance of buoyancy. The corresponding pressure rise is only a small fraction of the calculated adiabatic pressure rise. When turbulence is produced by turning on the fans, the rate of combustion is increased drastically and nearly 83% of the hydrogen initially present is burned. The peak pressure observed is close to the adiabatic pressure expected for 83% burn. The peak pressure measured is 15.2 psi (105 kPa) and the pressure calculated for adiabatic burning is 18.6 psi (128 kPa). The adiabatic pressure rise is 6.1 psi (42 kPa) with 26% burn and the measured is about 3.5 psi (24 kPa).

A further comparison of combustion with and without turbulence is shown in Figure 9 which is for 7% hydrogen. Data for both 7% and 8% (figure 9A) hydrogen cases show complete combustion with or without fan turbulence. For bottom ignition seven percent hydrogen with quiescent burning

appears to be the minimum concentration for complete combustion at 212° F (100° C). All other concentrations above 7% result in complete burning. This value is lower than the 8.5% hydrogen limit for complete combustion at 86°F (30° C). Increase in initial temperature results in an apparent shift in the downward propagation limit, thus allowing more complete combustion.

Figure 10 is a summary of several tests with and without turbulence. The mixtures were ignited either at the top or at the bottom as shown. For cases with the fan in operation, data consistenty revealed more complete combustion and a noteable increase in combustion peak pressure.

The lowest concentration at which the downward propagation could be achieved in a quiescent mixture was observed to be 8.5% hydrogen for top ignition.

4.4 EFFECT OF TURBULENCE WITH STEAM ADDITION

Figure 11 shows the effect of added steam when turbulence is present. Normally, 30% steam would exhibit limiting effects on combustion of the mixture when no turbulence is present (see Figures 5 and 6). But as can be seen from Figure 11, its affect on combustion in the presence of turbulence is minimal. The peak pressure with steam is reduced due to the increased heat capacity of the mixture.

Steam and turbulence have competing effects on combustion; whereas the addition of steam tends to reduce the rate and degree of combustion, turbulence promotes rapid and more complete combustion.

4.5 EFFECT OF HYDROGEN CONCENTRATIONS WITH TURBULENCE

As the hydrogen concentration is increased from 5.5% to 8%, combustion progresses from a partially burned to a fully burned situation. The rate of combustion also appears to increase with concentration.

Figure 12 presents the resulting pressure rise as a function of time for various hydrogen concentrations with turbulence. It can be noted that as the concentration is increased, the time to reach maximum pressure is shortened.

Though most of the results presented here are for bottom ignition, it is expected that similar arguments hold true for central ignition.

4.6 EFFECT OF STEAM ADDITION AND TURBULENCE ON COMBUSTION WITH CENTRAL IGNITION

Figure 13 shows the relative effects of steam and turbulence on the rate of burning. At 7% hydrogen in air the pressure rise at first is slow indicating that the fireball is moving upwards. When it reaches the top, the downward propagation starts and the entire combustion occurs in about 12 seconds. Hydrogen was nearly fully burned. Addition of 15% steam to such a mixture almost completely suppressed combustion. The pressure rise was trivial, indicating that only very little hydrogen was burned. Gas chromatography measurements showed that less than 0.5% hydrogen was consumed. The apparent difference in combustion behavior between what is shown on Figure 13 and Figure 5 can be ascribed to principally a hydrogen concentration difference and possibly the difference in igniter location.

The effect of steam disappeared once the fans were turned on indicative of the ability to promote combustion by turbulence.

4.7 EFFECT OF IGNITOR LOCATION

Ignitor location affects the degree and rate of burn significantly in lean quiescent mixtures. This is illustrated in Figures 14 and 15. Figure 14 shows the difference between central and bottom ignition with 8.5% hydrogen at room temperature and Figure 15 with 7% hydrogen at 100° C. It is clear from the figures that bottom ignition results in faster combustion at these concentrations. This is in contrast to combustion at hydrogen concentrations in excess of 10% where central ignition will exhibit faster combustion than bottom ignition due to the diminishing effects of buoyancy. For a spherical vessel, with central ignition the flame will propogate in all directions over a distance of the radius of the shere; whereas for bottom ignition at 10% hydrogen the flame will propogate over twice the distance of the radius.

4.8 TEMPERATURE EFFECTS ON FLAMMABILITY LIMITS

Though the purpose of the present series of experiments has not been one of establishing the limits of propagation, it does in a way shed some light on the process that must be taking place. Figure 16 shows the combustion peak pressures plotted against hydrogen concentration. For quiescent mixtures, the pressure rise is abrupt above about 8% hydrogen suggesting that the nature of flame propagation or combustion has changed. Agreement between the present data and the data of Furno et al (5) is good.

Figure 17 is similar to Figure 16 except that it is drawn for bottom ignition. Here also the threshold concentration is around 8% hydrogen. This can be compared with Figure 10. The shift to the left of threshold concentration at elevated temperature is obvious. A test was conducted to establish if indeed the downward propagation limit has shifted to 7%. A mixture containing 7% hydrogen was ignited at the top. The mixture failed to ignite even after several attempts under quiescent conditions. However, the mixture could be ignited down to 5.5% when fans were turned on.

Using the information provided in references (6) and (7) and assuming that the flammability limit for downward propagation as 9%, the estimated value for the downward limit at 100° C is about 8.5% hydrogen, agreeing with present work. The downward propagation in the sphere experiments, when ignited at the center or bottom, may not necessarily be related to the propagation limit. The propagation under these conditions may be due to some turbulence or circulation currents set up by the moving flame.

Figure 18 shows that combustion is possible even at 5.7% when turbulence is present. From these it could be inferred that the absolute limit of propagation is the limit for upward propagation.

5. CONCLUSIONS

The following conclusions can be made from the present investigations.

1. For small quantities of steam addition, the nature and degree of combustion is not affected very much with bottom ignition. Only at higher steam concentrations, around 30% or above would steam

begin to have significant effects on combustion.

2. Turbulence increases the rate and degree of burn in almost all cases.

3. Bottom ignition results in the highest degree of burn and is more effective in establishing a flame even at very low hydrogen concentrations, with or without fans.

4. Central ignition combustion is more susceptible to the influence of steam in lean mixtures than bottom ignition combustion.

5. For low steam concentrations, around 15%, steam effects if any are not significant in the presence of turbulence.

REFERENCES

1. Liu, D. D. S. et al, "Development of Instrument for Combustion Studies: Part I, Test of Ionization Probes for CTF Applications", WNRE-512-1, (1981).

2. Howe, P. T. and Myers, M. E., "On-Line Gas Analysis for the Containment Test Facility", WNRE Report, WNRE-217.

3. Liu, D. D. S. et al, "Canadian Hydrogen Combustion Studies Related to Nuclear Reactor Safety Assessment", paper 80-33, Western States Section/The Combustion Institute, 1980, 1980 Fall Meeting at Los Angeles, Calif, Oct. 20-21 (1980).

4. Abdel-Gayed, R. G. and Bradley. D., Sixteenth Combustion (International) Symposium pp. 1725-1735, (1976).

5. Furno, A. L. et al, "Some Observations of Near Limit Flames", 13th Combustion Symposium, pp. 593-599, (1971).

6. Shapiro, Z. M. et al, "Hydrogen Flammability Data and Application to PWR Loss-of-Coolant Accident", Bottis Plant, Pittsburgh, WAPD-SC-545, 1957.

7. Edmundson, H and Heap, M. P., "The Burning Velocity of Hydrogen-Air Flames", Combustion and Flame, 16, 161 (1971).

TABLE 1

CTF VESSEL DIMENSIONS

	Sphere	Interconnecting Pipe
Internal diameter (ft)	7.5	0.95
Length (ft)		19.7
Wall thickness (inch)	2.14	.67
Volume (ft^3)	223	17.7
Design pressure (psi)	1450	1450

TABLE 2

FAN DETAILS

Air Motor Speed	1850 RPM (Max)
Motor Horse Power	0.22
Fan Tip Diameter	16 inches
No. of Blades on the Fan	4
Fan Capacity	1500 CFM at 1100 RPM

Continuously Variable speed Motor

TABLE 3

Component	Concentration Range Volume%	Precision (2σ) Volume %
H₂	0.5 - 2.0	0.2
H₂	0 - 30	1.2
O₂	0 - 21	1.6
N₂	70 - 90	2.1
H₂O	3 - 8	0.7

E71351.29
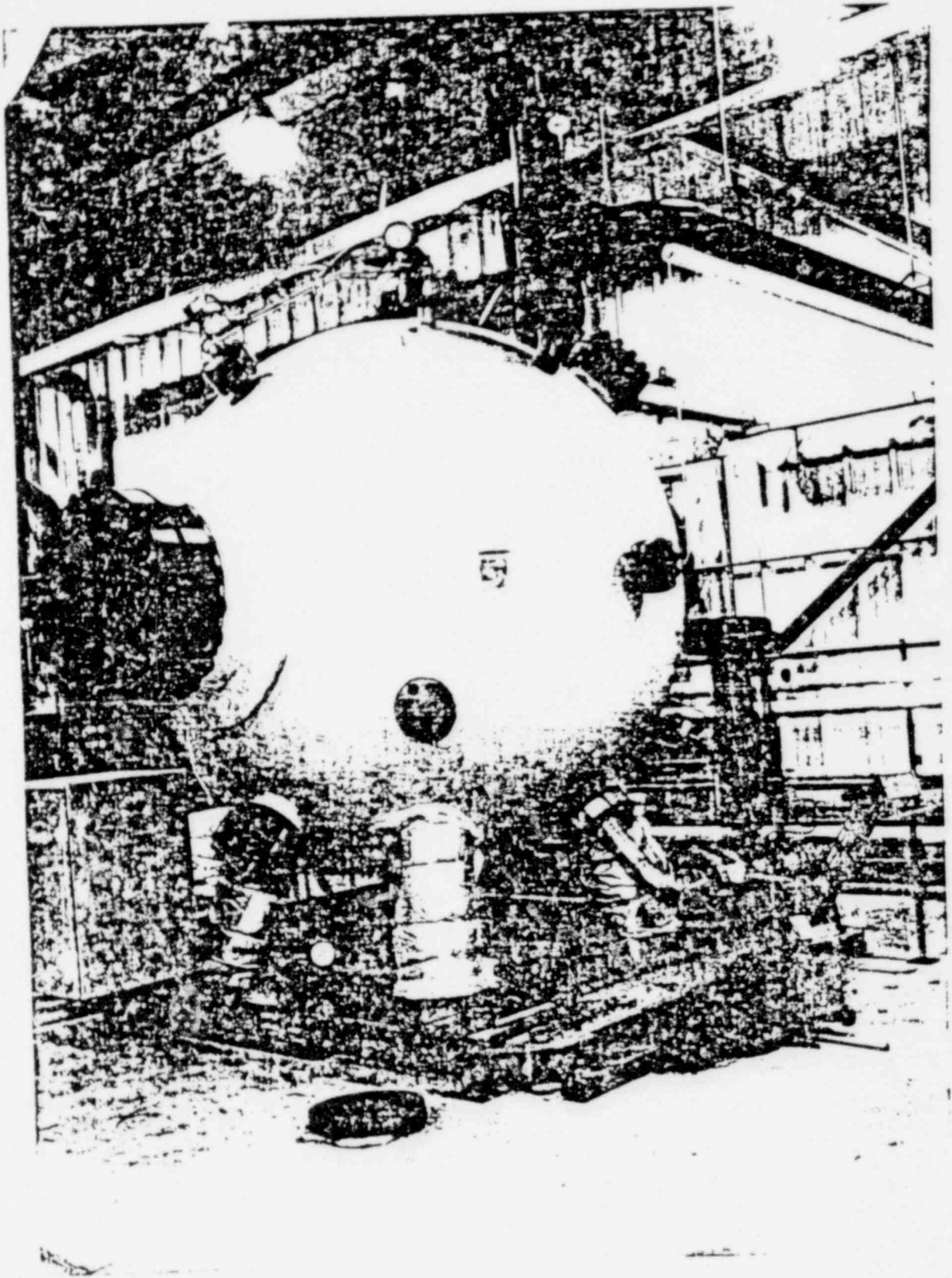
VIEW OF THE SPHERE   Figure-1

Rear fan

steam port

Air motor

Front fan
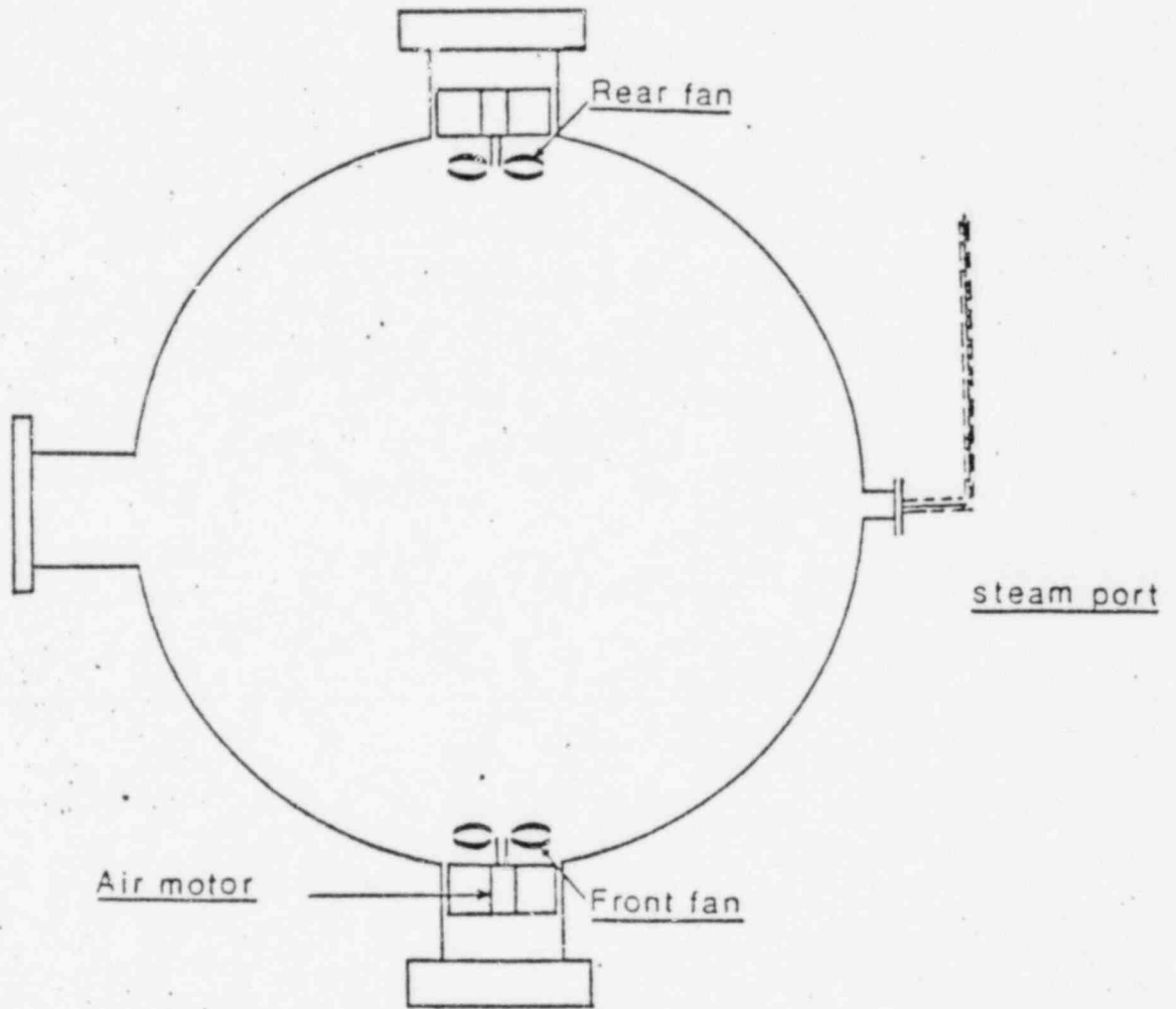
ARRANGEMENT OF FANS

Figure - 2
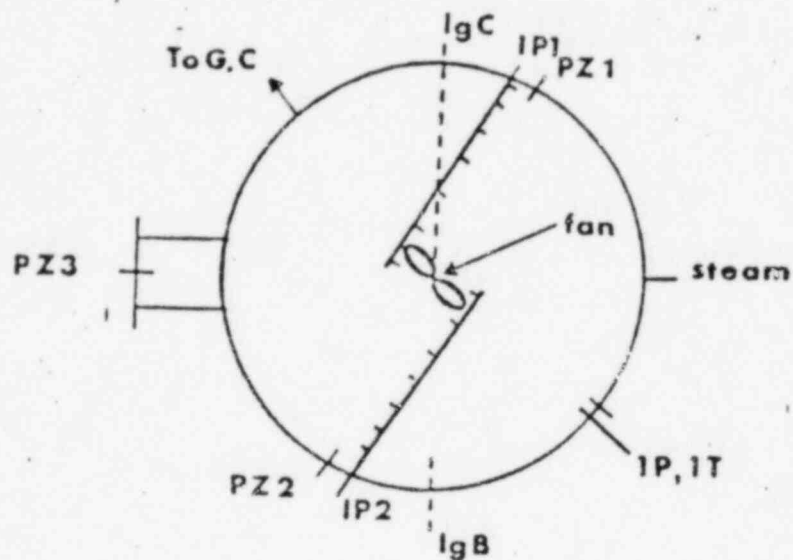
lgB, lgC — Ignitors

IP1, IP2 — Ion Probes

PZ1, 2, 3 — Piezo electric

IP — Process Pressure

SCHEMATIC OF INSTRUMENTATION

Figure −3

SCHEMATIC OF GAS SAMPLING LOOP
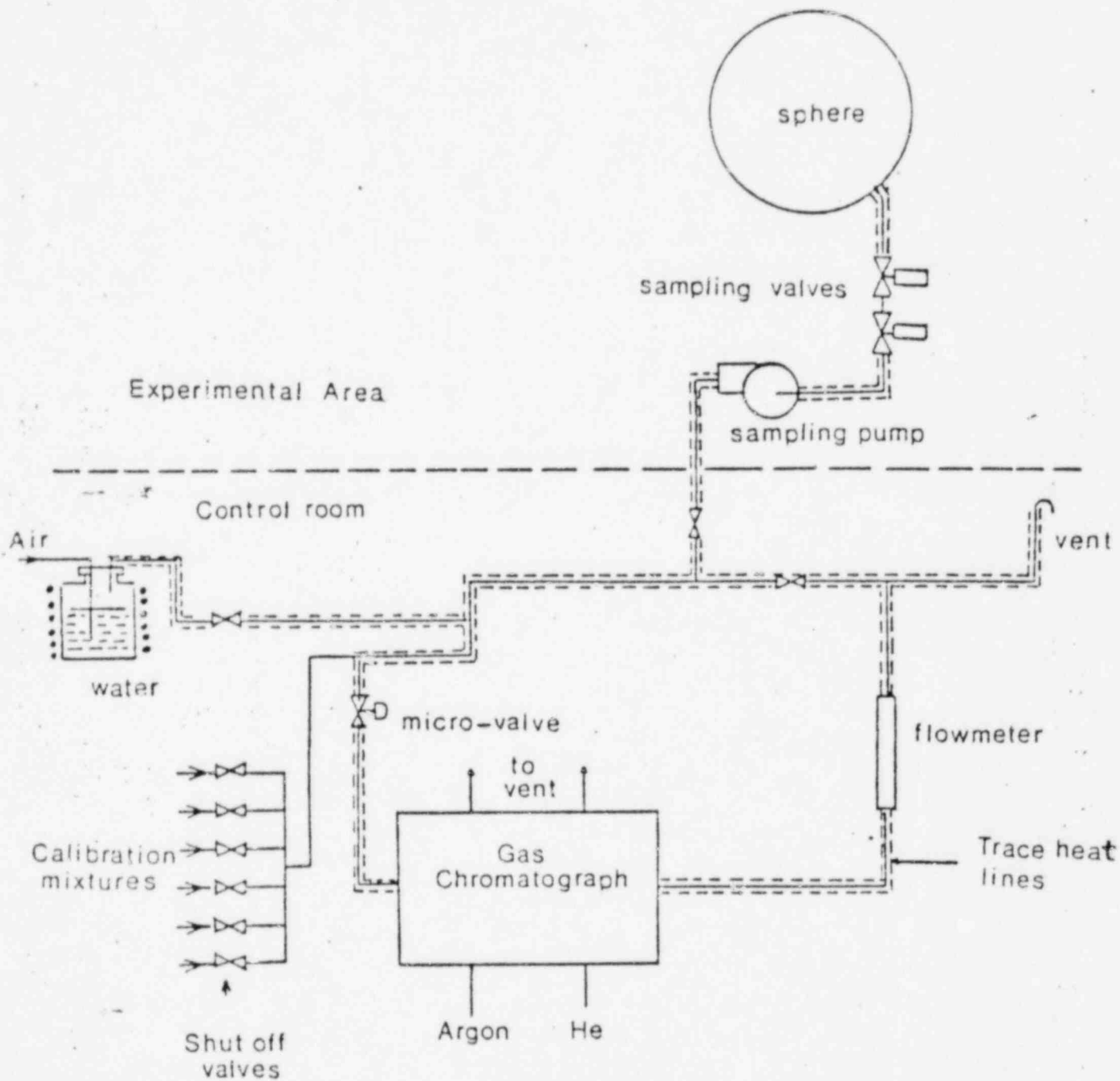
Figure _ 4
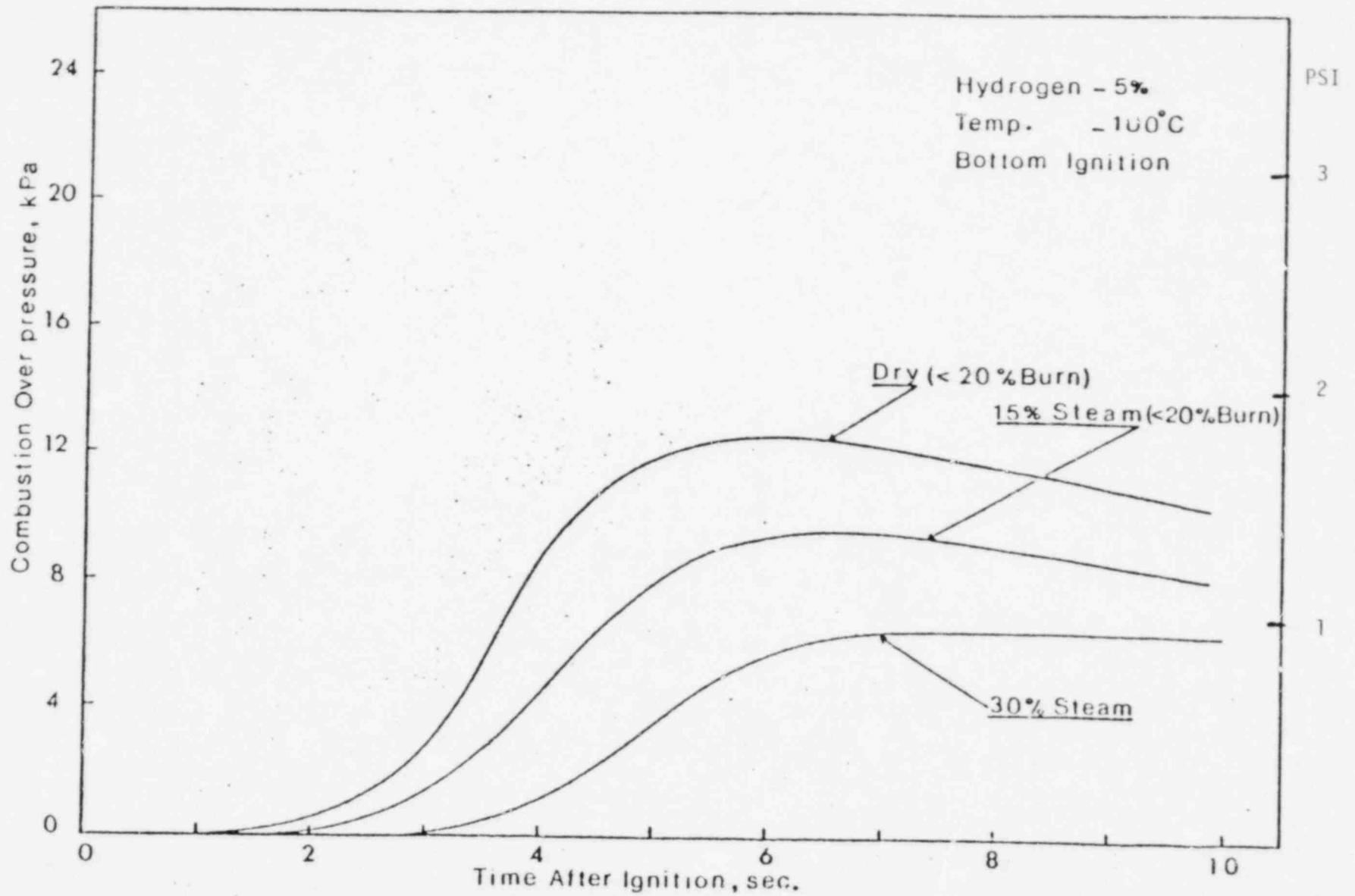
COMBUSTION NEAR LOWER LIMIT FOR UPWARD

FLAME PROPAGATION

Figure – 5
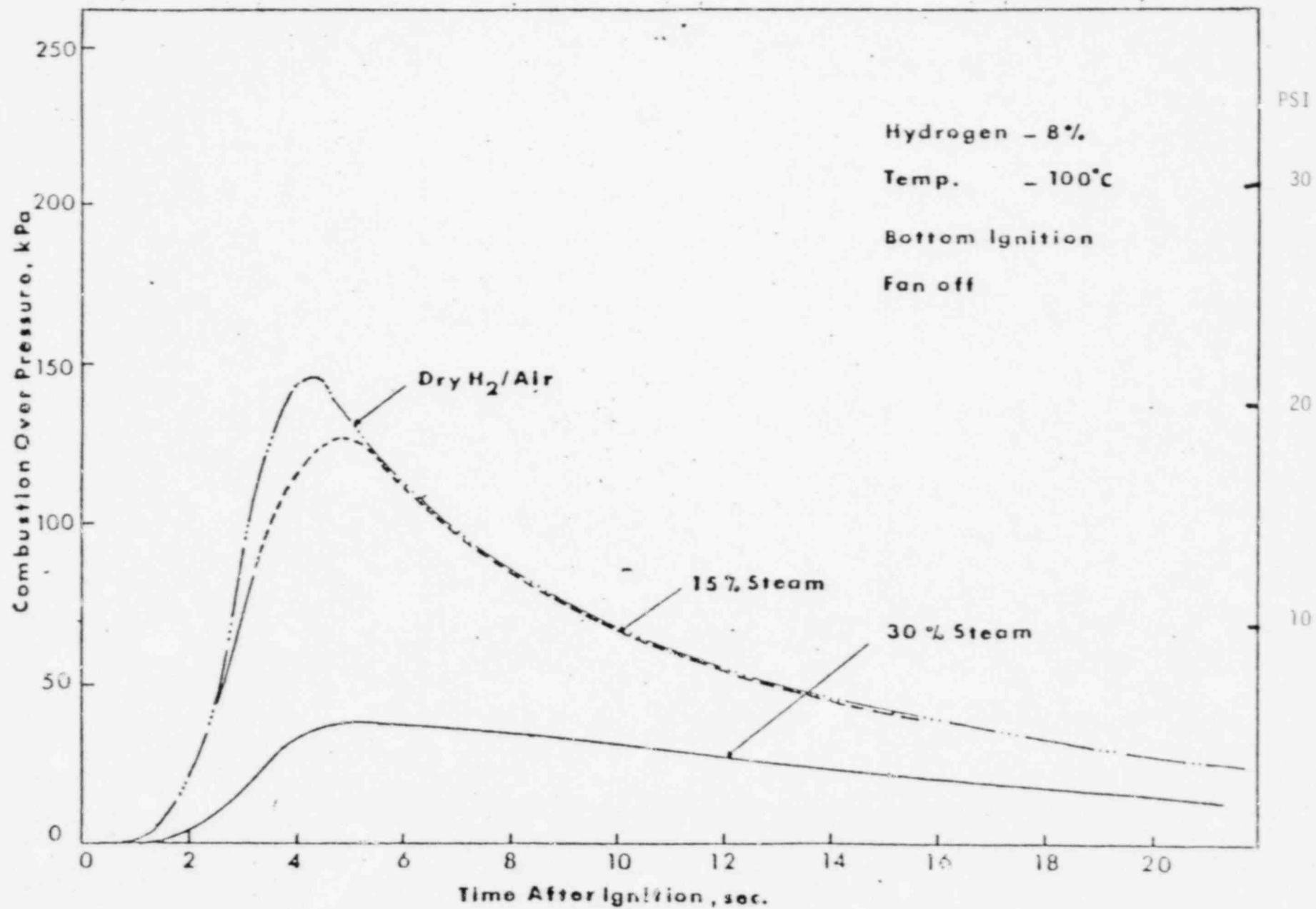
EFFECT OF STEAM ADDITION

Figure - 6
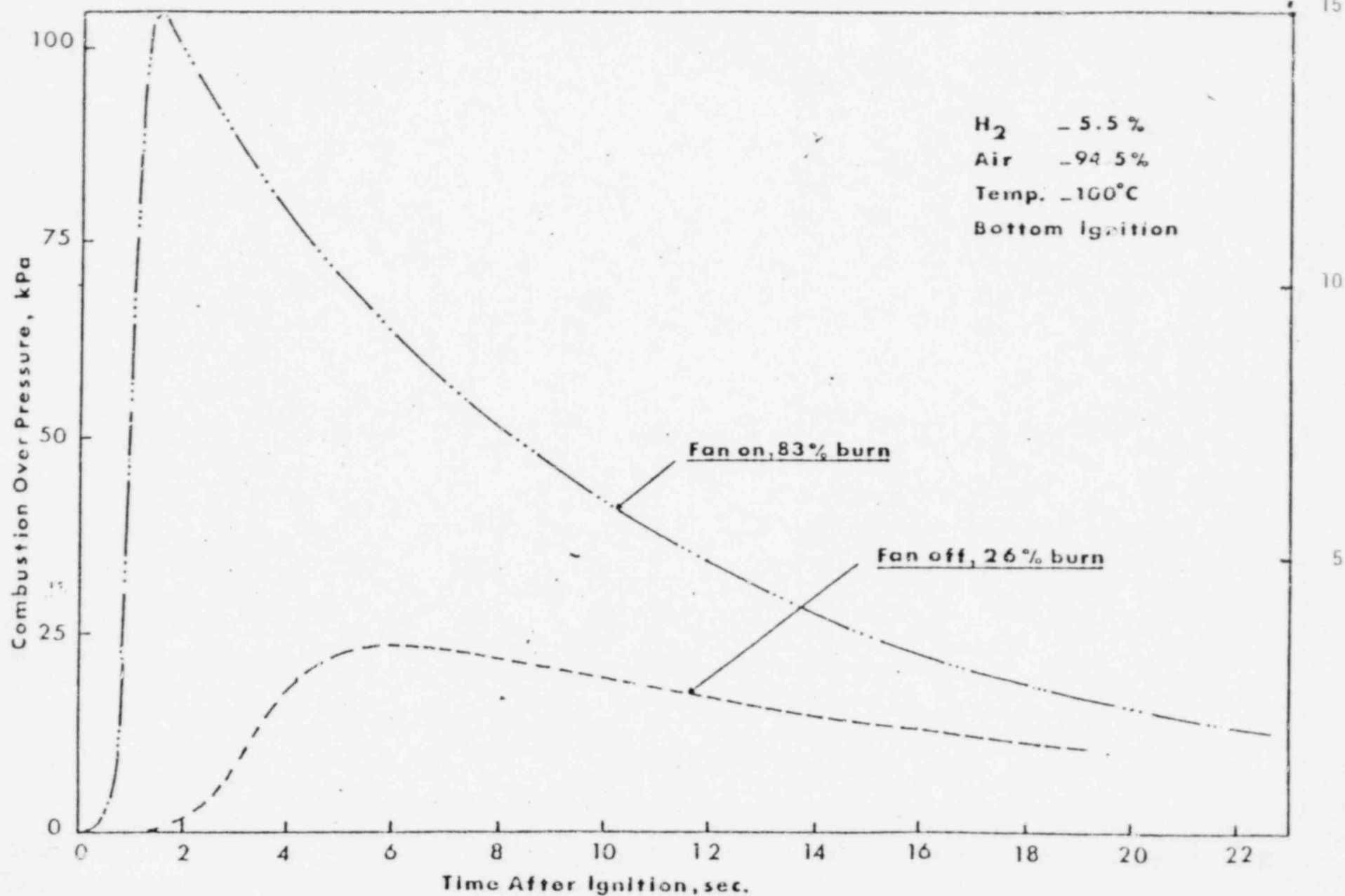
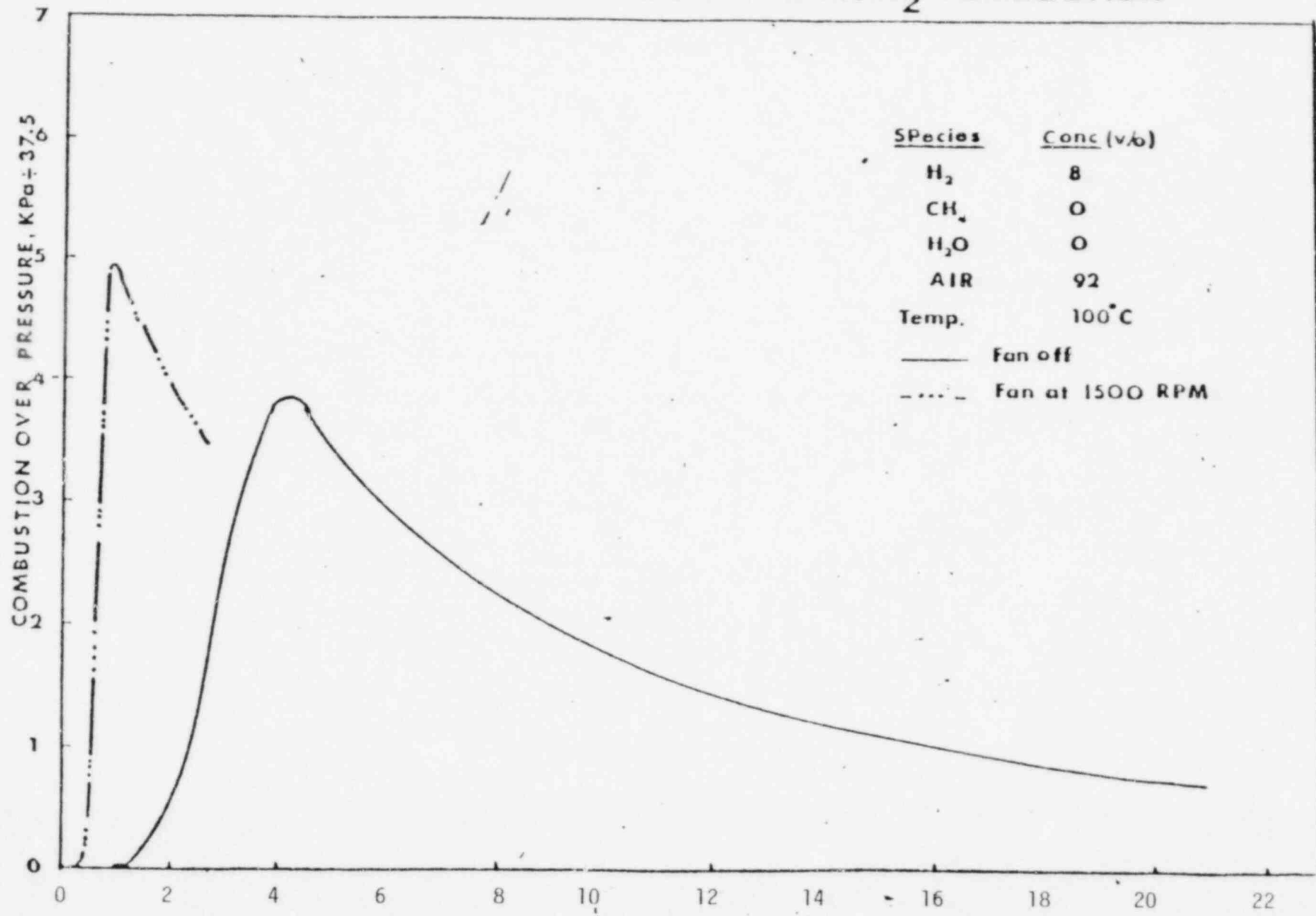EFFECT OF INITIAL TURBULENCE ON H₂ BURN

Figure-7
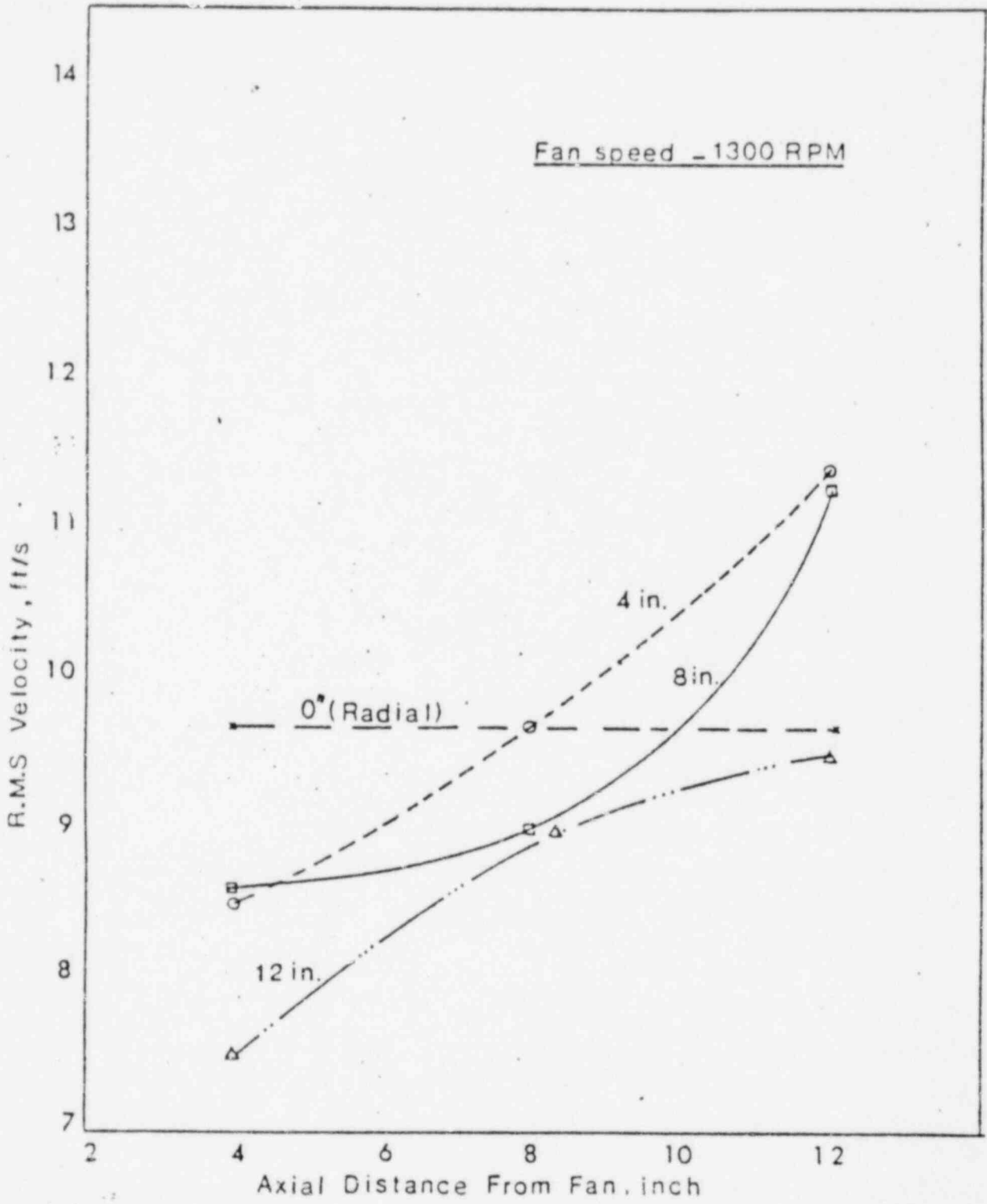
FAN TURBULENCE

Figure -8
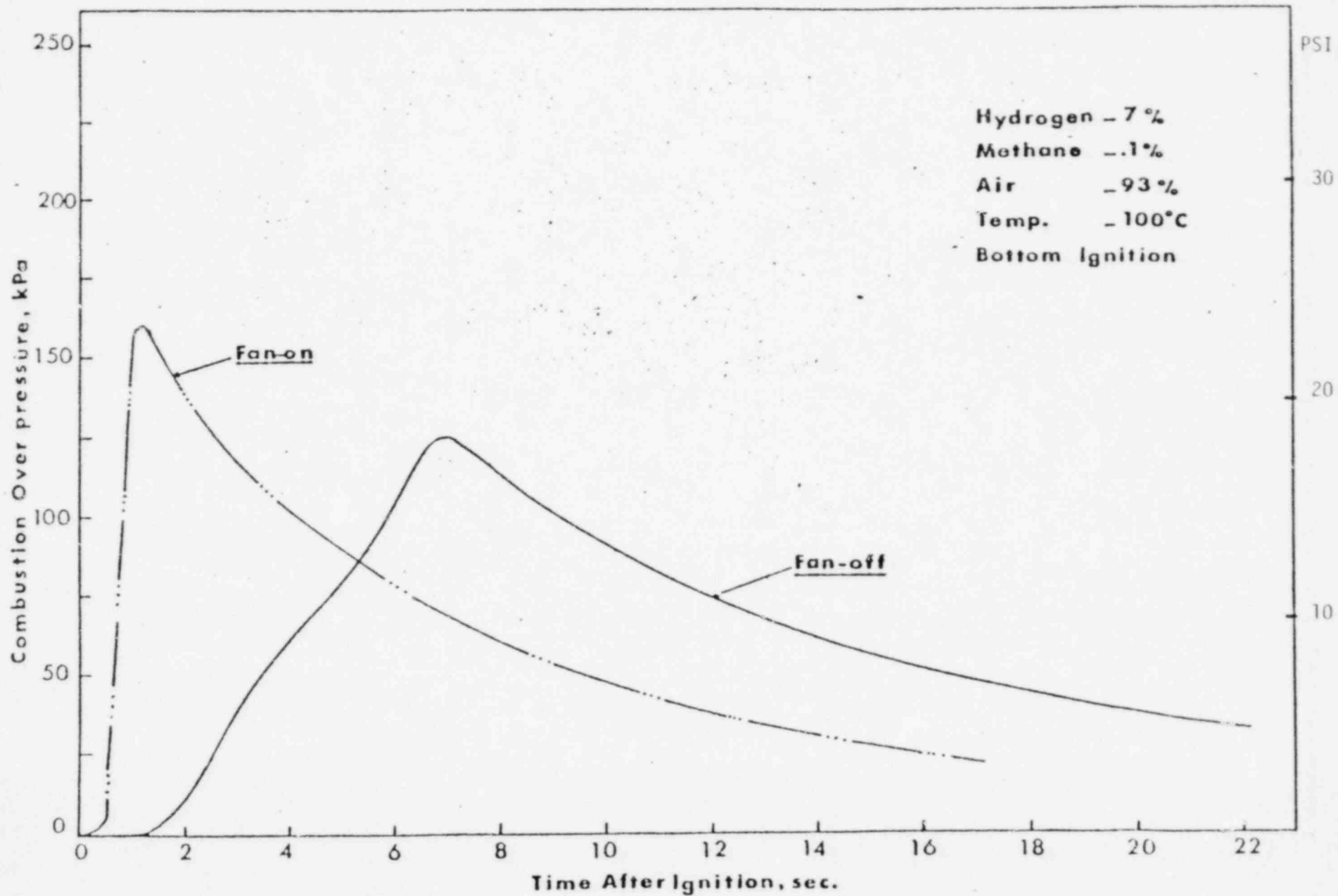
EFFECT OF INITIAL TURBULENCE ON COMBUSTION

Figure-9

EFFECT OF FAN TURBULANCE ON H_2 COMBUSTION

COMBUSTION OVER PRESSURE, KPa ÷ 37.6

Time After Ignition, sec. (Bottom Ignition)

SPecies	Conc (v/o)
H_2	8
CH_4	0
H_2O	0
AIR	92
Temp.	100°C

——— Fan off

–·····– Fan at 1500 RPM
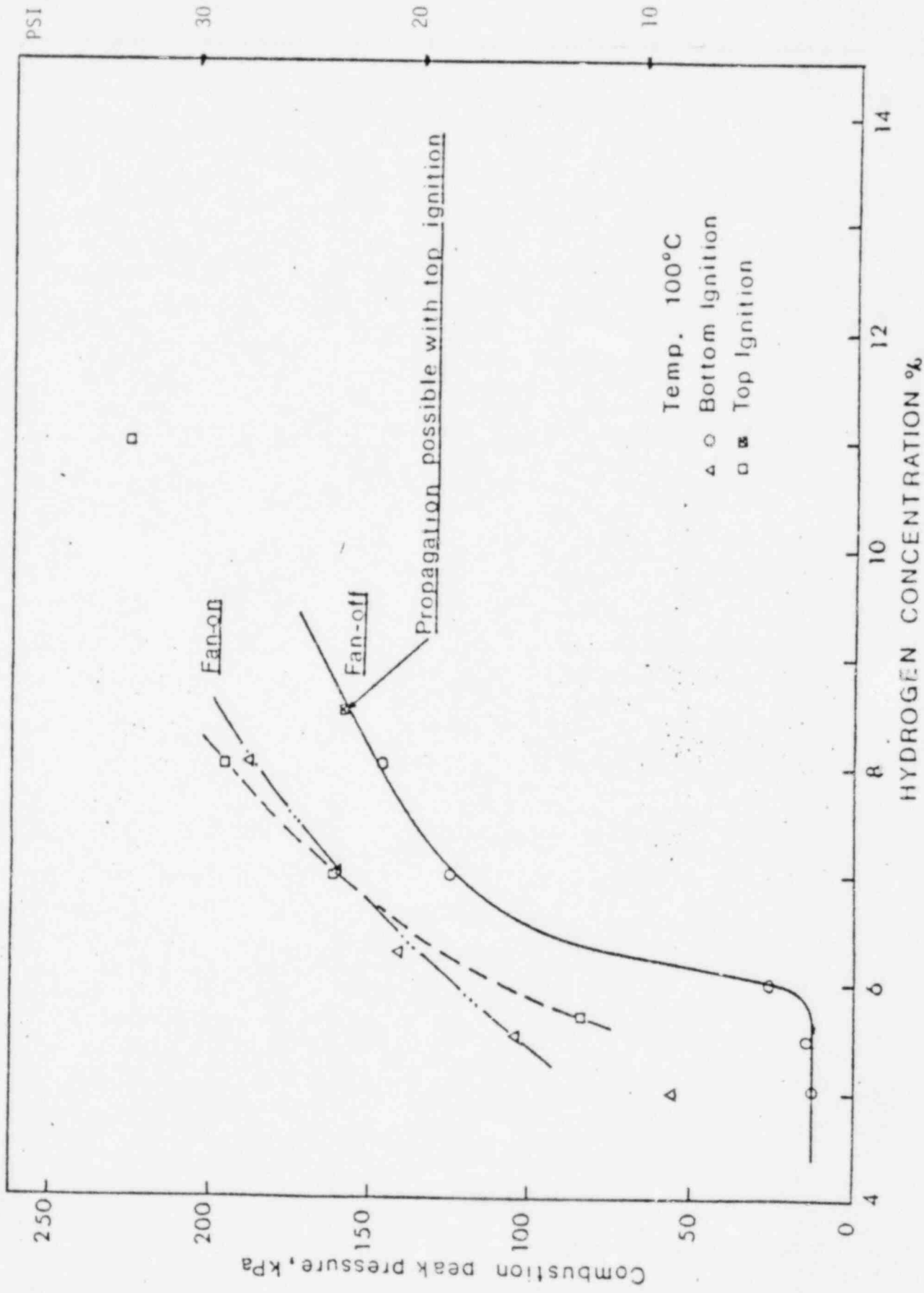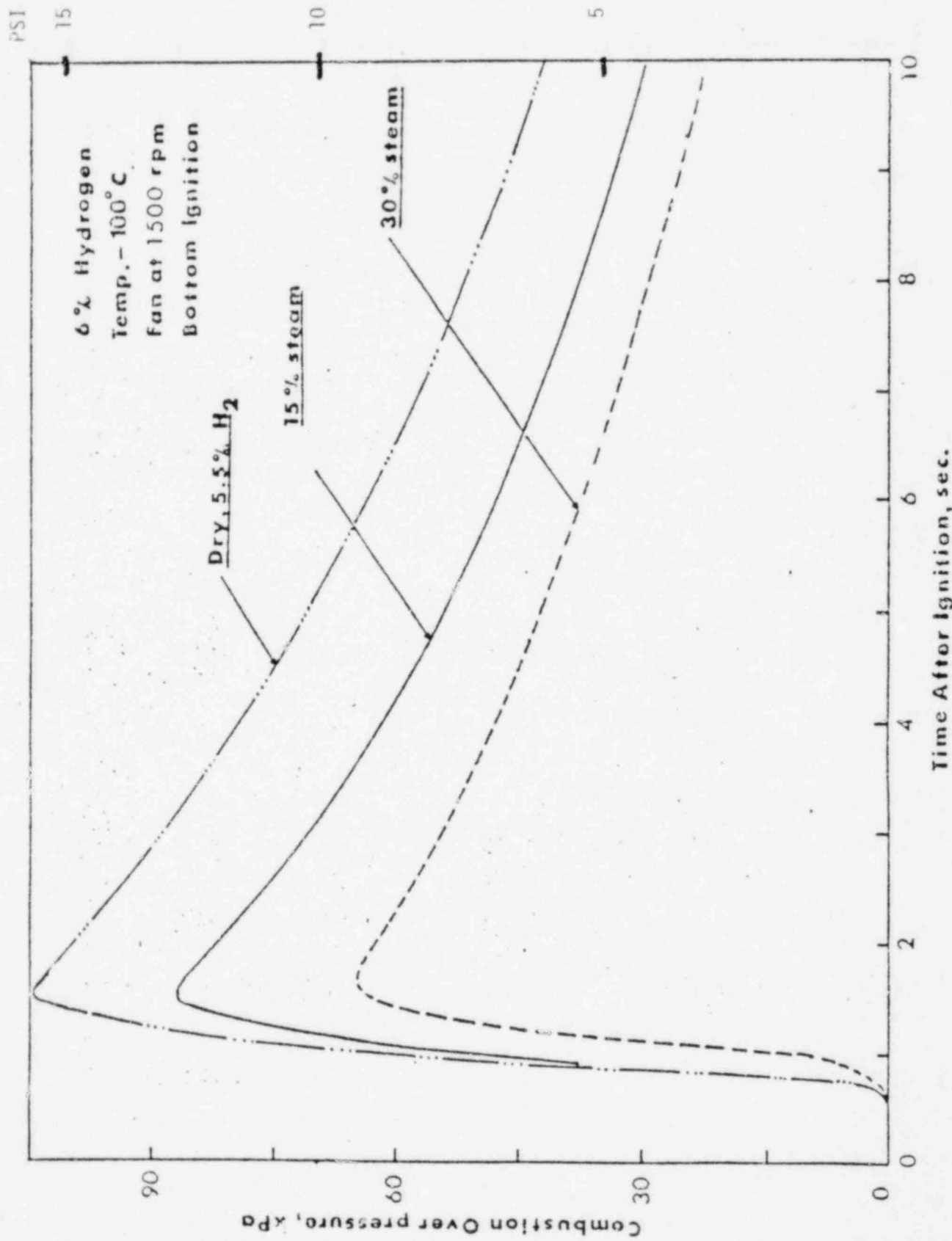
Figure - 9A

Figure - 10

EFFECT OF STEAM WITH TURBULENCE
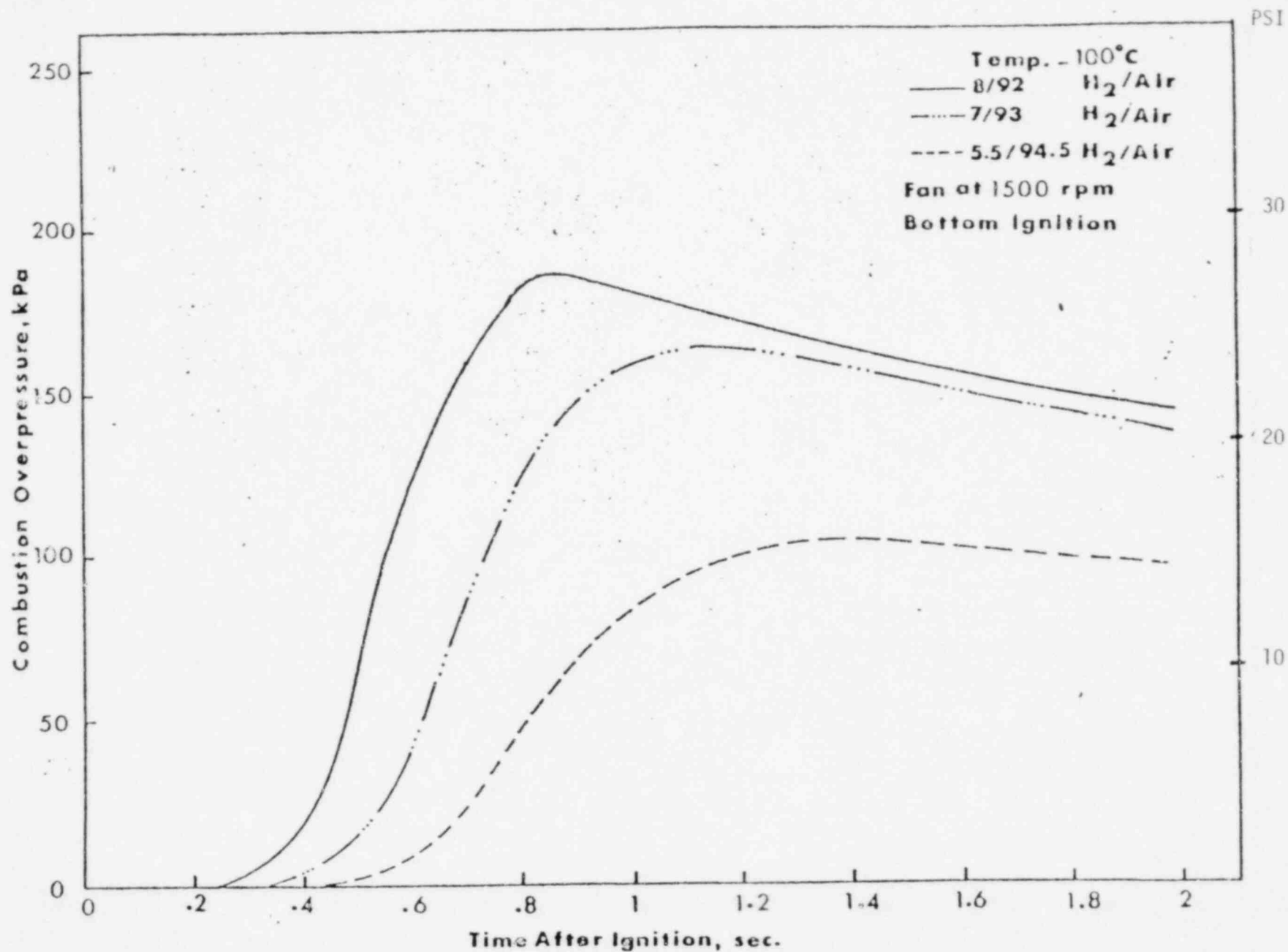
Figure - 11

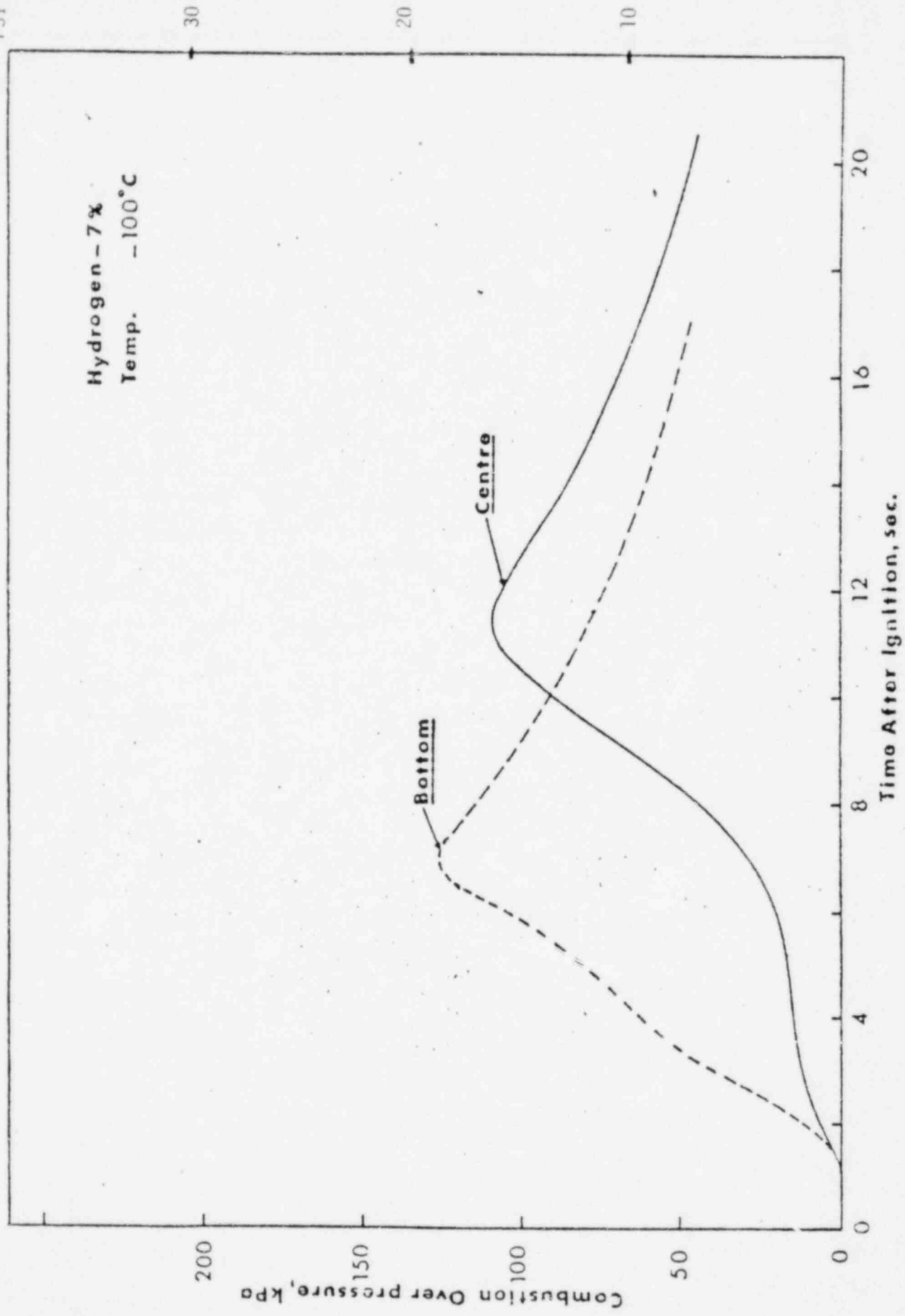**EFFECT OF CONCENTRATION AT CONSTANT FAN SPEED**
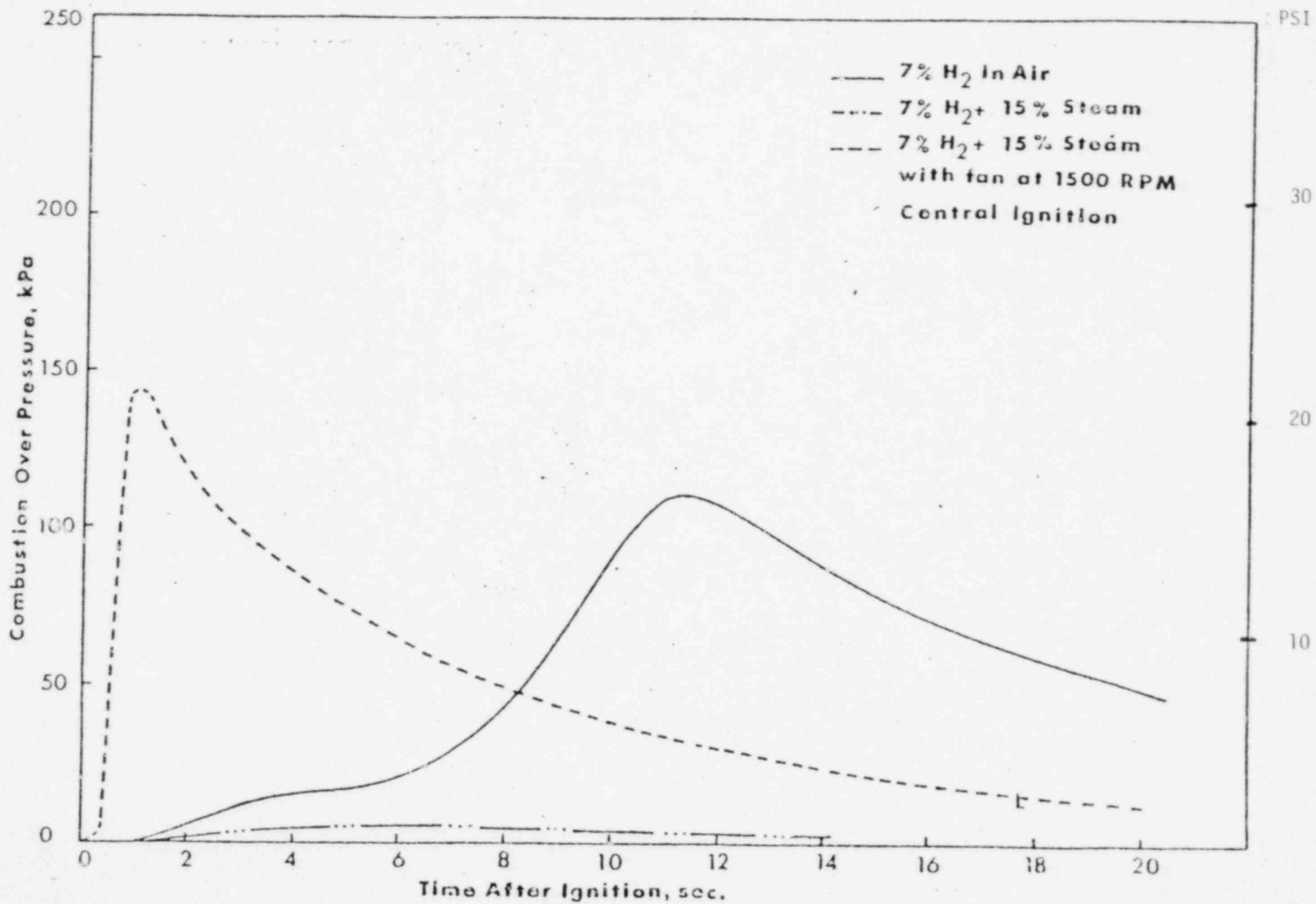
Figure - 12

RELATIVE EFFECTS OF STEAM AND TURBULENCE
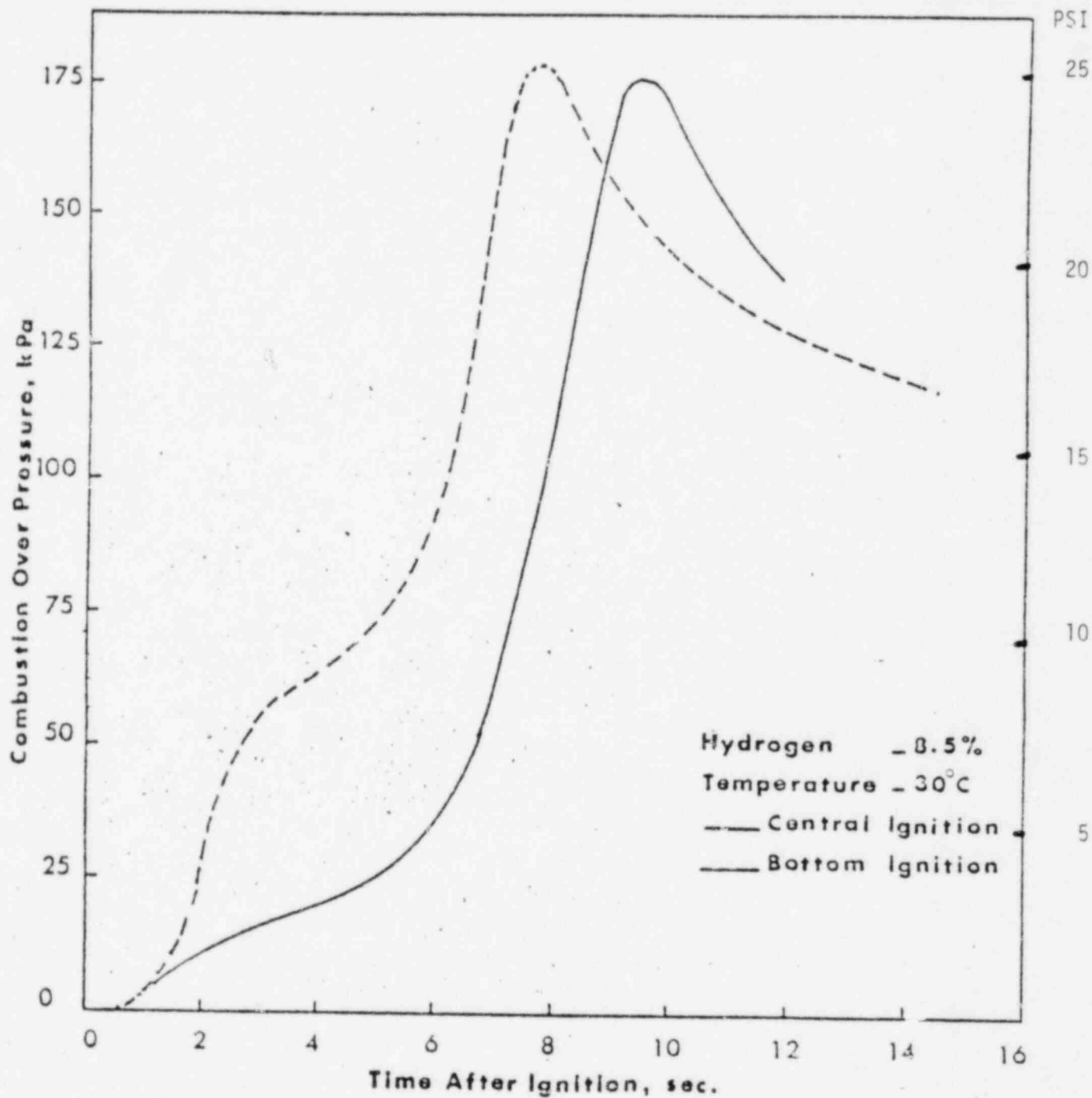
Figure - 13

EFFECT OF IGNITION SITE ON COMBUSTION

Figure - 14
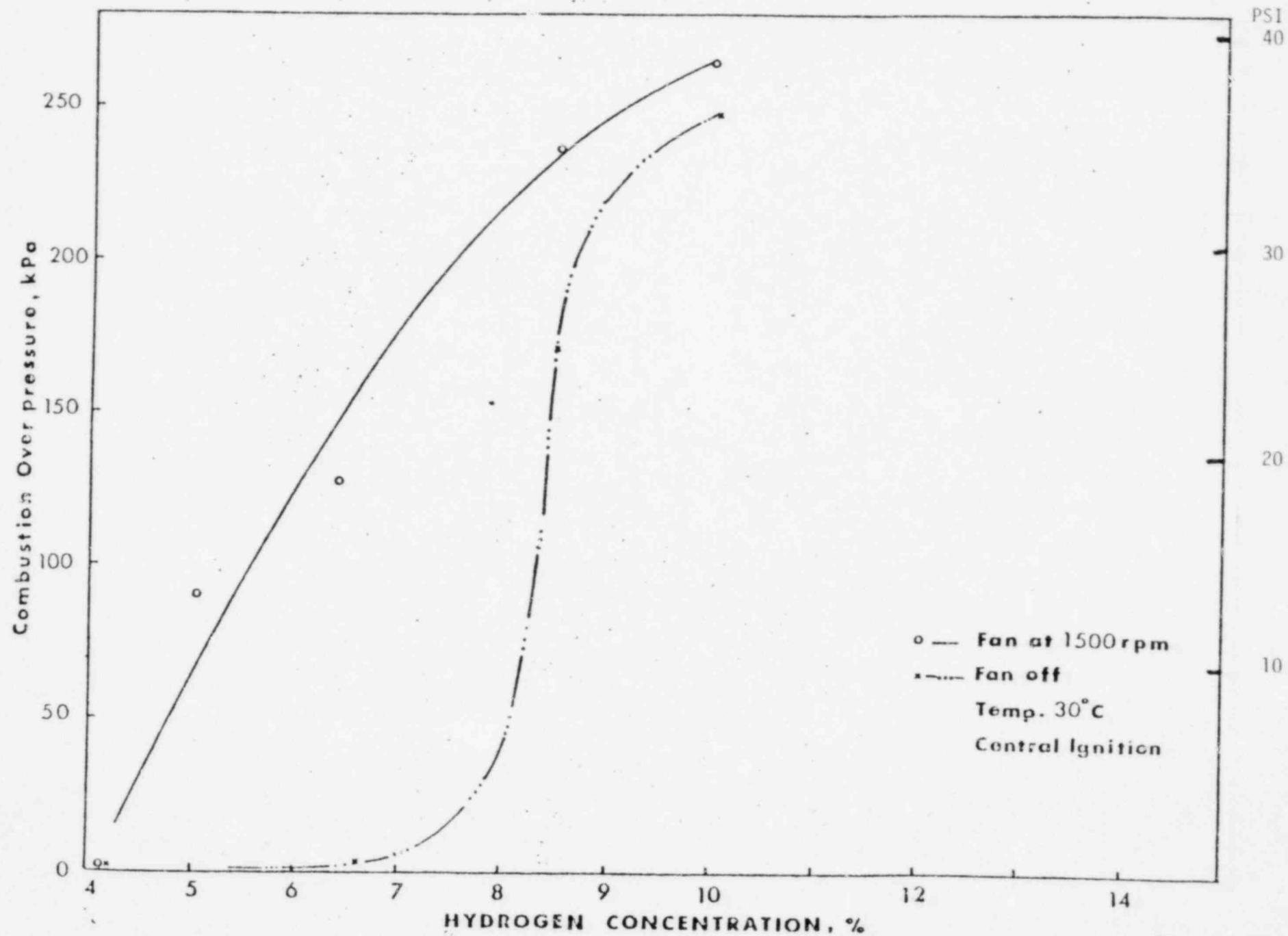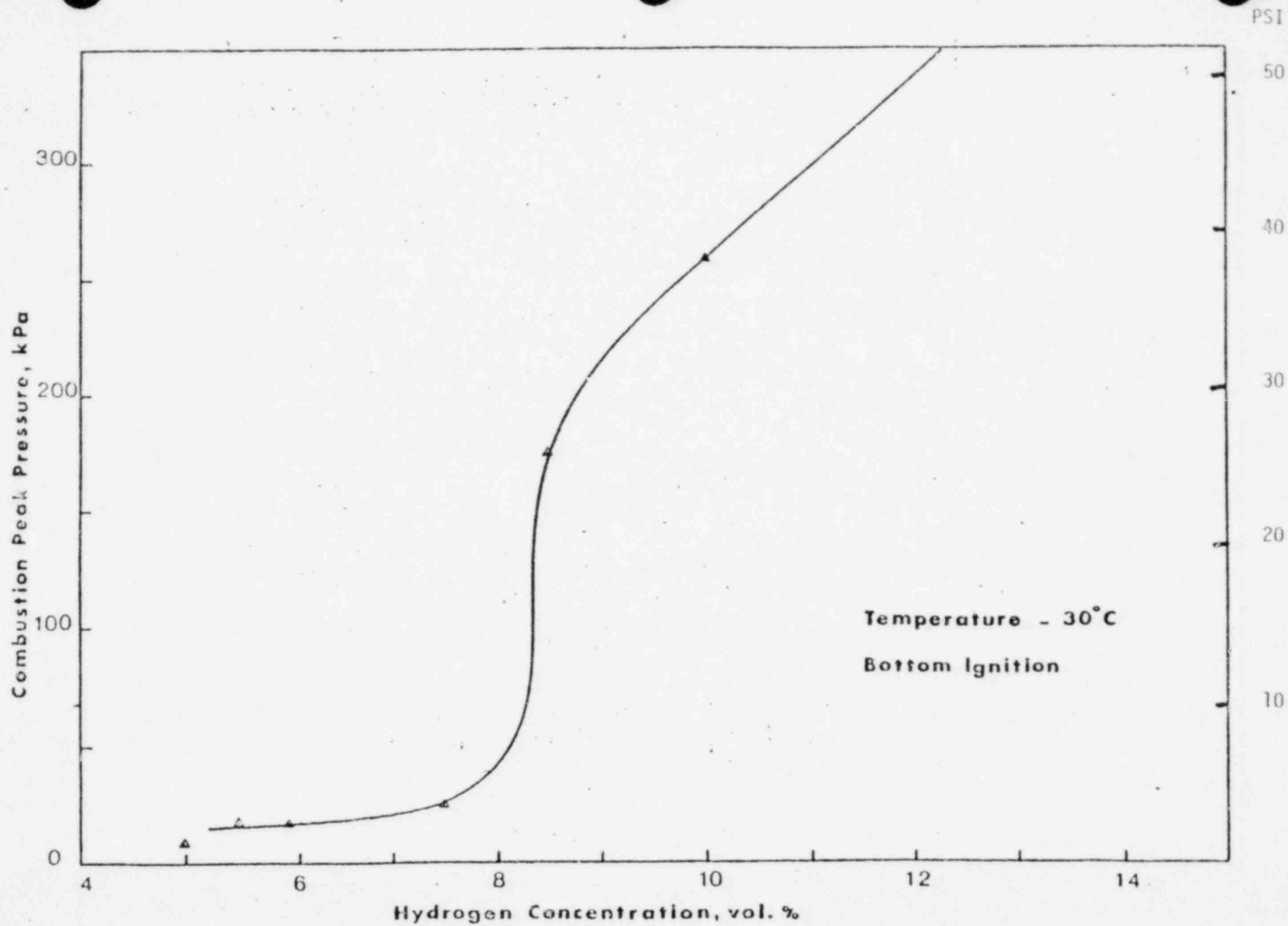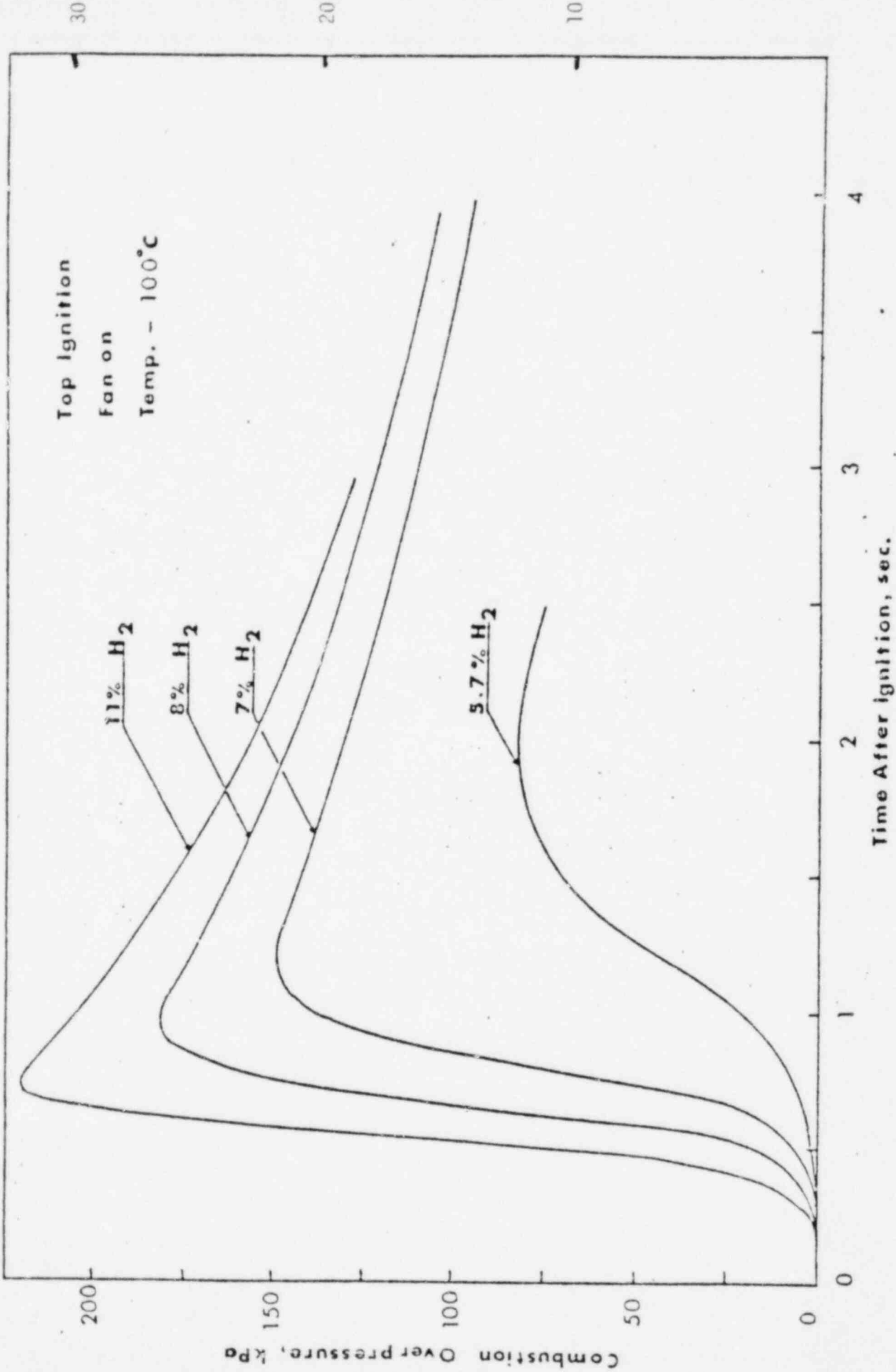
EFFECT OF IGNITOR LOCATION

Figure – 15

Figure - 16

COMBUSTION OF HYDROGEN NEAR FLAMMABILITY LIMITS

Figure - 17

TURBULENT COMBUSTION WITH TOP IGNITION

Figure - 18

APPENDIX 2K

HYDROGEN MIXING AND DISTRIBUTION

PRELIMINARY PROJECT REPORT

HYDROGEN MIXING AND DISTRIBUTION IN CONTAINMENT
ATMOSPHERES

PRELIMINARY PROJECT REPORT
DECEMBER 1981

Prepared by:

J. J. Wilder, Tennessee Valley Authority
F. G. Hudson, Duke Power Company
K. K. Shiu, American Electric Power

Project Conducted by:

Hanford Engineering Development Laboratory

Project Sponsors:

American Electric Power Service Corporation
Duke Power Company
Electric Power Research Institute
Tennessee Valley Authority

1

TABLE OF CONTENTS

1.0 INTRODUCTION

The objective of this program was to measure hydrogen mixing and
distribution in a simplified scaled light water reactor
subcompartment. The test matrix for this program was designed to
characterize hydrogen distribution in a typical lower compartment
region of an ice condenser containment under two different release
conditions. The test vessel used for these tests was modified to
geometrically simulate the lower compartment volume and the associated
flow paths into and out of that region. Hydrogen and steam release
rates used in these tests were scaled to model a small break loss of
coolant event based on analytical studies (MARCH computer code
analysis of Sequoyah Nuclear Plant) performed for the NRC by Battelle
Columbus.

The test results presented in section 4.0 are based on preliminary
results provided by G. R. Bloom and L. D. Muhlestein of the Hanford
Engienering and Development Laboratory. This report has been prepared
by the utilities.

2.0 TEST FACILITY

The Hanford Engineering Development Laboratory Containment Systems
Test Facility (CSTF) houses a carbon steel test vessel 25 feet in
diameter, 67 feet in overall height, which encloses a volume of 30,000
ft^3. The vessel has standard elliptical disked heads at the top and
bottom and models a scaled down LWR containment building with minimal
interior structures.

Hydrogen mixing in the upper compartment of an ice condenser
containment is expected to be very good. Upper containment sprays
will induce turbulent mixing of the gas and the upper compartment
geometry should prevent stratification or stagnant regions in that
large open area. This program, therefore, is focused on the lower
compartment where hydrogen from a degraded core event would be
expected to be released.

For the purposes of these tests, geometric similarity was retained
between the test compartment and the lower compartment of an ice
condenser containment. Dimensions of the compartment constructed in
the CSTF vessel are shown in Figure 8. By comparison, the ice
condenser crane wall diameter is 83 feet and the CSTF outside diameter
is 25 feet. The height to diameter ratio of the test compartment is
equal to that for the plant. The linear scaling factor between the
test compartment and the plant compartment is 0.3.

The high velocity jet nozzle shown on Figure 8 was located in one
corner of the test compartment directed horizontally 60 degrees away
from the center of the vessel at a height of approximately 5 feet from
the floor. This location was chosen because the majority of the
reactor coolant system piping in an ice condenser plant is located in
the bottom half of the lower compartment. The corner location was

chosen to be conservative. The second hydrogen release location was positioned vertically upward at approximately the 140 degree position on Figure 8 to be geometrically similar to the location of an ice condenser plant's pressure relief tank rupture disk.

3.0 TEST MATRIX

3.1 SCALING

As mentioned above, this test program was geometrically modeled to simulate hydrogen releases in the lower compartment of an ice condenser containment. The test parameters: hydrogen and steam flow rates, forced air flow into and out of the compartment, and release locations and sizes, also had to be modeled so that the results of these tests could be integrated into the full scale degraded core accident analysis.

Modeling is said to be ideal if all dimensionless groups characterizing the event (including geometric scale factors) are identical in the model and the prototype. However, in complex models it is often difficult or impossible to select model test parameters so that all dimensionless groups are identical to those of the prototype. For this reason non-ideal modeling is often used. In such non-ideal models, similitude for one or more of the dimensionless groups is compromised so that experiments can be carried out to evaluate the dominant controlling phenomena. When non-ideal models are used, it is obviously important that the dominant parameters be identified, and that test conditions be selected to yield parameters which are essentially the same in the prototype.

HEDL, with the help of their consultant, Dr. Arlin Postma, examined the dominant mixing processes and identified the following four dominant mixing processes in the ice condenser annular volume for the release conditions under consideration;

1. High speed horizontal jet mixing

2. High speed vertical jet mixing

3. Fan induced recirculating air flow and

4. Natural convection flows along surfaces

It was determined that in modeling these mixing processes that the following criteria would be met.

1. Preserve the similarity of the densimetric Froude
   numbers. The densimetric Froude number is the ratio of
   momentum forces to buoyancy forces.

2. Preserve geometric similarity.

3. Preserve scaled relative times which is required
   because of competing mixing processes.

4. Preserve density ratios of jet to ambient atmosphere.

One other important factor in modeling these tests was the
substitution of helium for hydrogen. The reason for a
substitute gas was that safety requirements at Hanford would
not allow hydrogen combustion at this facility. Helium was
selected because it has nearly the same buoyancy in air or
nitrogen as hydrogen and exhibits similar mixing
characteristics. The thermal conductivity of helium is near
that of hydrogen and the same thermal-conductivity type
concentration monitoring equipment was used for both gases,
thus, eliminating the need to reinstrument the test
compartment for the one hydrogen test. The hydrogen test
was conducted in an oxygen reduced atmosphere to confirm
test results using helium as a simulant.

3.2 Mixing Tests

The mixing test matrix is given in Table I. Hydrogen or
helium concentrations, gas velocities and temperature
profiles were measured during simulation of the two hydrogen
release scenarios. Mixing and distribution were determined
from the concentration, velocity, and temperature profiles.

The four preliminary tests, HM-P1 through HM-P4, were
designed to determine the separate and combined effects of
natural and forced convection air recirculation. Natural
convection air velocities were measured at near ambient and
at an elevated containment gas temperature of 150° F.
Forced air recirculation and gas velocity in the compartment
were measured in both ambient and elevated temperature
cases.

Mixing tests HM-1 through HM-5 were all simulations of a
steam-hydrogen release from a two inch pipe break. Tests HM-1
and HM-2 were cases without the air recirculation normally
provided during an accident scenario for an ice condenser
lower containment region. Tests HM-3 and HM-4 were
conducted with the modeled air recirculation flows. Tests
HM-1 and HM-3 were conducted with helium-steam release rates
arbitrarily set at one half the reference release rate to
determine the effect of reduced jet mixing in the test
compartment volume. Mixing test HM-5 was identical to test

HM-4 with the difference that hydrogen was used as the source gas and nitrogen was used as the containment gas. This test was conducted to determine whether helium was a valid simulant for hydrogen in these tests.

The final two tests HM-6 and HM-7 simulated a vertical hydrogen steam jet release directed upward from a location geometrically similar to that of a pressure relief tank (PRT). The helium-steam source rates were identical to those of tests HM-3 and HM-4 respectively. These flow rates taken from an S_2D type event were considered representative of the releases from a 2-inch pipe break as well as a rupture of the PRT rupture disk.

4.0 TEST RESULTS

Tests HM-P1 and HM-P3 demonstrated the difference in natural convection created by ambient (85° F) and elevated gas temperatures (150° F) in the lower compartment. When comparing the effect of natural convection forces in the ambient air test HM-P1 with test HM-P3 the local average air velocity in the lower and upper volume increased by a factor of four when the compartment was heated to 150° F. Tests HM-P2 and HM-P4 were conducted with ambient and elevated gas temperatures respectively with the added parameter of scaled forced air recirculation. In these forced air recirculation tests, ambient air case HM-P2 and elevated air case HM-P4, natural convection effects were the most significant in the bottom of the test compartment. The local air velocities in these two tests were of the same order of magnitude with the elevated temperature case being slightly higher.

Hanford experienced failure of several of their gas velocity probes in the middle region of the test compartment on test HM-P3. They could not repair them in time to keep the tests on schedule so they elected to proceed with the test series. Hanford felt that sufficient gas velocity information was available from the remaining probes to describe the gas mixing process.

The helium and hydrogen concentrations in these tests were measured by 12 thermal conductivity analyzers. Ten of the analyzers were located in the lower compartment and two in the upper compartment. The analyzers required a constant gas flow rate of 150 cc per minute. The gas sample was cooled, the condensate separated, and the gas dried prior to being injected into the analyzers. The concentrations presented in Figures 1 through 7 have not been corrected for steam and are therefore conservative.

There is a modeling time scale of approximately 3.33 to 1 from the test to the plant case. Test helium transients will happen three times faster in the test compartment; therefore, one should multiply the time scale of Figures 1 through 7 by 3.33 to predict transients in the plant containment.

Helium concentration transients for ten test compartment points are presented in Figures 1 through 7 for tests HM-1 through HM-7 respectively. During the helium-steam release in tests HM-1 and HM-2, the maximum concentration difference between all measurement points in the test compartment was 2 vol % He. Following the helium-steam release, the test compartment, unlike the plant, developed a vaccum as the steam in the compartment condensed. This reverse migration coupled with the lack of a mixing mechanism from either the fans or the jet itself created a concentration difference of 7 vol % He for test HM-2. This was the largest difference observed in any test. Hanford did not believe that this portion of the test was in any way prototypic of the plant. The maximum concentration difference occurred approximately two minutes after the jet release was stopped.

Mixing tests HM-3 and HM-4 both exhibited good distribution of the helium during and after the source was terminated. The maximum difference in the test compartment at any time was less than 2 percent for both tests.

The hydrogen concentration transients for test HM-5 is presented in Figure 5. The hydrogen release rate was 0.66 lb/min or about 27% lower than the modeled release rate of 0.9 lb/min due to problems with the hydrogen flowmeter. The low hydrogen flow rate is not considered serious since the hydrogen concentration data can be normalized for comparison purposes and the jet mixing Froude number for test HM-5 was near that calculated for test HM-4.

The hydrogen concentration transient in Figure 5 is identical to the helium concentration transient reported for test HM-4 if the concentration data is normalized. The data was normalized by dividing the concentration at any time by the peak concentration for the test. Comparison of the hydrogen and helium concentration transients demonstrates that the curves are identical in every detail. The agreement between the test results of tests HM-4 and HM-5 demonstrates that helium is a valid simulant for hydrogen.

During test HM-6 the helium flow rate was too high by a factor of two during the ninth minute of a 10 minute release. Extrapolation of the helium concentration transient prior to the inadvertant high helium release rate leads to a prediction of a peak helium concentration of 6%.

Comparing vertical and horizontal helium-steam release tests (HM-6 to HM-3 and HM-7 to HM-4) to each other shows relatively close agreement. The peak helium concentration of test HM-3 was 5.5 volume percent helium and the corrected peak for HM-6 was 6 volume percent.

The maximum observed helium concentration difference between points in the test compartment during the source release was 1.9 volume percent helium during test HM-6 and was 1.3 volume percent helium during test HM-3.

Tests HM-4 and HM-7 also had similar helium concentration transients. The peak helium concentration was 10.8 volume percent for both tests. The maximum helium concentration difference between points was 2.8 volume percent helium in tests HM-7 and 1.5 volume percent during test HM-3. The conclusion from these test results is that jet orientation plays an observable but minor role in the gas mixing process and the resulting gas concentration transients.

5.0 PRELIMINARY CONCLUSIONS

From the preliminary test results we have drawn the following conclusions concerning hydrogen mixing:

1. Helium is a valid simulant for hydrogen in these hydrogen mixing and distribution tests.

2. The test compartment volume is well mixed with less than 1 volume % concentration difference between points within 20 minutes after stopping the hydrogen-steam or helium-steam source for all cases.

3. In all cases with forced air recirculation, the concentration difference between points was less than 1 volume percent within 5 minutes after stopping the source gas.

4. The air recirculation fans minimize both the peak helium concentration and the maximum helium concentration difference between points in the test compartment.

5. Test compartment volume gas mixing is not strongly dependent on source jet release orientation.

TABLE 1

H_2 MIXING TEST MATRIX

Test No.	Cont. Gas	Recirc. Flow (CFM)	Source Gas	Orientation Source Gas Jet	He or H_2 Flow Rate (lb/min)	Steam Flow (lb/min)	Initial Containment Gas Temp (°F)
HM-P1	Air	0	--	--	--	--	85
HM-P2	Air	3700	--	--	--	--	85
HM-P3	Air	0	--	--	--	--	150
HM-P4	Air	3700	--	--	--	--	150
HM-1	Air	0	He-Steam	Horizontal	0.9	27	150
HM-2	Air	0	He-Steam	Horizontal	1.8	54	150
HM-3	Air	3700	He-Steam	Horizontal	0.9	27	150
HM-4	Air	3700	He-Steam	Horizontal	1.8	54	150
HM-5	N_2	3700	H_2-Steam	Horizontal	0.66	54	150
HM-6	Air	3700	He-Steam	Vertical	0.9	27	150
HM-7	Air	3700	He-Steam	Vertical	1.8	54	150
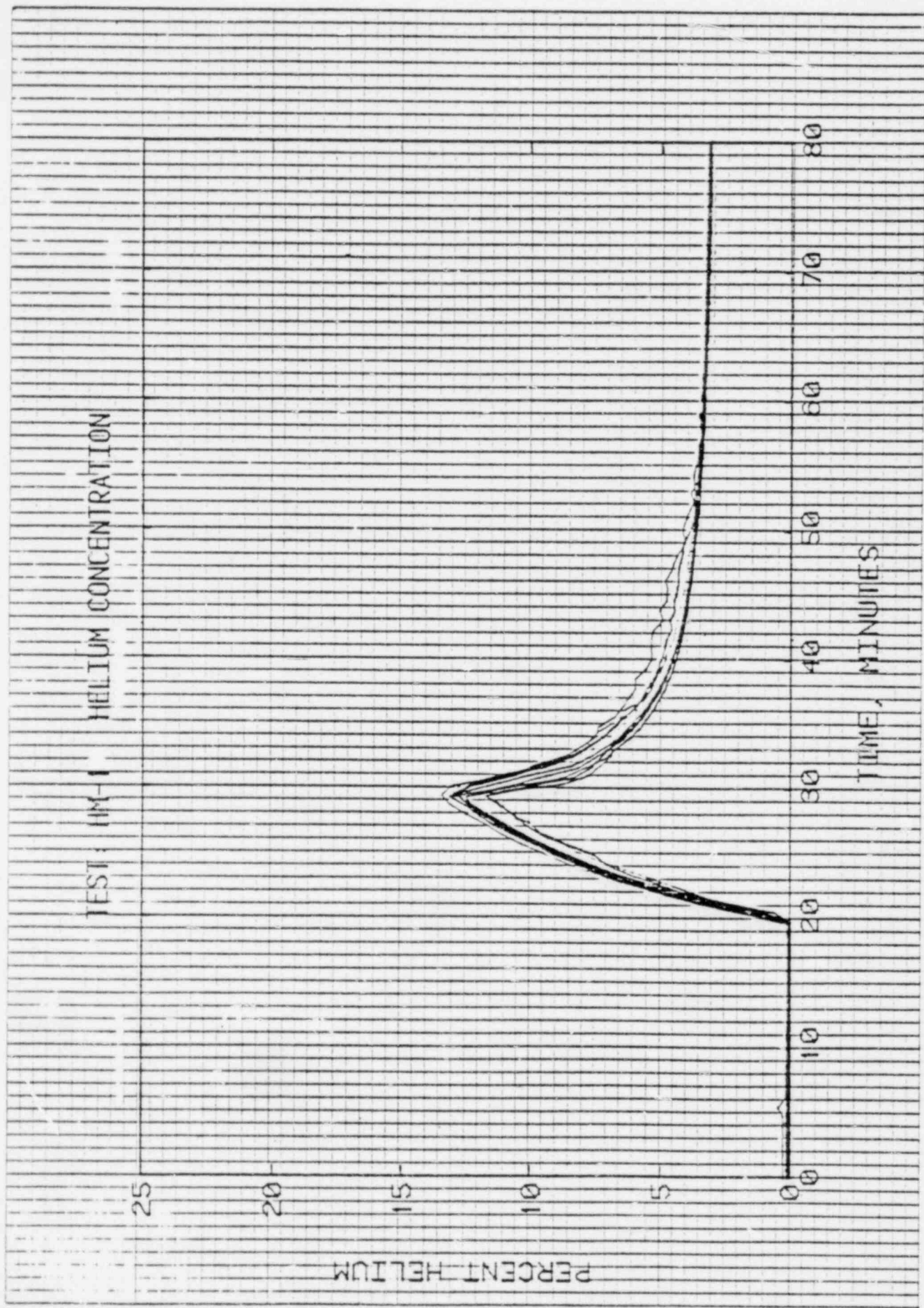
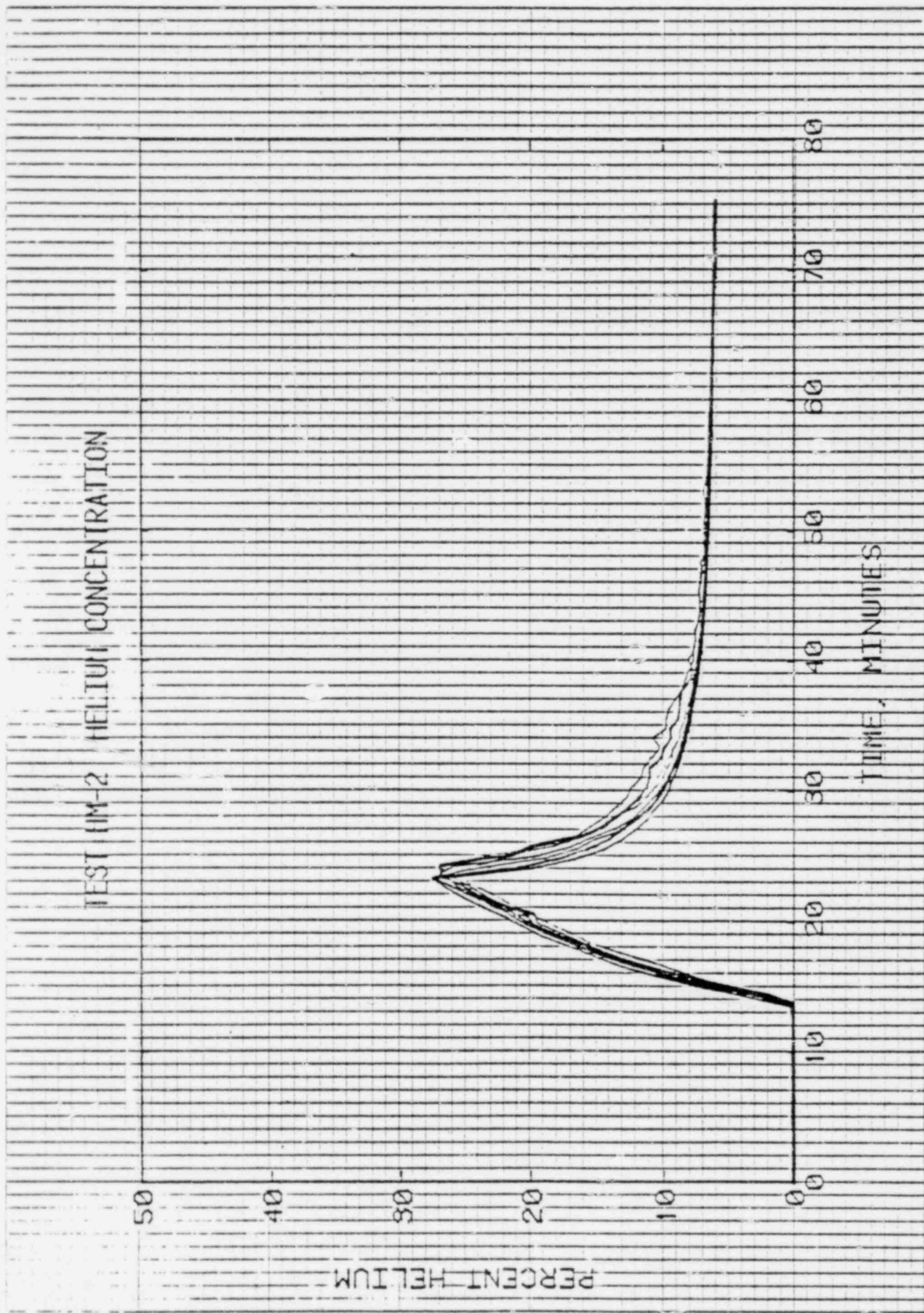Figure 1.   Test HM-1   Helium Concentration Transients.

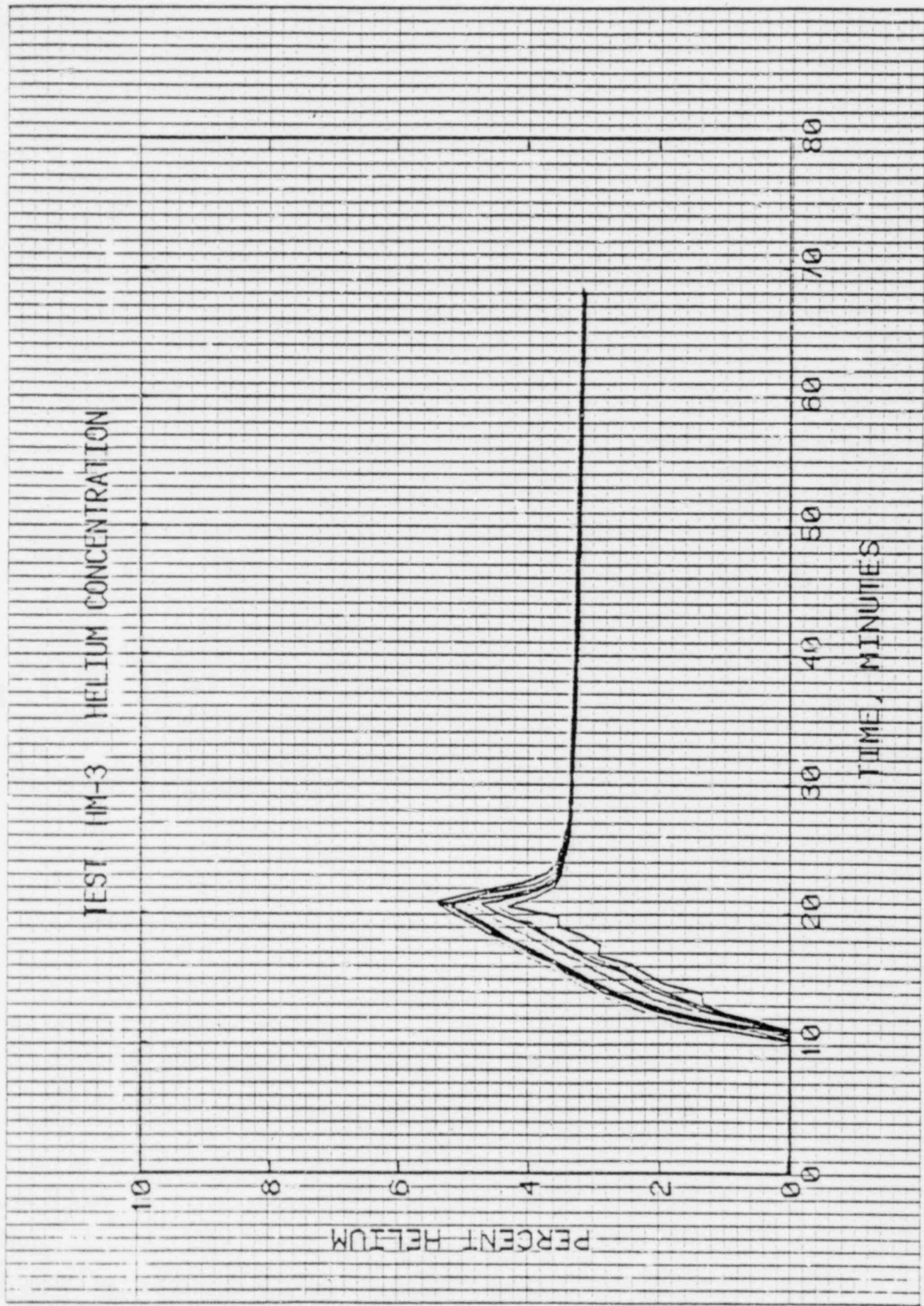Figure 2. Test HM-2 Helium Concentration Transients.

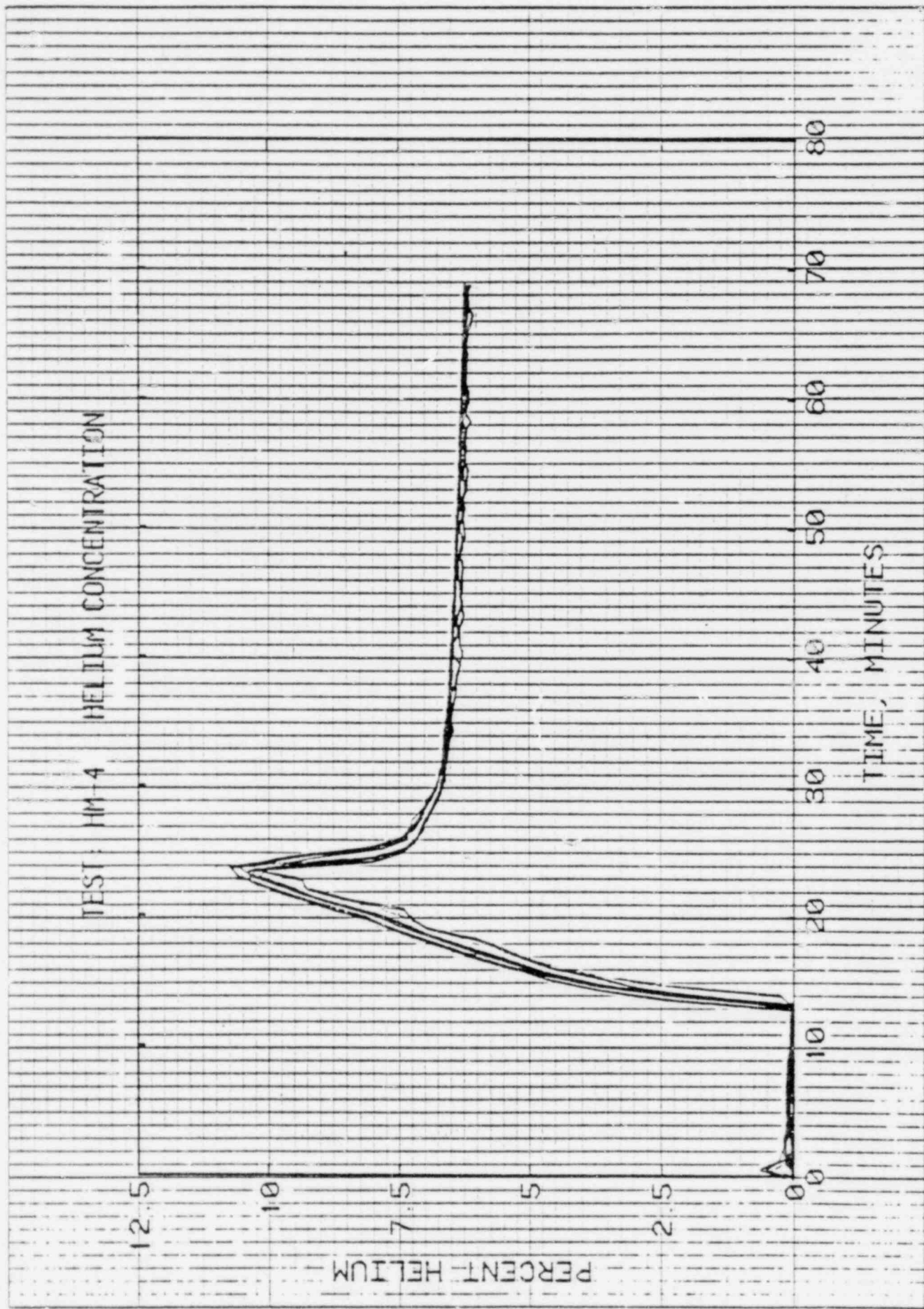Figure 3. Test IIM-3 Helium Concentration Transients.
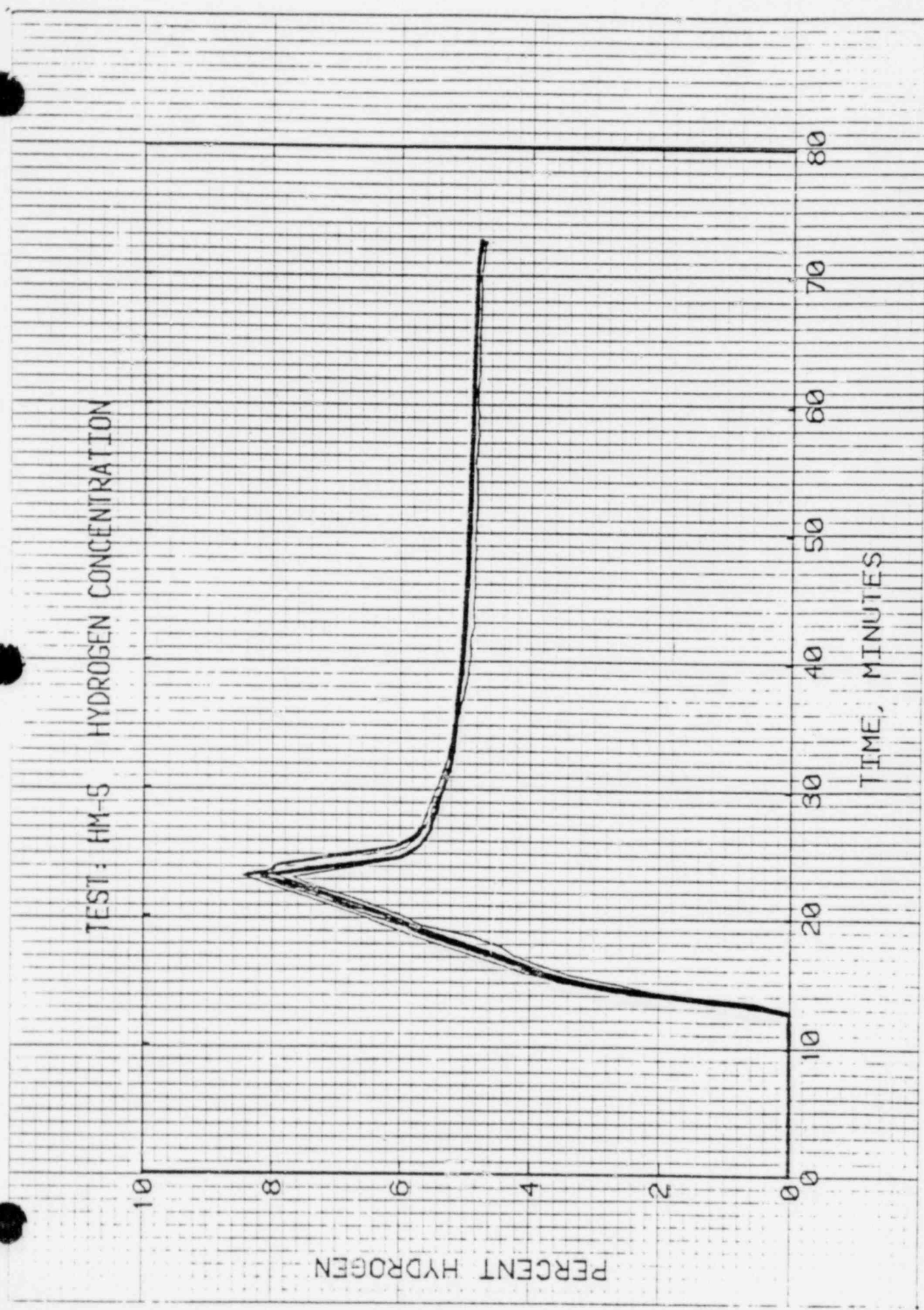
Figure 4. Test HM-4 Helium Concentration Transients.

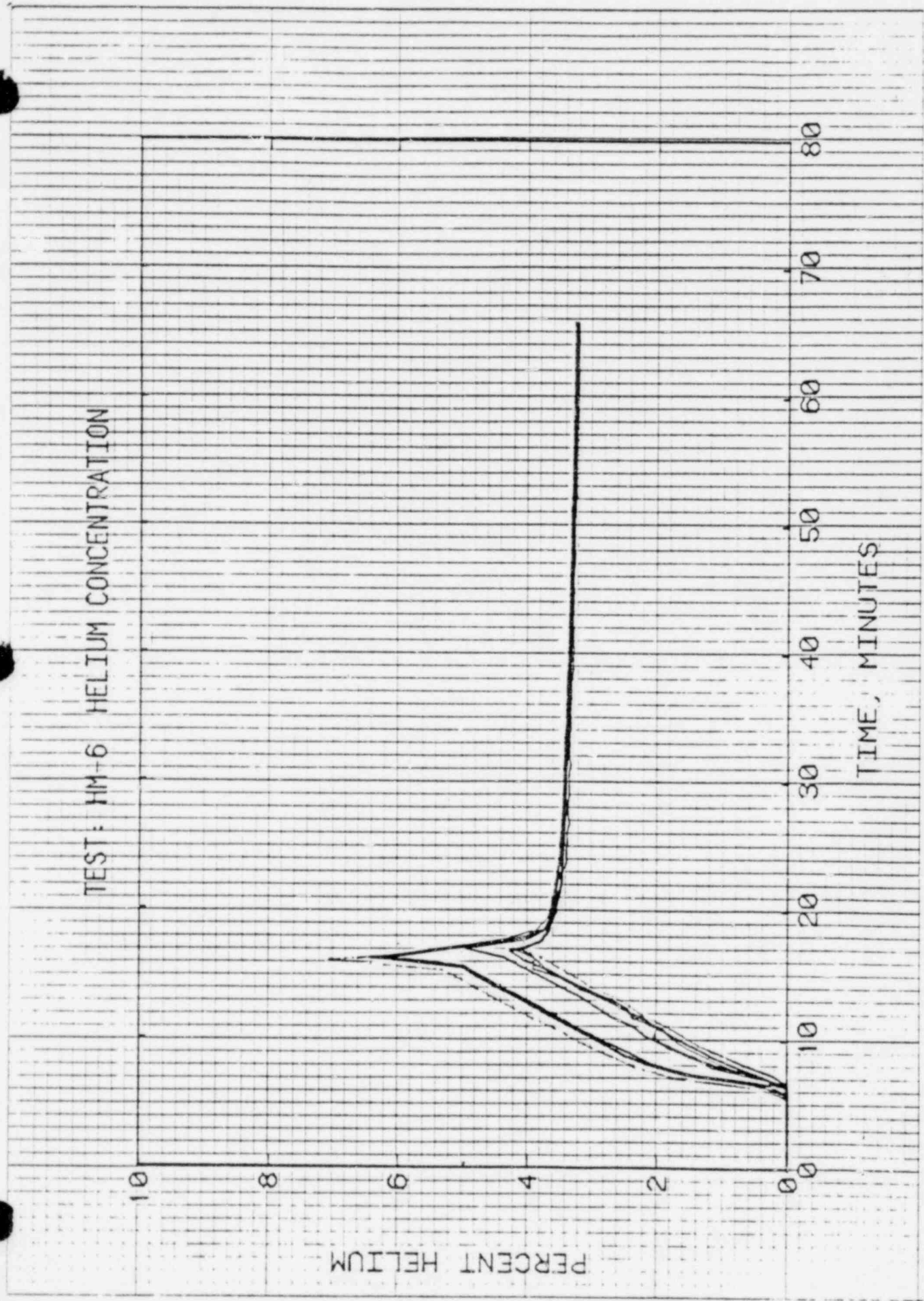Figure 5. Test HM-5 Hydrogen Concentration Transients

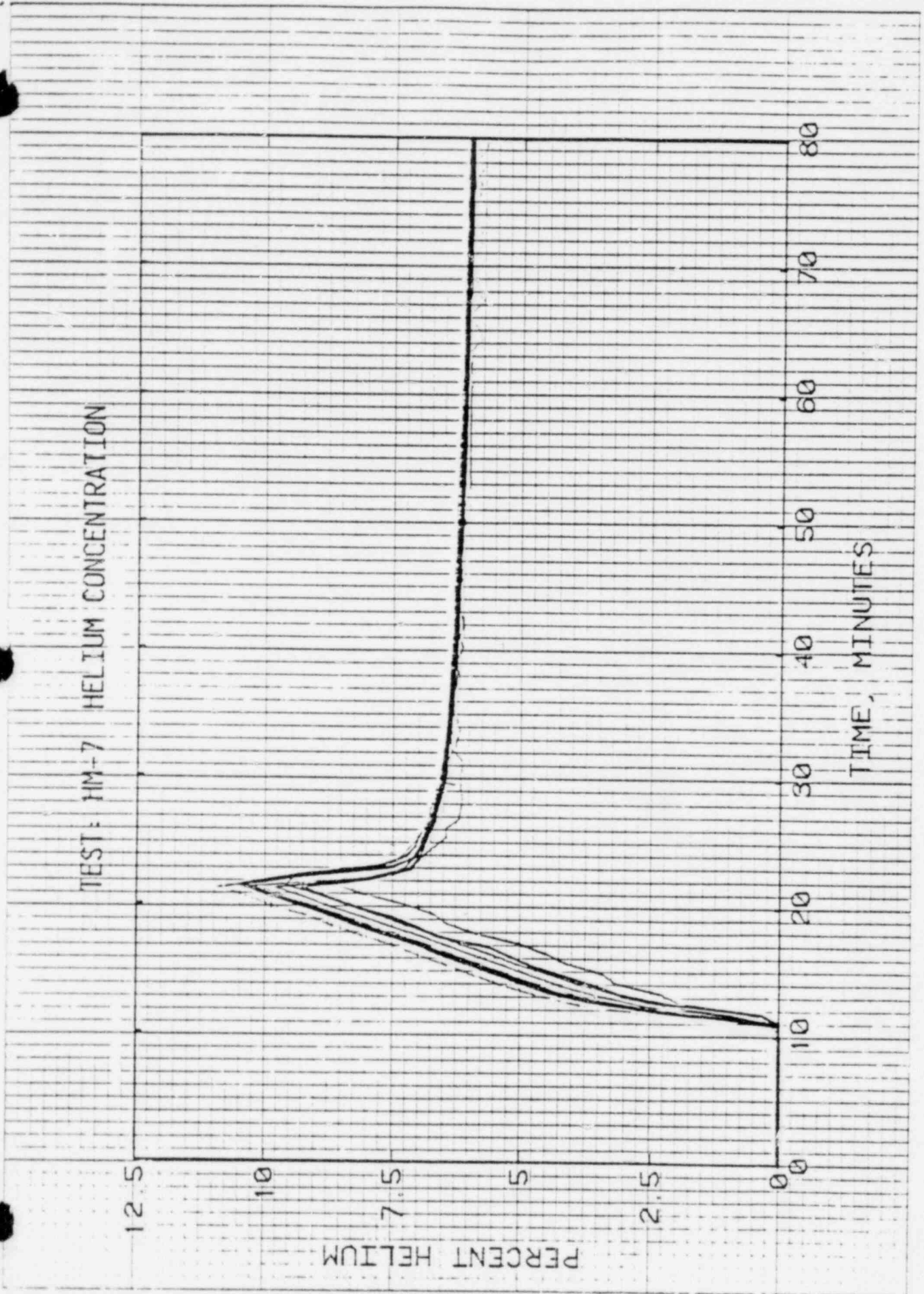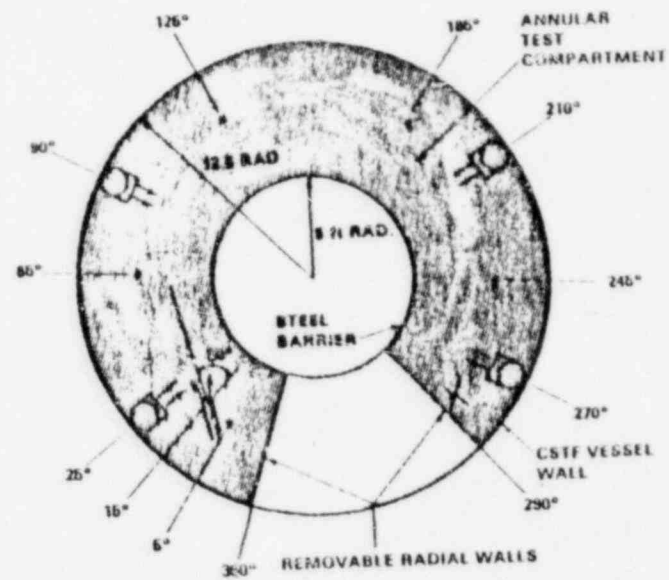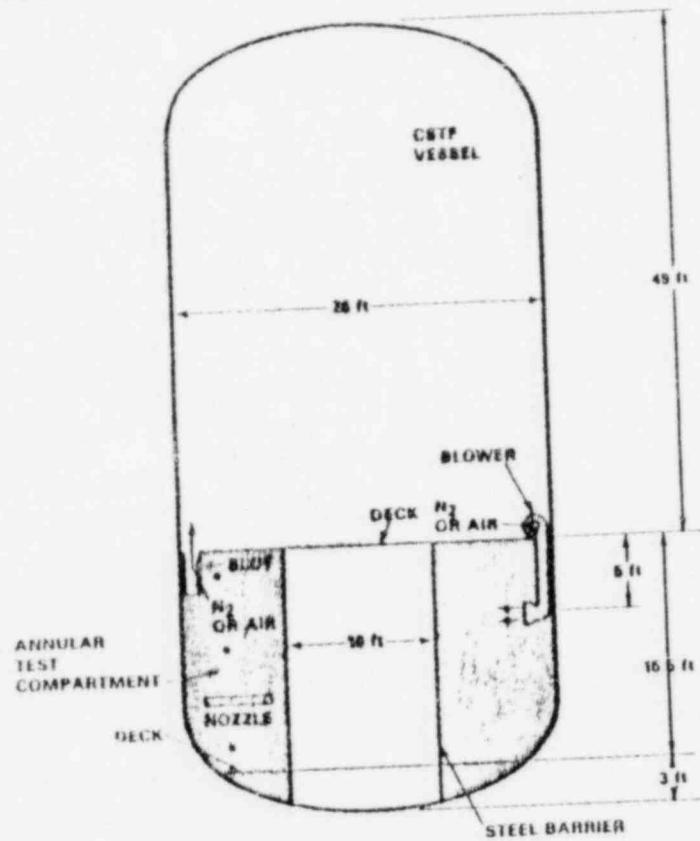Figure 6. Test HM-6 Helium Concentration Transients

Figure 7. Test HM-7 Helium Concentration Transients

TEST COMPARTMENT SCHEMATIC

Figure 8

system. Selection of the glow plug as the DIS ignition source precludes
further study of electromagnetic emissions and their effect on instru-
mentation. (Section 2.3)

4. Catalytic combustors are an effective means of hydrogen removal. How-
   ever, environmental effects of catalyst performance indicate significant
   support systems would be required to assure combustor performance. As
   a result of these demonstrated concerns, further study is precluded.
   (Section 2.4)

5. In order to significantly affect the lower flammability limit of hydro-
   gen, a micro-fog consisting of relatively large droplets must have a
   larger density then a fog with smaller droplets. (Section 2.5)

In addition to the results mentioned above, data obtained from the remaining
research projects appear to indicate the following:

1. Ignitor location does have an effect on the characteristics of hydrogen
   deflagrations. However, the observed results appear to be consistent with
   existing knowledge on combustion phenomena. Other tests show that with
   sufficiently small droplets, a micro-fog does reduce the pressure rise
   resulting from hydrogen deflagrations. (Section 2.6).

2. Operation of glow plug hydrogen ignitors at 14 volts provides sufficent
   margin for effective operation over a broad range of environmental
   conditions. Results generally agree with Shapiro-Moffette flammability
   curve. (Section 2.7)

3. Steam and turbulence produce competing effects on hydrogen combustion. Steam tends to minimize combustion, while turbulence tends to enhance combustion. (Section 2.8)

    | 2

4. Due to the inherent characteristics of a discharge jet, combined with the operation of the air return fans, localized accumulations of large hydrogen concentrations will not occur within an ice condenser containment. (Section 2.9)

    | 1

In undertaking a project which requires one to work at the edge of known technology without specific guidelines or design requirements, the best conclusion that can be obtained is one in which knowledgeable engineering personnel, applying the best tools available to them, reach what they consider to be a reasonable solution that has a high probability of being successful. Duke Power considers that such a stage has been reached with regard to protection of the McGuire containment from the effects of nuclear accidents which lie outside the station design basis. Additional investment in either research or analysis is extremely unlikely to change the hydrogen mitigation system itself or our conclusions concerning its effectiveness.